REVIEW ARTICLE

Adhesive organelles of Gram-negative pathogens assembled with the classical chaperone/usher machinery: structure and function from a clinical standpoint

Vladimir Zav'yalov[1], Anton Zavialov[2], Galina Zav'yalova[1] & Timo Korpela[1]

[1]Joint Biotechnology Laboratory, University of Turku, Turku, Finland; and [2]Department of Molecular Biology, Swedish University of Agricultural Sciences, Uppsala, Sweden

Correspondence: Vladimir Zav'yalov, Joint Biotechnology Laboratory, University of Turku, BioCity 6A, FIN-20520 Turku, Finland. Tel.: +35 8 2 333 8510; fax: +35 8 2 333 8080; e-mail: vlazav@utu.fi

Received 2 June 2009; revised 10 November 2009; accepted 17 November 2009.
Final version published online 7 January 2010.

DOI:10.1111/j.1574-6976.2009.00201.x

Editor: Mecky Pohlschroder

Keywords
fimbrial adhesions; Gram-negative pathogens; chaperone/usher machinery; mono- and polyadhesive binding; immunomodulatory activity; vaccines.

Abstract

This review summarizes current knowledge on the structure, function, assembly and biomedical applications of the superfamily of adhesive fimbrial organelles exposed on the surface of Gram-negative pathogens with the classical chaperone/usher machinery. High-resolution three-dimensional (3D) structure studies of the minifibers assembling with the FGL (having a long F1–G1 loop) and FGS (having a short F1–G1 loop) chaperones show that they exploit the same principle of donor-strand complementation for polymerization of subunits. The 3D structure of adhesive subunits bound to host-cell receptors and the final architecture of adhesive fimbrial organelles reveal two functional families of the organelles, respectively, possessing polyadhesive and monoadhesive binding. The FGL and FGS chaperone-assembled polyadhesins are encoded exclusively by the gene clusters of the γ3- and κ-monophyletic groups, respectively, while gene clusters belonging to the γ1-, γ2-, γ4-, and π-fimbrial clades exclusively encode FGS chaperone-assembled monoadhesins. Novel approaches are suggested for a rational design of antimicrobials inhibiting the organelle assembly or inhibiting their binding to host-cell receptors. Vaccines are currently under development based on the recombinant subunits of adhesins.

Introduction

A necessary step for the development of an infectious disease in the host organism is the formation of a firm link between the pathogen and the target cells of the host. The link is mediated by surface-exposed adhesive organelles and is required for internalization of bacteria or extracellular colonization of host tissues. The adhesive organelles mediate bacterial adhesion via a specific interaction with surface structures present on host cells. The adhesin binding to the target cells triggers subversive signals that allow pathogens to evade immune defense and facilitate bacterial colonization or invasion (reviewed by Zavialov *et al.*, 2007).

There are two major classes of protein adhesins of Gram-negative pathogens:

(1) The fimbrial adhesins, represented by the linear homopolymers or heteropolymers (up to seven distinct subunits) of hundreds to thousands of subunits.

(2) The nonfimbrial adhesins consisting of a single protein or homotrimers.

The fimbrial adhesins in Gram-negative bacteria are typically formed by noncovalent homo- or heteropolymerization of subunit proteins (reviewed by Zavialov *et al.*, 2007; Fronzes *et al.*, 2008; Kline *et al.*, 2009; Waksman & Hultgren, 2009). In contrast, the more recently discovered fimbrial adhesins in Gram-positive bacteria are formed by covalent polymerization of protein subunits in a process that requires a dedicated sortase enzyme (reviewed by Proft & Baker, 2009).

The assembly of fimbrial and nonfimbrial adhesins of Gram-negative pathogens involves different secretion systems. Protein transport across the outer membrane of Gram-negative bacteria can be subdivided into Sec-independent and Sec-dependent pathways (reviewed by Gerlach & Hensel, 2007). Depending on the system of secretion, adhesive proteins present on the surface of Gram-negative bacteria can be divided into a few major families:

(1) The fimbrial adhesins, assembled on the outer membrane through the classical chaperone/usher pathway (Hung *et al.*, 1996; Thanassi *et al.*, 1998; Choudhury *et al.*, 1999; Sauer *et al.*, 1999, 2000, 2002, 2004; Knight *et al.*, 2000; Zavialov *et al.*, 2001, 2002, 2003, 2005, 2007; Remaut *et al.*, 2006, 2008; Verger *et al.*, 2007; Zavialov & Knight, 2007; Fronzes *et al.*, 2008; Waksman & Hultgren, 2009; Yu *et al.*, 2009).
(2) CS (coli surface) pili, assembled on the outer membrane through the 'alternate chaperone/usher pathway' (Soto & Hultgren, 1999). The assembly of the surface antigen 1 (CS1) pili of enterotoxigenic *Escherichia coli* (ETEC) shows high functional similarities to the classical chaperone/usher pathway, but the proteins involved share no detectable sequence similarities. Poole *et al.* (2007) demonstrated that, like the classical chaperone/usher pathway, the donor-strand complementation mechanism governs the intersubunit interaction of fimbriae of the alternate chaperone/usher pathway.
(3) Type IV pili, formed in distinction to (1) and (2) by polymerization of pilin subunits at the cytoplasmic membrane. The assembled pilus structure is extruded across the outer membrane and forms long and flexible surface appendages (Craig *et al.*, 2004; Fronzes *et al.*, 2008, 2009a, b). Components of the type IV pilus assembly machinery are structurally related to the type II secretion system, where homologous proteins are called 'pseudopilins.'
(4) Curly or thin aggregative fimbrial adhesins, assembled at the bacterial surface through extracellular nucleation precipitation: the major fiber subunit CsgA polymerizes on the surface-exposed nucleator CsgB (Hammar *et al.*, 1996; Fronzes *et al.*, 2008).
(5) The nonfimbrial 'trimeric autotransported adhesins,' secreted by the type V secretion system (Linke *et al.*, 2006). Adhesin YadA is the prototypical member of nonfimbrial adhesins. YadA is expressed by several *Yersinia* species and is a member of the family of very stable trimeric autotransporter adhesins anchored in the outer membrane with a β-barrel.
(6) Integral outer membrane proteins (e.g. OmpA, invasin and intimin), anchored to the outer membrane by a unique mechanism in which the bacteria provide the cognate receptor for the adhesin intimin by translocating it into the host cell in a type III secretion system-dependent manner (Niemann *et al.*, 2004).
(7) Nonfimbrial adhesins, secreted by the type I secretion system (Delepelaire, 2004). For example, two-partner-secreted filamentous hemagglutinins from *Bordetella pertussis* exist in a membrane-bound and in a secreted form, each having distinct functions.

Dominant class (1) of the fibrillar adhesive organelles of Gram-negative pathogens is assembled by the conserved classical chaperone/usher protein secretion system (Hung *et al.*, 1996; Thanassi *et al.*, 1998; Choudhury *et al.*, 1999; Sauer *et al.*, 1999, 2000, 2002, 2004; Knight *et al.*, 2000; Zavialov *et al.*, 2001, 2002, 2003, 2005, 2007; Remaut *et al.*, 2006, 2008; Verger *et al.*, 2007; Zavialov & Knight, 2007; Fronzes *et al.*, 2008; Waksman & Hultgren, 2009; Yu *et al.*, 2009). This system can assemble fimbrial organelles of diverse subunit composition, architecture and function. The assembled organelles consist of two families that are structurally and functionally distinct. One family consists of only one or two types of subunits, and at a low resolution typically shows a nonpilar, amorphous or capsule-like morphology (Hung *et al.*, 1996; Soto & Hultgren, 1999; Zavialov *et al.*, 2003, 2005, 2007; Le Bouguénec, 2005; Remaut *et al.*, 2006). The assembly of this family is assisted by the FGL (having a long F1–G1 loop) family of periplasmic chaperones (Zav'yalov *et al.*, 1995b; Hung *et al.*, 1996; Zavialov *et al.*, 2003, 2005, 2007; Remaut *et al.*, 2006; Zavialov & Knight, 2007). The notable property of the organelles is that all subunits possess two independent binding sites specific to different host-cell receptors (Anderson *et al.*, 2004a, b; Pettigrew *et al.*, 2004; Korotkova *et al.*, 2006a, b, 2008a). Because of this function–structure property, they were named 'FGL chaperone-assembled polyadhesins' (Zavialov *et al.*, 2007). The other family consists of thick rigid and thin flexible adhesive pili (also known as adhesive fimbriae) of a complex subunit composition (up to seven different subunits). The majority of the pili display only one adhesive domain on the tip of the pilus (monoadhesive fimbriae/pili) (Hung *et al.*, 1996; Thanassi *et al.*, 1998; Choudhury *et al.*, 1999; Sauer *et al.*, 1999, 2000, 2002, 2004; Knight *et al.*, 2000; Verger *et al.*, 2007; Fronzes *et al.*, 2008; Remaut *et al.*, 2008; Waksman & Hultgren, 2009). The assembly of monoadhesive pili/fimbriae is assisted by the FGS (having a short F1–G1 loop) family of periplasmic chaperones (Hung *et al.*, 1996).

The discovery of two families of organelles and chaperones was based on the different morphologies of organelles and the sequence comparison of chaperones (Zav'yalov *et al.*, 1995b; Hung *et al.*, 1996). The relevance of the division was confirmed later by high-resolution three-dimensional (3D) analysis of the typical representatives of the two families of chaperones and the organelle subunits folded by them (Choudhury *et al.*, 1999; Sauer *et al.*, 1999, 2002; Zavialov *et al.*, 2003, 2005, 2007; Remaut *et al.*, 2006; Verger *et al.*, 2007; Zavialov & Knight, 2007; Salih *et al.*, 2008; Waksman & Hultgren, 2009). Both types of organelles are made of fibers of linearly polymerized subunits. The subunits are connected via the donor-strand exchange mechanism (Sauer *et al.*, 1999; Zavialov *et al.*, 2003, 2005, 2007; Verger *et al.*, 2007; Salih *et al.*, 2008; Waksman & Hultgren, 2009). Comparison of the subunit 3D structures in fibers and bound to chaperone (Sauer *et al.*, 2002; Zavialov *et al.*, 2003) together with calorimetric studies (Zavialov *et al.*, 2005) revealed that the fiber formation in both of the families is driven by the chaperone-preserved folding energy.

The last comprehensive review on the superfamily of Gram-negative bacterial adhesins assembled via the classical

chaperone/usher pathway was published a decade ago (Soto & Hultgren, 1999). Since that time, remarkable progress has been made in understanding the structure and function of the classical chaperone/usher assembly-translocation machinery (Remaut *et al.*, 2008; Yu *et al.*, 2009), the structure and function of the surface-exposed adhesive organelles (Zavialov *et al.*, 2003, 2005, 2007; Anderson *et al.*, 2004a, b; Pettigrew *et al.*, 2004; Bouckaert *et al.*, 2005, 2006; Westerlund-Wikström & Korhonen, 2005; Korotkova *et al.*, 2006a, b, 2008a; De Greve *et al.*, 2007; Li *et al.*, 2007; Verger *et al.*, 2007; Salih *et al.*, 2008) and the phylogenesis of ushers/chaperones (Nuccio & Bäumler, 2007). It has now become evident that adhesins trigger subversive signals directed to mislead the immune system (Betis *et al.*, 2003a, b; Sodhi *et al.*, 2004; Bergsten *et al.*, 2005; Sharma *et al.*, 2005a, b; Diard *et al.*, 2006; Cane *et al.*, 2007). Numerous applications of the organelles for the development of vaccines have been described (Eyles *et al.*, 2000; Langermann *et al.*, 2000; Strindelius *et al.*, 2004; Glynn *et al.*, 2005; Goluszko *et al.*, 2005; Powell *et al.*, 2005; Williamson *et al.*, 2005; Alvarez *et al.*, 2006; Elvin *et al.*, 2006; Honko *et al.*, 2006; Jones *et al.*, 2006; Lopes *et al.*, 2006; Santi *et al.*, 2006; Chichester *et al.*, 2009; Del Prete *et al.*, 2009; Hu *et al.*, 2009; Remer *et al.*, 2009; Verdonck *et al.*, 2009). In addition, it has been demonstrated that adhesive domains of monoadhesins and the chaperone/usher assembly-translocation machinery are promising targets for new generations of antimicrobials that specifically inhibit adhesion (Wellens *et al.*, 2008) or interfere with the fimbrial adhesion assembly (Pinkner *et al.*, 2006; Aberg & Almqvist, 2007).

Although several excellent reviews have been published recently, they either focused on specialized aspects of the chaperone–usher assembly (Sauer *et al.*, 2004; Fronzes *et al.*, 2008) or covered the results of studies of only a particular chaperone–usher system (Waksman & Hultgren, 2009). Our previous review was also devoted only to FGL chaperone-assembled polyadhesins (Zavialov *et al.*, 2007). We believe that significant recent knowledge accumulated on different aspects of biogenesis of the superfamily of Gram-negative bacterial adhesins assembled via the classical chaperone/usher pathway and their medical applications require new analysis and generalizations. During this work, we found that a number of different types of subunits, of which the organelles are built up, strongly correlate with the length of the F1–G1 loop of chaperone proteins. Based on this, here, we suggest a novel function–structure classification of the superfamily of adhesive organelles assembled via the classical chaperone/usher machinery.

General properties of adhesive organelles

Adhesive organelles assembled via the classical chaperone/usher machinery are found in Gram-negative bacteria, primarily in genera *Escherichia*, *Klebsiella*, *Photorhabdus*, *Proteus*, *Salmonella* and *Yersinia* of *Enterobacteriaceae*. The organelles are also found in species from genera *Bordetella* of *Alcaligenaceae*, *Hemophilus* of *Pasteurellaceae* family, *Pseudomonas* of *Pseudomonadaceae* family and *Acinetobacter* of *Moraxellaceae*. These bacteria cause various diseases including fatal systemic diseases, such as bubonic and pneumonic plague (*Yersinia pestis*), enteric typhoid fever (*Salmonella typhi* and *Salmonella paratyphi A*), sepsis or extraintestinal focal infections (*Salmonella choleraesuis*), gastroenteritis (*Yersinia pseudotuberculosis*, *Salmonella typhimurium* and *Salmonella enteritidis*), pyelonephritis, cystitis, diarrhea (different pathogenic *E. coli* strains and *Proteus mirabilis*), whooping cough (*B. pertussis*), Brazilian purpuric fever, meningitis, otitis media (*Hemophilus influenzae*), pneumonia (*Klebsiella pneumoniae*), insect infections (*Photorhabdus temperata*) and plant infections (*Pseudomonas syringae*).

Table 1 describes the assembly-assisting proteins, species distribution and associated diseases for 50 currently known adhesive organelles, whose assembly on the bacterial surface has been confirmed experimentally and which is assisted by the classical chaperone/usher machinery. The information is in alphabetical order of the names of the chaperone/usher proteins.

Gene clusters encoding for adhesive organelles

Genes of proteins involved in the expression and assembly of adhesive fibers via the classical chaperone/usher pathway are arranged into compact gene clusters, which are located either on the chromosome or on the plasmids of Gram-negative bacteria. Depending on the structural properties of periplasmic chaperones, they can be divided into two families:

(1) FGL chaperone-comprising gene clusters and

(2) FGS chaperone-comprising gene clusters.

FGL chaperone-comprising gene clusters

Encoded by the *caf* gene cluster fraction 1 (F1), capsular antigen from *Y. pestis* comprises aggregated high-molecular-weight linear polymers of a single subunit Caf1 (Zavialov *et al.*, 2002, 2003, 2005, 2007). The genes of the *caf* gene cluster, *caf1*, *caf1M*, *caf1A* and *caf1R*, encode, respectively, for Caf1 subunit, periplasmic chaperone Caf1M, an outer membrane assembler, the molecular usher Caf1A and the protein Caf1R regulating gene cluster transcription (Galyov *et al.*, 1990, 1991; Karlyshev *et al.*, 1992a, b, 1994).

The *psa* gene cluster from *Y. pestis* encodes proteins for expression and assembly of the fimbrial pH6 antigen comprising the high-molecular-weight polymer of the PsaA subunit (Lindler & Tall, 1993). PsaB functions as the periplasmic chaperone and PsaC as the molecular usher. Two additional proteins, PsaE and PsaF, have been shown to

Table 1. Adhesive fimbrial organelles assembled on the Gram-negative pathogen cell surface via the classical chaperone/usher pathway*

Organelle	Chaperone/usher	Bacterium	Disease	Reference(s)
Aggregative adherence fimbria II, AAF/II	AafD/C	*Escherichia coli*	Diarrhea	Elias *et al*. (1999)
ND	ACIAD0120/0121	*Acinetobacter* sp. strain ADP1	ND	Barbe *et al*. (2004); Gohl *et al*. (2006)
Thin pili, an external diameter of 2–3 nm	AcuD/C	*Acinetobacter* sp. strain BD413	ND	Barbe *et al*. (2004); Gohl *et al*. (2006)
Afimbrial adhesin, AFA-III	Afa-3B/C	*E. coli*	Diarrhea or cystitis	Garcia *et al*. (1994)
Afimbrial adhesin, AfaE-VIII	Afa-8B/C	*E. coli*	Diarrhea/septicemia	Lalioui & Le Bouguénec (2001)
AF/R1 pili	AfrC/B	*E. coli*	Diarrhea in rabbits	Cantey *et al*. (1999)
Aggregative adherence fimbria Type I, AAF-I	AggD/C	*E. coli*	Diarrhea	Savarino *et al*. (1994)
Aggregative adhesion fimbria type III, AAF-III	Agg-3D/C	*E. coli*	Diarrhea	Bernier *et al*. (2002)
Ambient-temperature fimbriae	AtfB/C	*Proteus mirabilis*	Urinary tract infections	Massad *et al*. (1996
Capsular F1 antigen	Caf1M/A	*Yersinia pestis*	Plague	Galyov *et al*. (1990, 1991); Karlyshev *et al*. (1992a, b, 1994)
Colonization factor-3, CS-3 fimbriae	CS3-E/D	*E. coli*	Diarrhea	Jalajakumar *et al*. (1989)
Colonization factor, CS6	CssC/D	*E. coli*	Diarrhea	Wolf *et al*. (1997)
CS12 fimbria	CswB/C	*E. coli*	Diarrhea	EMBL accession number Q9ALL0
CS31A capsule-like antigen	ClpE/D	*E. coli*	Diarrhea	Bertin *et al*. (1993)
F1845 (DaaE) fimbrial adhesin	DaaB/C	*E. coli*	Diarrhea	Bilge *et al*. (1989)
Diffuse adherence fibrillar adhesin	DafaB/C	*E. coli*	Diarrhea	Keller *et al*. (2002)
Dr hemagglutinin flexible fimbriae	DraB/C	*E. coli*	Pyelonephritis	Piątek *et al*. (2005); Servin (2005); Van Loy *et al*. (2002)
F17 pili	F17D/C	*E. coli*	Diarrhea	Lintermans *et al*. (1988)
987P fimbriae	FasB/D	*E. coli*	Diarrhea in piglets	Emmerth *et al*. (1999)
K99 pili	FaeE/D	*E. coli*	Neonatal diarrhea in calves, lambs, and piglets	Bakker *et al*. (1991)
K88 pili	FanE/D	*E. coli*	Neonatal diarrhea in piglets	Bakker *et al*. (1991)
Type 2 and 3 pili	FimB/C	*Bordetella pertussis*	Whooping cough	Willems *et al*. (1992)
Type 1 pili	FimC/D	*E. coli*	Cystitis	Jones *et al*. (1993)
F1C pili	FocC/D	*E. coli*	Cystitis	Riegman *et al*. (1990)
CS18 fimbriae	FotB/D	*E. coli*	Diarrhea	Honarvar *et al*. (2003)
Haemophilus influenzae biogroup aegyptius fimbriae	HafB/E	*H. influenzae*	Meningitis, Brazilian purpuric fever	Read *et al*. (1996)
H. influenzae fimbriae	HifB/C	*H. influenzae* type b	Otitis media	van Ham *et al*. (1994)
Afimbrial adhesin	LdaE	*E. coli*	Diarrhea	Scaletsky *et al*. (2005)
Long polar fimbriae	LpfB/C	*Salmonella typhimurium*	Gastroenteritis	Bäumler & Heffron (1995)
Mannose-resistant fimbriae	MrfD/C	*Photorhabdus temperata*	Insect pathogen	Meslet-Cladiere *et al*. (2004)
Type 3 fimbriae	MrkB	*Klebsiella pneumoniae*	Pneumonia	Allen *et al*. (1991)
Mannose-resistant/*Proteus*-like MR/P pili	MrpD/C	*P. mirabilis*	Nosocomial urinary tract infections	Bahrani & Mobley (1994)
Mucoid *Yersinia* factor, Myf fimbriae	MyfB/C	*Y. enterocolitica*	Enterocolitis	Iriarte & Cornelis, (1995)
Nonfimbrial adhesin, NFA-I	NfaE/C	*E. coli*	Urinary tract infections	Ahrens *et al*. (1993); Servin (2005)
P pili	PapD/C	*E. coli*	Pyelonephritis or cystitis	Marklund *et al*. (1992)
Pef pili	PefD/C	*S. typhimurium*	Gastroenteritis	Bäumler *et al*. (1996)
PMF pili	PmfC/D	*P. mirabilis*	Nosocomial urinary tract infections	Massad & Mobley (1994)
Fimbrial pH6 antigen	PsaB/C	*Y. pestis, Y. pseudotuberculosis*	Plague Gastroenteritis	Massad & Mobley (1994)

Table 1. Continued.

Organelle	Chaperone/usher	Bacterium	Disease	Reference(s)
Putative adhesin	PSPPH_A0063/ A0064	*Pseudomonas syringae*	Halo blight of bean	Joardar *et al*. (2005)
REPEC fimbriae	RalE/D	*E. coli*	Diarrhea in rabbits	Adams *et al*. (1997
Atypical fimbriae Saf	SafB/C	*S. typhimurium*	Gastroenteritis	Folkesson *et al*. (1999); McClelland *et al*. (2001)
Putative atypical fimbriae	SafB/C	*S. typhi*	Enteric typhoid fever	Deng *et al*. (2003)
Putative atypical fimbriae	SafB/C	*S. choleraesuis*	Sepsis, extraintestinal focal infections	Chiu *et al*. (2005)
Putative atypical fimbriae	SafB/C	*S. paratyphi A*	Enteric typhoid fever	McClelland *et al*. (2004)
Filamentous fimbriae-like structures SEF14/18	SefB/C	*S. enteritidis*	Gastroenteritis	Clouthier *et al*. (1993, 1994)
Putative fimbriae	SefB/C	*S. typhi*	Enteric typhoid fever	EMBL accession number A212T7
Putative fimbriae	SefB/C	*S. paratyphi A*	Enteric typhoid fever	McClelland *et al*. (2004)
S pili	SfaE/F	*E. coli*	Urinary tract infections	Dobrindt *et al*. (2001)
Sfp fimbriae	SfpD/C	*E. coli*	Diarrhea	Brunder *et al*. (2001)
Stf fimbriae	StfD/C	*S. typhimurium*	Systemic and fatal infection in inbred mice	Emmerth *et al*. (1999)

*The information is placed in alphabetical order of the names of chaperone/usher proteins.
Nondetected.

regulate the transcription of the *psaA* gene (Yang & Isberg, 1997). Another transcriptional regulator, RovA, interacts with the *psaE* and *psaA* promoter regions, suggesting that RovA is an upstream regulator of the *psa* gene cluster (Cathelyn *et al*., 2006). Identical *psa* gene clusters are present in *Y. pestis* and *Y. pseudotuberculosis* (Lindler & Tall, 1993).

Closely related to the *psa* gene cluster of *Y. pestis*, *Yersinia enterocolitica* contains *myf* encoding the Myf fimbriae, which are built up of MyfA subunits. The *psa* and *myf* clusters have a similar general organization. Moreover, proteins encoded by these gene clusters display a significant sequence similarity, suggesting that the pH6 antigen and Myf fibriae have a common function in the different species of *Yersinia*. Like PsaE and PsaF encoded by *psa*, the MyfE and MyfF proteins encoded by *myf* play a role in the regulation of cluster transcription (Iriarte & Cornelis, 1995).

The *cs-3* gene cluster from *E. coli* encodes for proteins for expression and assembly of the colonization factor-3 that forms CS-3 fimbriae comprising the high-molecular-weight polymer of the CS-3 subunit (Jalajakumar *et al*., 1989). CS3-E functions as the periplasmic chaperone and CS3-D as the molecular usher.

The *nfa* gene cluster from *E. coli* encodes proteins for the expression and assembly of the nonfimbrial adhesin, NFA-I, comprising the high-molecular-weight polymer of the NfaA subunit (Ahrens *et al*., 1993). NfaE functions as the periplasmic chaperone and NfaE as the molecular usher.

A group of *E. coli* gene clusters, *afa-3*, *afa-8*, *agg*, *aaf*, *agg-3*, *dafa*, *dra* and *daa*, which encode proteins for the expression and assembly of the afimbrial adhesins Afa-III and AfaE-VIII, the aggregative adherence fimbria type I, II and III (AAF/I, AAF/II and AAF-III), the diffuse adherence fibrillar adhesin (Dafa), the Dr hemagglutinin flexible fimbriae and the F1845 (DaaE) fimbrial adhesin, respectively, have a peculiar feature: each gene cluster encodes additional subunit D, for which an invasive function was suggested (putative invasin subunit; Jouve *et al*., 1997; Servin, 2005). DraE and AfaE-III adhesins may assemble into a flexible fiber, which provides the link between the usher at the outer membrane and the putative invasin subunit located at the tip of the fiber (Anderson *et al*., 2004a, b; Pettigrew *et al*., 2004). However, expression of DraD invasin subunit is independent of the DraC usher and DraE fimbrial subunit (Zalewska *et al*., 2005). In addition, polymerization of DraE fimbrial subunits into fimbrial structures does not require the expression of DraD. Recently, Zalewska-Piątek *et al*. (2008) showed that type II secretion in *E. coli* strain Dr^+ leads to DraD translocation to the bacterial cell surfaces. Very recently, Korotkova *et al*. (2008b) and Guignot *et al*. (2009) demonstrated that the DraD subunit is not required for β_1 integrin recruitment or bacterial internalization. Therefore, the function of D subunits is still in question.

The *Salmonella* spp. gene clusters *saf*, *sef*, *cs6-1* and *cs6-2*, which encode proteins for the expression and assembly of the atypical fimbriae Saf, the filamentous fimbriae-like structures SEF14/18 and the colonization factors CS6-1 and -2, respectively, have another common peculiar feature: all of these gene clusters encode two adhesin subunits. The SefB chaperone of *S. enteritidis* assists in the assembly of two

distinct cell-surface structures, SEF14 and SEF18, which are homopolymers of SefA and SefD subunits, respectively (Clouthier *et al.*, 1994). The CssC chaperone assists in assembling thin CS6 fibrillae, which are composed of two heterologous CssA and CssB subunits (Wolf *et al.*, 1997).

FGS chaperone-comprising gene clusters

Two gene clusters *atf* and *pef* that encode proteins for expression and assembly of the ambient-temperature fimbriae ATF of *P. mirabilis* (Massad *et al.*, 1996) and plasmid-encoded (PE) fimbriae of *S. typhimurium*, respectively, have a common peculiar feature: they encode only one structural subunit, which probably functions as an adhesin subunit. Recently, a cosmid carrying the *pef* operon was introduced into *E. coli* and expression of fimbrial filaments composed of PefA was confirmed by flow cytometry and immune-electron microscopy (Chessa *et al.*, 2008). PE fimbriae were purified from the surface of *E. coli* and the resulting preparation was shown to contain PefA as the sole major protein component. Binding of purified PE fimbriae to a glycan array suggested that this adhesin specifically binds the trisaccharide Galss1-4 (Fuca1-3) GlcNAc, also known as the Lewis X (Lex) blood group antigen.

The *aciad* gene cluster of *Acinetobacter* sp., strain ADP1 (Barbe *et al.*, 2004; Gohl *et al.*, 2006), encodes only one structural subunit, which may function as an adhesin subunit. This cluster contains genes for two periplasmic chaperones.

The gene clusters *f17a*, *acu* and *fim/fha* encode proteins for the expression and assembly of the F17 pili of *E. coli* (Lintermans *et al.*, 1988), thin pili of *Acinetobacter* sp., strain BD413 (Barbe *et al.*, 2004; Gohl *et al.*, 2006) and type II and III pili of *B. pertussis* (Willems *et al.*, 1992). They encode one structural and one adhesin subunit, which are exposed on the tip of pili.

The gene clusters *hif*, *haf*, *mrk*, *lpf* and *pmf* that encode proteins for the expression and assembly of the *H. influenzae* fimbriae (van Ham *et al.*, 1994), *H. influenzae* biogroup aegyptius fimbriae (Read *et al.*, 1996), *K. pneumoniae* type III fimbriae (Allen *et al.*, 1991), *S. typhimurium* long polar fimbriae (Bäumler & Heffron, 1995) and *P. mirabilis* PMF pili (Massad & Mobley, 1994) encode two structural subunits and one adhesive subunit, which is exposed on the tip of fimbriae.

The gene clusters *fas*, *csw* and *fot* that encode proteins for the expression and assembly of the 987P (Edwards *et al.*, 1996), CS12 (EMBL accession number Q9ALL0) and CS18 (Honarvar *et al.*, 2003) fimbriae of *E. coli* have a very unusual feature in that they encode three distinct chaperones that assist in the assembling of fibers composed of two structural subunits and one adhesive subunit exposed on the tip of fimbriae. For example, in the case of 987P fimbriae, the FasB was shown to be a periplasmic chaperone for the major fimbrial subunit, FasA (Edwards *et al.*, 1996). The periplasmic chaperone FasC specifically interacts and stabilizes the adhesin FasG (Edwards *et al.*, 1996). FasE, a chaperone-like protein, is also located in the periplasm and is required for optimal export of FasG and possibly for other subunits (Edwards *et al.*, 1996).

Two gene clusters *fos* and *stf*, which encode proteins for the expression and assembly of the F1C pili of *E. coli* (Riegman *et al.*, 1990) and Stf fimbriae of *S. typhimurium* (Emmerth *et al.*, 1999), encode three structural and one adhesin subunit exposed on the tip of fimbriae.

The gene clusters *fim*, *sfp*, *sfa* and *mrp* encode proteins for the expression and assembly of the type I pili of *E. coli* (Jones *et al.*, 1993), Sfp fimbriae of *E. coli* (Brunder *et al.*, 2001), S pili of *E. coli* (Dobrindt *et al.*, 2001) and mannose-resistant/*Proteus*-like MR/P pili of *P. mirabilis* (Bahrani & Mobley, 1994). They encode four structural subunits and one adhesin subunit, which is exposed on the tip of fimbriae.

The gene clusters *fan*, *lda*, *fae* and *ral* encode proteins for the expression and assembly of the F4 (K88), Lda and F5 (K99) thin flexible pili and rabbit-specific enteropathogenic *Escherichia coli* (REPEC) fimbriae of *E. coli*, respectively (Bakker *et al.*, 1991; Adams *et al.*, 1997; Scaletsky *et al.*, 2005). These pili/fimbriae consist of four or five subunits. However, F4 (K88), F5 (K99) and Lda pili do not display specialized adhesive domains on the tip of the pilus, but carry binding sites on their main structural subunit (FanH, FaeH and LdaH) (Bakker *et al.*, 1991; Scaletsky *et al.*, 2005). The overall arrangement of the *ral* gene cluster closely resembles that of the *fae* cluster, with homologous genes occupying the same relative position in each cluster. The *ral* cluster also has some of the more specific features of the *fae* cluster, such as the overlapping reading frames of the gene-encoded chaperone and usher and the apparent absence of promoters within the region carrying the structural genes (Adams *et al.*, 1997). This general similarity, together with the significant levels of homology exhibited by individual genes, makes it reasonable to propose functions for the *ral* gene products based on the known roles of their Fae counterparts. Thus, Adams *et al.* (1997) proposed that RalC, RalF and RalH are minor fimbrial subunits of the fimbrial structure, which is primarily composed of RalG, the major fimbrial subunit. The gene cluster *afr* encodes proteins for the expression and assembly of the *E. coli* AF/R1 pili (Cantey *et al.*, 1999). The subunits encoded by the *afr* gene cluster have the highest percentage amino acid identity with the subunits encoded by the *ral* cluster (Adams *et al.*, 1997).

The *mrf* and *pap* gene clusters that encode proteins for the expression and assembly of mannose-resistant fimbriae of *P. temperata* (Meslet-Cladiere *et al.*, 2004) and P pili of *E. coli* (Marklund *et al.*, 1992) have the most complex composition: they encode six structural and one adhesin subunit that is exposed on the tip of fimbriae.

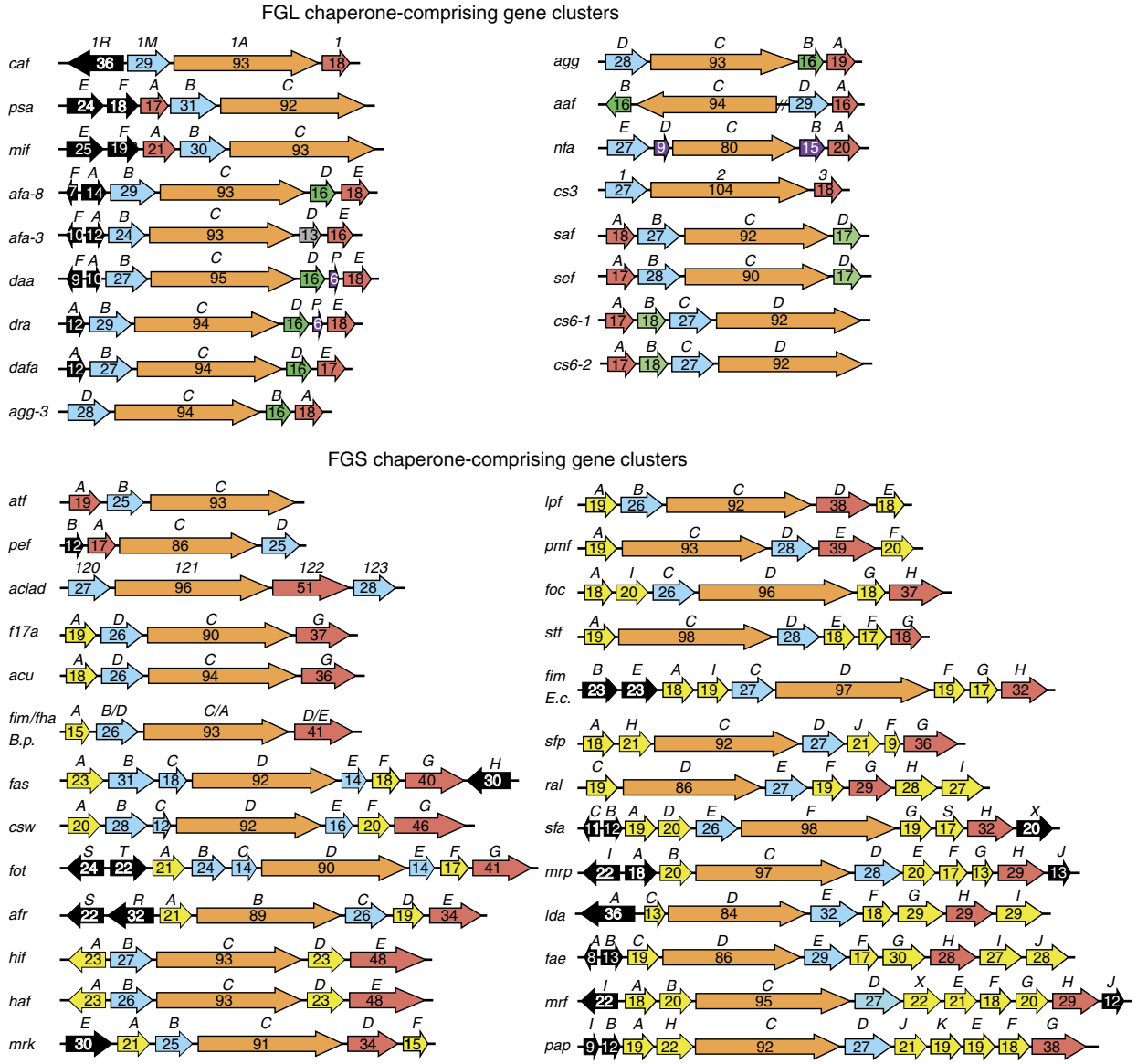

Fig. 1. General organization of gene clusters encoding adhesive organelles assembled with classical chaperone/usher machinery (elaborated by the authors). The genes encoding periplasmic chaperones and outer membrane ushers are blue and light orange, respectively. The genes encoding adhesin subunits, structural subunits and subunits with unknown function are red and yellow, respectively. The genes encoding regulatory proteins are black. The proteins with a putative function are green. The proteins with an unknown function are pink. The numbers designate a molecular weight of encoded protein in kDa.

Figure 1 shows the general organization of gene clusters for which the expression has been experimentally confirmed.

Structure and mechanism of the function of the chaperone/usher machinery

Molecular functions

Periplasmic chaperones and outer membrane molecular usher proteins function in cooperation as the chaperone/usher machinery that drives the assembly of surface-exposed fimbrial adhesins (Fig. 2).

Periplasmic chaperones possess the following main functions (Zav'yalov *et al.*, 1995b; Hung *et al.*, 1996; Thanassi *et al.*, 1998; Knight *et al.*, 2000; Sauer *et al.*, 2000, 2004; Zavialov *et al.*, 2001, 2003, 2005, 2007; Remaut *et al.*, 2006; Verger *et al.*, 2007; Zavialov & Knight, 2007):

(**1**) Binding to nascent subunits as they enter the periplasm via the Sec pathway.

(**2**) Protection of subunits from nonproductive aggregation and proteolytic degradation by capping their assembly surfaces.

(3) Transport of subunits to an outer membrane molecular usher.

Periplasmic chaperones either form stable complexes with subunits emerging to the periplasm or form dimers (PapD) (Hung *et al.*, 1999) or tetramers (Caf1M) (Zavialov & Knight, 2007), where the subunit-binding sequences are protected against proteolysis and unspecific binding (see 3D structure of chaperones).

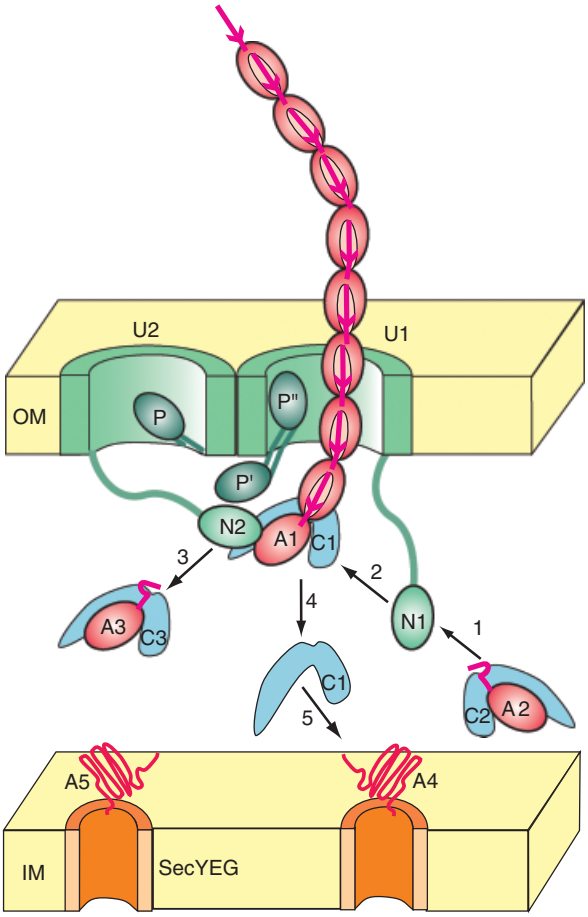

Fig. 2. General scheme of functioning of the chaperone/usher machinery that drives the formation of adhesive protein fibers on the bacterial surface. The subunits are connected in fiber by the 'donor strand complementation' (shown by red arrows). The fiber is secreted through the pore (illustrated by the split cylinder) in the outer membrane (OM) formed by the 'usher protein' (marked by letter U). N1 and N2 indicate the N-terminal domains of two different ushers (U1 and U2, respectively). Letter P indicates the position of the plug domain in U2, and P′ and P″ indicate two different positions of the plug domain in U1 for the two alternative models of gating. The free N1 recruits the C2:A2 complex (step 1), and bring the complex within proximity of the N2-bound C1–A1 complex (step 2). Donor-strand exchange then releases N2 for the recruitment of the C3–A3 complex (step 3) and releases C1 (step 4) for the recruitment of the next A4 subunit (step 5). The redrawing is based on the data published by Remaut *et al.* (2008).

Outer membrane molecular ushers possess the following main functions (Nishiyama *et al.*, 2005; Remaut *et al.*, 2006, 2008; Fronzes *et al.*, 2008; Yu *et al.*, 2009):
(1) release of a subunit from the chaperone;
(2) formation of an assembly platform for polymerization of subunits in linear fibers; and
(3) formation of a twinned-pore translocation machinery for secretion of linear fibers on the cell surface.

The recently decoded structure and proposed mechanism of the function of molecular usher proteins are described in Structure of outer membrane molecular usher proteins and Mechanism of function of the chaperone–usher machinery.

Structures of chaperones

3D structure of chaperones

For a long time, the PapD chaperone has been serving as a prototype protein for the superfamily of periplasmic chaperones (Holmgren & Branden, 1989). The PapD chaperone structure consists of two domains joined at an approximately right angle with a large cleft between the domains (Fig. 3). Both domains are seven-stranded β-sandwiches with an immunoglobulin-like topology (Holmgren & Branden, 1989). The F1 and G1 β-strands in the N-terminal domain of PapD are connected by a long and flexible loop that protrudes like a handle from the body of the domain.

Two families of the periplasmic chaperones were suggested with sequence analysis: FGS (having a short F1–G1 loop) and FGL (having a long F1–G1 loop) (Zav'yalov *et al.*, 1995a; Hung *et al.*, 1996) (Fig. 4). The PapD chaperone represents the FGS class of chaperones. High-resolution crystal structures for two FGL chaperones, Caf1M from *Y. pestis* and SafB from *S. typhimurium*, in complex with the corresponding subunits, Caf1 of the F1 capsular antigen and SafA of atypical fimbriae Saf, have been determined (Zavialov *et al.*, 2003, 2005; Remaut *et al.*, 2006). Like FGS chaperones (Holmgren & Branden, 1989; Choudhury *et al.*, 1999; Sauer *et al.*, 1999, 2002; Knight *et al.*, 2000; Verger *et al.*, 2007), FGL chaperones consist of two domains joined at an approximately right angle with a large cleft between the domains (Fig. 3). Both domains are seven-stranded β-sandwiches with an immunoglobulin-like topology (Zavialov *et al.*, 2003, 2005; Remaut *et al.*, 2006). The F1 and G1 β-strands in the N-terminal domain of Caf1M and SafB are connected by a flexible loop that is much longer than that in the PapD chaperone (Fig. 4).

When PapD is not engaged in binding to subunits, it is capable of interacting transiently with itself to form a weakly, but specifically bound dimer (Hung *et al.*, 1999). The crystal structures of two dimeric forms of PapD were solved to gain an insight into the molecular basis of PapD

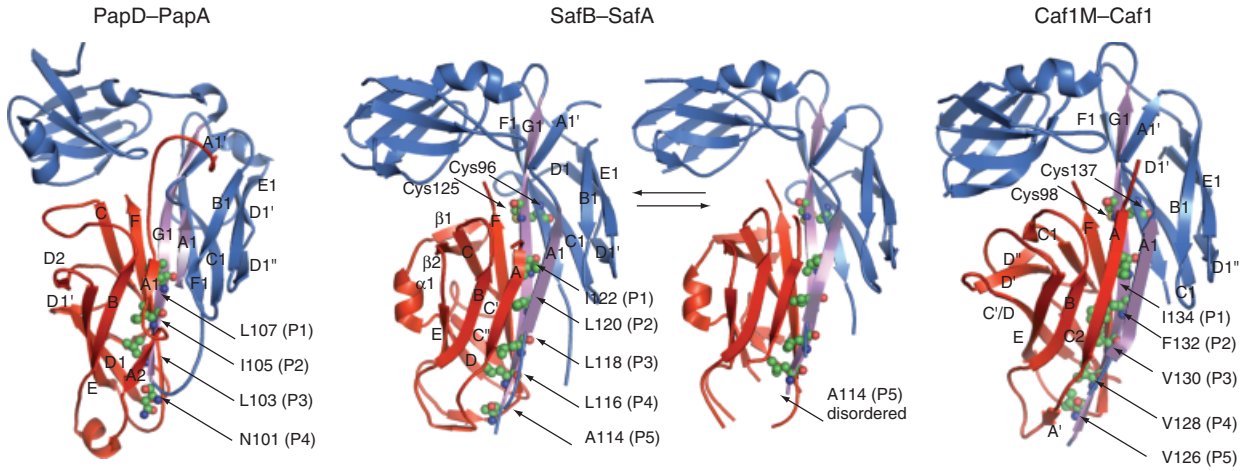

Fig. 3. Ribbon presentation of the crystal structures of PapD–PapA, SafB–SafA and Caf1M–Caf1 complexes. The chaperones are blue with G1 and A1 edge strands in violet; the subunits are red. The two conserved Cys residues in the whole FGL family that form disulfide bond are shown as ball-and-stick. The hydrophobic residues in the G1 strand of the chaperones that interact with the P5–P1 pockets of the subunits are also shown as ball-and-stick. The SafB residue A114, which interacts with the P5 pocket, is in equilibrium between a bound (left, type I structure) and an unbound (right, type II structure) state in the P5 pocket. The structures were redrawn based on the coordinates of atoms published by Remaut *et al.* (2006) (PDB accession numbers 2CO6 and 2CO7), Verger *et al.* (2007) (PDB accession number 2UY6) and Zavialov *et al.* (2003, 2005) (PDB accession number 1P5V). All figures were prepared with PYMOL (DeLano, 2002).

dimer formation (Hung *et al.*, 1999). The structure–function analysis revealed that PapD interacts with itself by means of the same interactive surfaces that it uses to bind subunits, possibly representing a self-capping mechanism that protects the subunit-binding sequences against proteolysis and unspecific binding.

Zavialov & Knight (2007) found that a typical representative of FGL chaperones, subunit-free Caf1M, exists predominantly as a tetramer. The 2.9 Å resolution crystal structure of the Caf1M tetramer revealed that each of the four molecules contributes to its subunit-binding sequences (the A1 and G1 strands) to form an eight-stranded hetero-sandwich with a well-packed phenylalanine-rich hydrophobic core (Zavialov & Knight, 2007). Tetramerization protects chaperone molecules against enzymatic proteolysis. Deletions in the subunit-binding motifs completely abolish tetramer assembly, suggesting that the hetero-sandwich is the main structural feature holding the tetramer together. Deletions in the VGVFVQFAI motif abolish both tetramer assembly and aggregation, consistent with the predicted high β-aggregation propensity for this motif. Such a packing of the aggregation-prone subunit-binding sequences into the hetero-domain is a novel molecular mechanism preventing unspecific aggregation of free chaperones.

The assembly of F4 fimbriae of ETEC indicates that self-capping of the pilin-interactive interfaces is not the mechanism that is consistently applied by all periplasmic chaperones, but is rather a case-specific solution to cap aggregation-prone surfaces (Van Molle *et al.*, 2009). FaeE crystal structure shows a dimer formed by an interaction between pilin-binding interfaces of two monomers. Thermodynamic and biochemical data show that FaeE occurs as a stable monomer in solution (Van Molle *et al.*, 2009).

Characteristic features of FGL and FGS chaperones

Comparison of structures of FGS and FGL chaperones reveals differences that appear to be located in functionally important segments. These class-specific differences were correctly predicted earlier based on sequence comparison and modeling using the known structure of the FGS chaperone PapD (Zav'yalov *et al.*, 1995b; Hung *et al.*, 1996; Chapman *et al.*, 1999) and functional studies (Zav'yalov *et al.*, 1997; Chapman *et al.*, 1999; MacIntyre *et al.*, 2001):

(1) FGL chaperones contain a significantly longer binding motif in the F1–G1 loop and the G1 β-strand than FGS chaperones, due to the extension of this motif into the F1–G1 loop region (typically by two hydrophobic alternating residues) (Fig. 4) (Zav'yalov *et al.*, 1995b; Hung *et al.*, 1996; MacIntyre *et al.*, 2001; Zavialov *et al.*, 2003, 2005; Remaut *et al.*, 2006).

(2) FGL chaperones also contain a longer binding motif at the N-terminus with three alternating bulky hydrophobic residues compared with that in FGS chaperones (two), which extends to the A1 strand in FGL chaperones (at least three residues) (Chapman *et al.*, 1999; Zavialov *et al.*, 2003, 2005, 2007; Remaut *et al.*, 2006).

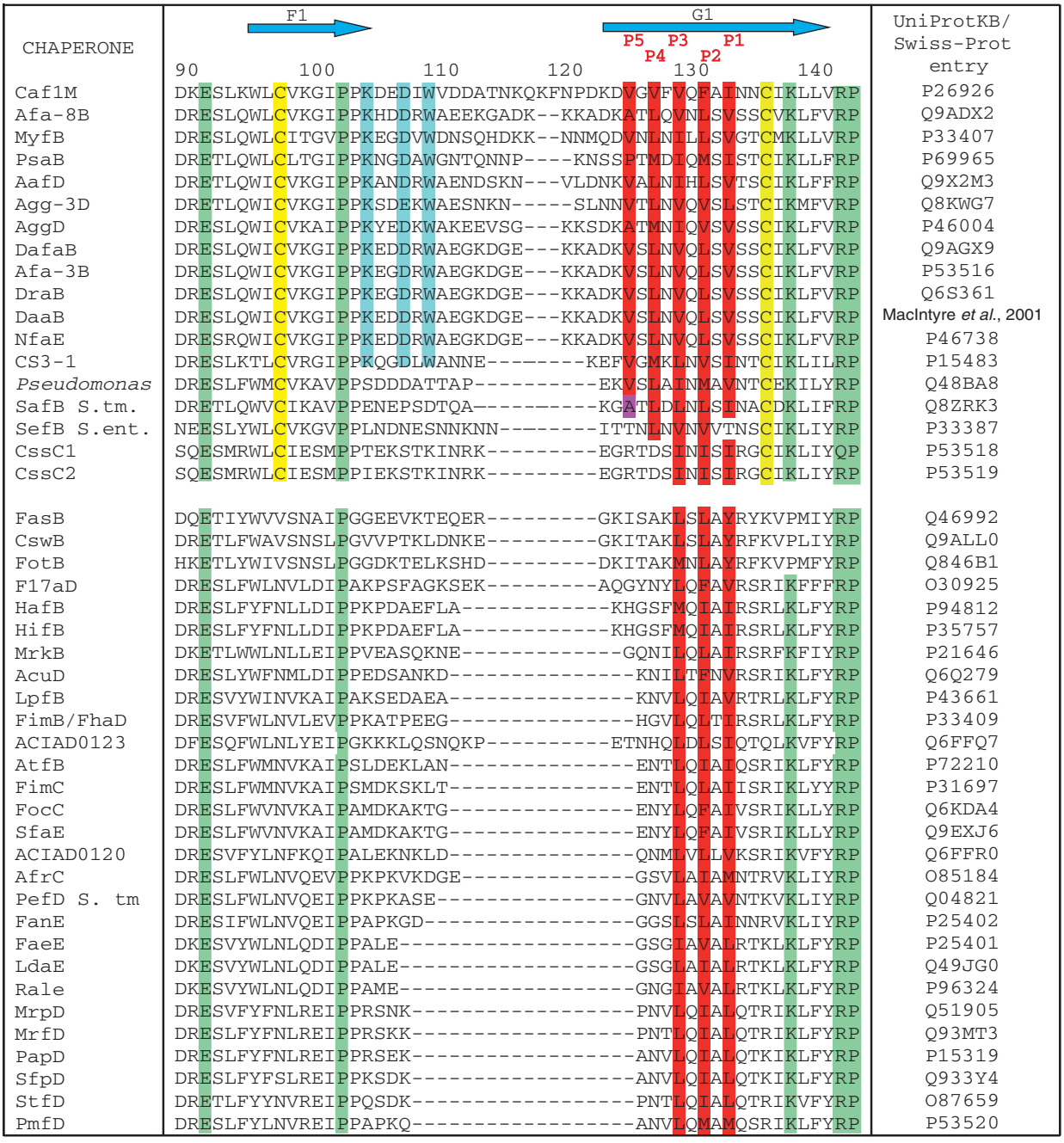

Fig. 4. Functionally important sequences of the chaperones assembling fimbrial adhesins via the chaperone/usher pathway (elaborated by the authors). Numbering in the CafM sequence is indicated. Conserved Cys residues involved in disulfide bond formation in the FGL chaperones are yellow. Other residues conserved in the whole superfamily are green, including subunit anchoring Lys, which is replaced by Pro in FasB, CswB and FotB operating only with adhesin subunits. Alternating bulky hydrophobic residues (from five to three in the FGL family, and three in the FGS family) extending from the beginning of the G1 β-strand are red. The conservative positions typical for the Caf1M-like subfamily of FGL chaperones are in cyan. F1 and G1 β-strands are shown by arrows (see Fig. 3 for details).

(3) In contrast to FGS chaperones, the massive subunit-binding hairpin F1 strand–loop–G1 strand of FGL chaperones is stabilized by a disulfide bridge between two conserved Cys-residues, one of which is localized in the F1 β-strand and the other in the G1 β-strand (Figs 3 and 4; C98 and C137 in Caf1M and C98 and C125 in SafB) (Zavialov *et al.*, 2003, 2005; Remaut *et al.*, 2006).

Biochemical and mutagenesis studies showed that the unique structural features of FGL chaperones are crucial for function.

Importance of the disulfide bond in the provision of FGL chaperone functions *in vitro* and *in vivo*

Reduction of the disulfide bond and alkylation of the cysteine residues in an FGL chaperone considerably increase the dissociation constant for the Caf1M–Caf1 complex (Zav'yalov *et al.*, 1997). Later, it was also shown that cysteine residues of FGL chaperone DraB form a disulfide bond and are crucial for the formation of the DraB–DraE binary complex (Piątek *et al.*, 2005). Probing of the conformation and stability of Caf1M at different temperatures, pH and concentration of urea by measurements of circular dichroism and fluorescence suggested that a disulfide bond does not affect the general conformation, but induces changes in the local structure around the bond (Zav'yalov *et al.*, 1997). However, the level of expression of Caf1M in *E. coli* was clearly affected by disulfide isomerase DsbA. Caf1M accumulated in considerably larger quantities in the $DsbA^+$ strain than in the $DsbA^-$ strain, suggesting an important role of the disulfide bond in the provision of Caf1M functions *in vivo* (MacIntyre *et al.*, 2001).

G1 and A1 β-strands are crucial for chaperone function

The studies of MacIntyre *et al.* (2001) highlighted the importance of G1 β-strand hydrophobic residues in protecting newly secreted Caf1 from proteolytic degradation. This could be explained in part by the observed importance of some residues (F132) in stabilizing the chaperone–subunit complex. However, the mutation, Caf1MV128A, which also resulted in subunit degradation, enhanced chaperone–subunit stability (A. Zavialov, pers. commun.). In contrast to FGS chaperones, the A1 β-strand of Caf1M also significantly adds to the binding contact in this region (Figs 3 and 6). Deletion of the sequence 10–15 of Caf1M in the A1 β-strand (A. Zavialov, pers. commun.) led to complete loss of the chaperone function. The structure of the Caf1M–Caf1 complex suggests that the chaperone A1 and G1 strands are likely to form a binding platform rigid enough to prevent collapse of the open subunit conformation in this very unstable region (Fig. 3).

Correlation between the length of the FG loop and the number of different types of subunits operated by the chaperones

Figure 6 shows the plot of the correlation between the number of deleted residues in the F1–G1 loop of chaperones (in comparison with the longest F1–G1 loop of the Caf1M chaperone) and the number of different types of subunits operated by the chaperones. These parameters show a strong correlation, but the slopes of the plots of correlation for FGL and FGS chaperones are different. This might be explained by an influence of the disulfide bond connecting F1 and G1 strands in FGLs. The coefficient of correlation for FGL chaperones is equal to 0.80 and 0.72 for FGS chaperones. The longer F1–G1 sequence creates a longer subunit recognition motif for a more specific binding of one or two subunits forming FGL chaperone-assembled fimbrial polyadhesins (Zavialov *et al.*, 2003, 2007). Probably, the shorter F1–G1 sequence in FGS chaperones evolved as a consequence of a need for less specific binding of subunits, as monoadhesive fimbriae/pili are composed of up to seven different subunits.

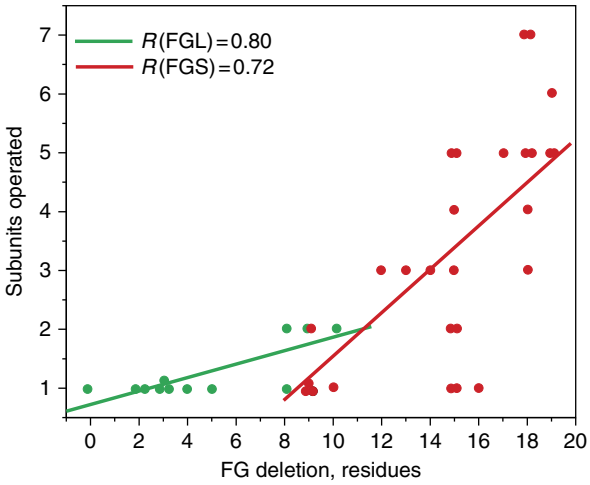

Fig. 5. Plot of correlation (elaborated by the authors) between the number of deleted residues in the F1–G1 loop in the chaperones (FG deletion in residues shown on abscissa) in comparison with the F1–G1 loop of the Caf1M chaperone and the number of different types of subunits operating by the chaperone (subunits operated shown on ordinate). The slopes of plots of correlation for FGL and FGS chaperones are different and are shown in green and red, correspondingly. The coefficient of correlation for FGL chaperones is equal to 0.80 and 0.72 for FGS chaperones.

Structure of subunits and the molecular architecture of adhesive organelles

3D structure of chaperone-complemented subunits

Chaperone-free subunits of fimbrial polyadhesins (Zav'yalov *et al.*, 1997; Zavialov *et al.*, 2005) and monoadhesive fimbriae/pili (Nishiyama *et al.*, 2003; Bann *et al.*, 2004) are highly unstable and prone to form aggregates. Hence, structural information on many subunits of these organelles was obtained by studying chaperone–subunit complexes (Choudhury *et al.*, 1999; Sauer *et al.*, 1999, 2002; Zavialov *et al.*, 2003, 2005; Remaut *et al.*, 2006; Verger *et al.*, 2007).

The crystal structures of the type I pilus FimC–FimH (Choudhury *et al.*, 1999) and the P pilus PapD–PapK,

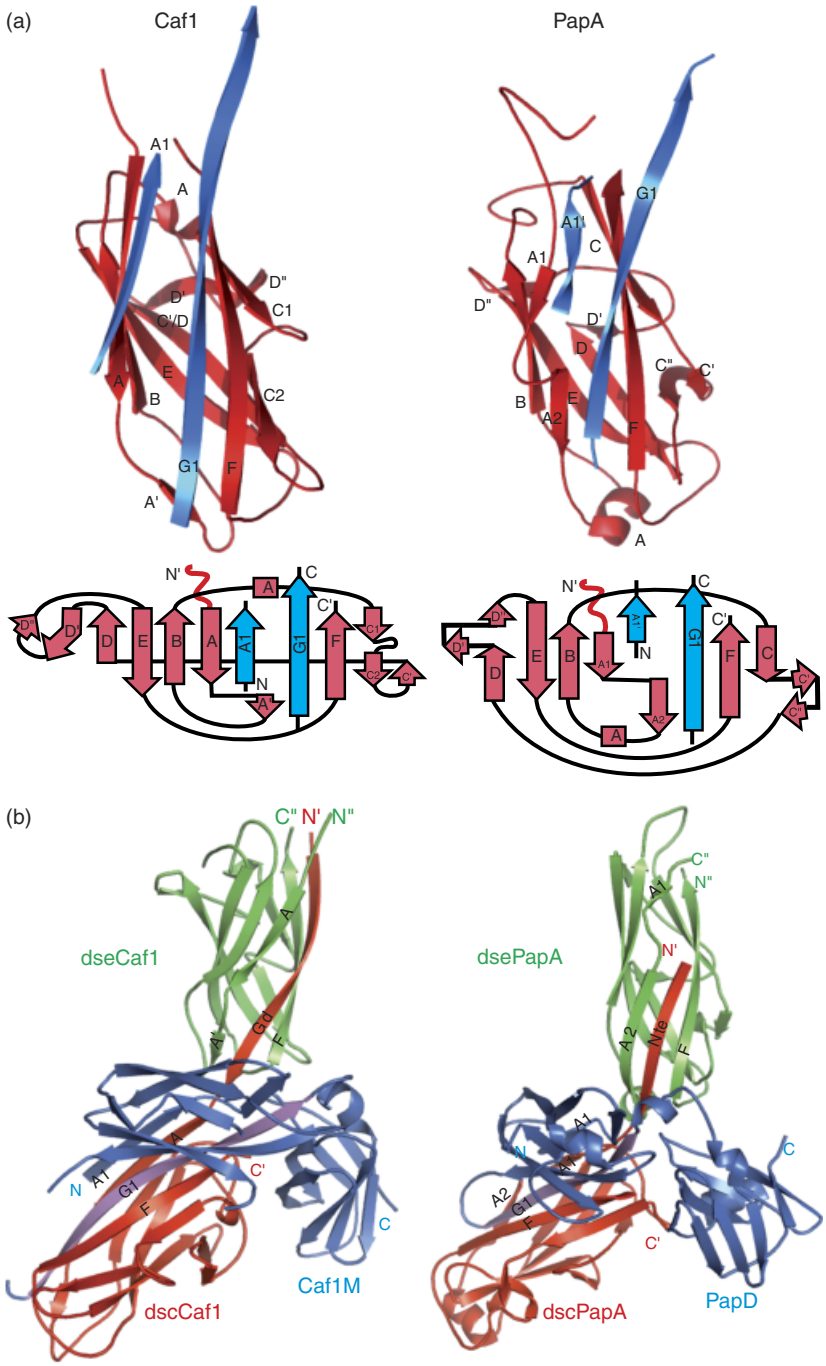

Fig. 6. (a) Comparison of the PapA pilin domain and Caf1 polyadhesin subunit complemented with chaperones. The PapA pilin domain and Caf1 polyadhesin subunit are shown in red with donor strands from PapD and Caf1M chaperone (blue). Only interacting chaperone–subunit strands are shown. (b) Ribbon diagrams of the native PapD–PapA′–PapA″ and Caf1M–Caf1′–Caf1″ complexes. Caf1M and PapD are blue, except for G1 and A1 β-strands (violet). The chaperone-bound Caf1′ and PapA′ subunits and N-terminal donor strands (Gd or Nte) are red; the Caf1″ and PapA″ subunits corresponding to the tip of growing fibers are green. The N- and C-termini are labeled in the same colours as the ribbons. The redrawing is based on the coordinates of atoms of structures published by Verger *et al*. (2007) (PDB accession number 2UY6) and Zavialov *et al*. (2003, 2005) (PDB accession numbers 1P5V and 1Z9S).

PapD–PapE and PapD–PapA (Sauer *et al*., 1999, 2002; Verger *et al*., 2007) chaperone–subunit complexes show that pilus subunits (pilins), like chaperones, have immunoglobulin-like folds (Figs 3 and 5). However, the C-terminal (G) β-strand of the fold is missing, creating a deep hydrophobic groove on the surface of the subunit (Figs 3 and 5). Chaperones bind pilins by inserting their G1 β-strand into this groove in a process called donor-strand complementation (Choudhury *et al*., 1999; Sauer *et al*., 1999, 2002; Verger *et al*., 2007) (Figs 3 and 5). Three hydrophobic side chains in the conserved G1 motif are inserted into the hydrophobic acceptor groove and become an integral part of the subunit hydrophobic core.

The crystal structures of the Caf1M–Caf1 and SafB–SafA chaperone–subunit complexes reveal the chaperone-bound conformation of FGL chaperone-assembled polyadhesin subunits (Zavialov *et al*., 2003, 2005; Remaut *et al*., 2006). As pilins, the polyadhesin subunits Caf1 and SafA have an

incomplete immunoglobulin-like fold (Figs 3 and 5). Despite the lack of significant sequence similarity, polyadhesin subunits and pilins display similar organization of the B, C, E and F β-strands (Fig. 5a), which are known to form a common structural core of the immunoglobulin-like fold (Bork *et al.*, 1994). However, the β-strand A has different structures. In pilins, the β-strand A starts hydrogen bonding to the β-strand B, participating in the formation of the ABED β-sheet; it then makes a switch in the middle and continues as part of the A'G1FC β-sheet (Fig. 5a). In polyadhesin subunits, the A β-strand either switches very late (in Caf1) or becomes disordered (in SafA). A region between C and E β-strands shows a large structural variability for both pilus and polyadhesin subunits (Fig. 5a). Pilins tend to have a larger loop between the β-strands D″ and E. Polyadhesin subunits have considerably longer sequences that are involved in the region between the β-strands C and D″. This region is clearly more structurally variable in polyadhesin subunits than in pilins and it might potentially participate in the formation of binding sites and organelle-specific epitopes (see 'Binding of polyadhesins to host-cell receptors and serum proteins').

The major differences between the two classes of subunits and corresponding chaperones are found in the chaperone–subunit interactive area. Figure 3 shows ribbon diagrams of the PapD–PapA (Verger *et al.*, 2007), SafB–SafA (Remaut *et al.*, 2006) and Caf1M–Caf1 (Zavialov *et al.*, 2003, 2005) complexes. The end of the F1–G1 loop and the beginning of the G1 β-strand in PapD harbor a four-residue subunit-binding motif of one small hydrophilic (N101) and three alternating bulky hydrophobic residues (L107, I105 and L103) (Verger *et al.*, 2007). The same region in the SafB molecule harbors a similar five-residue motif of one small hydrophobic (A114) and four bulky hydrophobic residues (L116, L118, L120 and I122) (Remaut *et al.*, 2006). The end of the F1–G1 loop and the beginning of the G1 β-strand in Caf1M harbor a subunit-binding motif of five alternating bulky hydrophobic residues (V126, V128, V130, F132 and I134) (Zavialov *et al.*, 2003, 2005). The rest of the F1–G1 loop (residues 96–102 in PapD, 104–113 in SafB and 104–123 in Caf1M) is disordered in the crystal structures. Another subunit-binding motif in FGL chaperones of three alternating hydrophobic residues (Y12 in Caf1M/F12 in SafB, V14 and I16) is localized in a long N-terminal sequence, which forms the A1 strand. A1 and G1 β-strands are the edge strands of the β-sandwich fold of the N-terminal domain. In the complex A1 and G1, β-strands are extended due to the partial ordering of the N-terminal sequence and the F1–G1 loop, respectively, to form a binding platform, exposing the hydrophobic residues of the binding motifs. In addition to this binding structure, PapD, Caf1M and SafB chaperones apply a pair of conserved positively charged residues (R8 and K112 in PapD, R20 and K127 in SafB, R20 and K139 in Caf1M) to bind subunits by anchoring their C-terminal carboxyl groups.

Figure 5a illustrates how the Caf1 subunit is complemented by the Caf1M chaperone (Zavialov *et al.*, 2003, 2005). The absence of the seventh (G) strand results in a six-stranded β-sandwich where the hydrophobic core of Caf1 is partially exposed in a long and deep hydrophobic groove. Caf1 interacts mainly with the N-terminal domain in Caf1M (Fig. 3). These two proteins bind via edge strands in Caf1 and in the N-terminal domain of Caf1M to form a closed barrel with a common core (Zavialov *et al.*, 2003). Strand G1 in Caf1M is hydrogen-bonded to strand F in Caf1. Chaperone A1 strand is hydrogen-bonded to subunit strand A. As in FGS chaperone–pilin complexes (Choudhury *et al.*, 1999; Sauer *et al.*, 1999, 2002; Verger *et al.*, 2007), hydrophobic residues from the Caf1M chaperone G1 strand are donated to the Caf1 subunit to compensate for the missing G strand (Figs 3 and 5). The longer G1 donor strand of the Caf1M chaperone inserts a motif of five bulky hydrophobic residues (P1–P5 residues; seeFigs 3 and 4) into five binding pockets in the hydrophobic groove of the Caf1 subunit (P1–P5 binding pockets). As a result, the acceptor groove of the Caf1 subunit is significantly longer than that in the pilus subunits (Fig. 5a). The longer A1 strand in Caf1M also interacts more extensively with the subunit compared with the A1 strand in FGS chaperone–pilin complexes.

The crystal structure of the SafB–SafA complex also shows a considerably larger interactive area between the chaperone and the subunit than that found in the FGS chaperone–pilin complexes (Fig. 3). As in the Caf1M–Caf1 complex, this is a result of the presence of a more extended hydrophobic groove in the SafA subunit than in pilus subunits, which is complemented by subunit-binding motifs of SafB containing the additional FGL-specific sequences. However, the major F1–G1–loop–G1 β-strand-binding motif of SafB contains four rather than five bulky hydrophobic residues (L116, L118, L120 and I122), which interact with the hydrophobic P4–P1 pockets of the subunit's groove. The fifth donor residue inserting into pocket P5 is a small A114. Two crystal forms of the SafB–SafA complex were observed that differ in the extent of ordering around A114 (Fig. 3) (Remaut *et al.*, 2006). In type I crystals, A114 is ordered and is inserted into the P5 pocket of the SafA subunit (Fig. 3). In type II crystals, this residue is disordered and does not insert into the P5 pocket (Fig. 3). As a result, the loops and secondary structure elements in the SafA subunit that form this P5 pocket are also disordered and are not observed in the electron density map. These two structures suggest an equilibrium between the two states of the SafB–SafA complex as a result of a weak binding of the chaperone G1 donor strand at the P5 site of the SafA-binding groove (Remaut *et al.*, 2006).

3D structure of fiber subunits

The elucidation of the crystal structure of *Y. pestis* F1 minimal fiber Caf1M–Caf1′–Caf1″ (ternary complex) was an important step in understanding the general principles of subunit assembly via the chaperone/usher pathway, revealing the fiber conformation of the organelle subunit (Caf1″) and subunit–subunit interactions in fibers (Zavialov *et al.*, 2003, 2005). The structure of Caf1M and the chaperone-bound Caf1′ subunit is virtually the same as in the Caf1M–Caf1 binary preassembling complex. However, in contrast to the disordered N-terminal region of Caf1 in binary complex, the N-terminal region of Caf1′ is ordered and forms an antiparallel donor β-strand interaction with the last (F) β-strand of the chaperone-free Caf1″ subunit (Fig. 5b). The donated strand produces a bona fide immunoglobulin-like topology in the fiber subunit. The N-terminal donor strand was denoted as 'Gd' (d for donor) because it plays the same structural role in the fiber as it does in the (C-terminal) G strand of the canonical immunoglobulin fold (Zavialov *et al.*, 2003). Thus, the release of the subunit from the chaperone–subunit complex and its incorporation into a growing fiber involves an exchange of G1 and A1 donor strands of the chaperone to the Gd strand of the neighboring subunit in the fiber. The replacement of the G1 strand by the Gd strand also involves a change of direction of the donor strand from parallel to antiparallel to the F β-strand of the subunit. This process was predicted earlier for FGS chaperone-assembled adhesive pili (Choudhury *et al.*, 1999; Sauer *et al.*, 1999) and for FGL chaperone-assembled polyadhesins (Zavialov *et al.*, 2002) and was termed 'donor-strand exchange.' A similar 'topological transition' (Sauer *et al.*, 2002) was also observed for the P pilus subunit PapE bound to a peptide designed to have the sequence of the proposed donor strand of the PapK subunit, suggesting that the donor-strand exchange takes place during assembly of both types of organelles.

Recently, the structure of a ternary complex of PapD bound to PapA (through donor-strand complementation) was solved (Verger *et al.*, 2007). The structure of this complex is shown in Fig. 5b. The structure provides a snapshot of PapA before and after donor-strand exchange. The PapD–PapA′–PapA″ complex is similar to the one obtained for the Caf system (Zavialov *et al.*, 2003, 2005). The core sheet structure of donor strand-exchanged PapA is in a closer conformation than that of donor strand-complemented PapA, as the β-strands on each side of the groove of donor strand-exchanged PapA are nearer to each other. Also, the '63–74' loop is ordered in donor strand-exchanged PapA and not in donor strand-complemented PapA, as this molecule is missing residues 70–73 in this region.

High-resolution structures of several other subunits of fimbrial polyadhesins, AfaE/DraE, DraD, DaaE and SafA, have been determined (Anderson *et al.*, 2004a, b; Cota *et al.*, 2004, 2006; Pettigrew *et al.*, 2004; Jedrzejczak *et al.*, 2006; Korotkova *et al.*, 2006b; Remaut *et al.*, 2006). Artificially engineered constructs were prepared to facilitate the structure determination in each of these studies. Structural information on the DaaE and AfaE/DraE subunits was obtained by structure determination of cytoplasm-assembled trimers of these subunits (Anderson *et al.*, 2004a; Pettigrew *et al.*, 2004; Korotkova *et al.*, 2006b; Remaut *et al.*, 2006). The crystal structures revealed that the trimers are connected together by a β-strand-swapping mechanism. Although non-native, the β-strand-swapping is similar to the donor-strand complementation. A different approach was chosen to determine an nuclear magnetic resonance (NMR) structure of a circularly permuted self-complemented AfaE subunit (Anderson *et al.*, 2004b). This construct contains the donor sequence fused at the C-terminus rather than at the N-terminus, which allows insertion of this self-complementing Gd strand into the acceptor groove, restoring the classical immunoglobulin-like fold. To determine the structure of the fiber form of the SafA subunit, the group of Gabriel Waksman (Remaut *et al.*, 2006) used the same technique that they used earlier for structure determination of PapE (Sauer *et al.*, 2002). SafA was cocrystallized with a peptide corresponding to the N-terminal sequence, which was predicted to form the donor strand. The biological relevance of the constructs used by Anderson *et al.* (2004b) and Remaut *et al.* (2006) in their structural studies relies on the correctness of the prediction of the donor sequence, which is not easy to prove. Hence, these structures may potentially contain errors. The self-complemented AfaE (Anderson *et al.*, 2004b) has a slightly distorted structure at the beginning of the donor strand, which makes it dissimilar to Caf1 and SafA subunits (authors' observation). Comparison with the crystal structure of the cytoplasm-assembled trimers of the same subunit suggests that this could be a result of changes introduced by the artificially engineered linker connecting the donor strand to the C-terminus of the subunit. Nevertheless, all these structures show a similar incomplete immunoglobulin-like fold for the subunits and suggests that subunit–subunit interactions in polyadhesin fibers involve N-terminal Gd donor-strand complementation.

The Caf1 polyadhesin subunit (Zavialov *et al.*, 2003, 2005) has a longer acceptor groove, which accommodates a longer Gd donor strand compared with the P pilus subunit PapA (Verger *et al.*, 2007) (Fig. 5b). This is in agreement with the observation of a more extended contact area between the FGL chaperone and the polyadhesin subunit in structures of Caf1M–Caf1 and SafB–SafA complexes compared with the contact area between the FGS chaperone and the pilus subunit in structures of FimC–FimH, PapD–PapK, PapD–PapE and PapD–PapA complexes (Choudhury *et al.*, 1999; Sauer *et al.*, 1999, 2002; Zavialov *et al.*, 2003, 2005; Verger *et al.*, 2007).

Chaperone preserves folding energy of subunit for driving fiber assembly

No energy input from external sources is required to convert periplasmic chaperone–subunit preassembly complexes to free chaperone and secreted fibers (Jacob-Dubuisson *et al.*, 1994), in spite of a much more extensive interface between a chaperone and a subunit than that between fiber subunits (Zavialov *et al.*, 2003). Some clues as to how the process can be energetically driven have been provided by structural studies (Sauer *et al.*, 2002; Zavialov *et al.*, 2003, 2005; Verger *et al.*, 2007). Comparison of a chaperone complemented (Caf1′) with a fiber subunit (Caf1″) revealed a large conformational difference (Zavialov *et al.*, 2003, 2005). The fiber conformation was referred to as the 'closed' or the 'condensed' conformation (Zavialov *et al.*, 2005). The observed difference between open and closed conformations, involving a rearrangement and condensation of the subunit hydrophobic core, suggested that periplasmic chaperones might trap subunits in a high-energy molten globule-like folding intermediate state (Zavialov *et al.*, 2003). A model was proposed in which release of the subunit, followed by Gd donor-strand complementation, allows folding to be completed, driving fiber formation (Zavialov *et al.*, 2003). In contrast to the bulky hydrophobic donor residues in the chaperone G1 donor strand, many smaller donor residues in the subunit N-terminal Gd donor segment do not intercalate between the two sheets of the subunit β-sandwich, allowing close contact between the two sheets (Zavialov *et al.*, 2003, 2005).

A significant stabilizing contribution from the final fine packing of the hydrophobic core of the subunit is suggested by the melting of the native ternary complex. The structurally observed complete collapse of the Gd-complemented fiber Caf1″ subunit results in a dramatic increase in enthalpy and transition temperature for melting the fiber module. Thermodynamic studies provide strong evidence for the hypothesis that collapse of the subunit hydrophobic core shifts the equilibrium toward fiber formation (Zavialov *et al.*, 2005).

Zip-in–zip-out mechanism of the donor-strand exchange

Zavialov *et al.* (2003) proposed a model for the usher-catalyzed fiber assembly involving a sequential concerted donor-strand exchange in which G1 is gradually replaced by Gd with a zip-in–zip-out mechanism. Remaut *et al.* (2006), using real-time electrospray ionization MS, detected a transient ternary complex between the chaperone–subunit complex and a peptide mimicking the donor strand of the subunit, providing experimental support for the hypothesis. Exchange of the donor strand of the chaperone to the peptide was highly dependent on the interactions at the P5 pocket of the subunit (Fig. 7). This site may recruit the incoming subunit donor strand. Indeed, the observation of two crystal forms with the SafB – SafA complex (Fig. 3) (Remaut *et al.*, 2006) suggests that the acceptor cleft of the SafA subunit could be easily uncapped at this site, providing a starting point for the donor-strand exchange.

Recently, Verger *et al.* (2008) solved the structure of the PapD–PapF complex to explain why PapF undergoes slow donor-strand exchange. The structure reveals that the PapF P5 pocket is partially obstructed. Molecular dynamic simulations show that this region of PapF is flexible compared with its equivalent in PapH, a subunit that also has an obstructed P5 pocket and is unable to undergo donor-strand exchange. Using electrospray ionization MS, Verger *et al.* (2008) showed that mutations in the P5 region result in increased donor-strand exchange rates. Thus, the partial obstruction of the P5 pocket serves as a modulating mechanism of donor-strand exchange.

Rose *et al.* (2008) used molecular dynamic simulations to probe the donor-strand exchange mechanism during the formation of the Saf pilus from *Salmonella enterica* at the atomic level, allowing the direct investigation of the zip-in–zip-out hypothesis. The simulations provide an explanation of how the incoming Gd is able to dock and initiate donor-strand exchange due to inherent dynamic fluctuations within the chaperone–subunit complex. In the simulations, the chaperone donor strand was seen to unbind from the pilus subunit, residue by residue, in direct support of the zip-in–zip-out hypothesis. In addition, an interaction of a residue toward the N-terminus of the Gd with a specific binding pocket on the adjacent pilus subunit was seen to stabilize the donor-strand exchange product against unbinding, which also proceeded in the simulations by a zippering mechanism. The study provides an in-depth picture of donor-strand exchange, including the first atomistic insights into the molecular events occurring during the zip-in–zip-out mechanism. Figure 7 schematically presents the donor-strand exchange mechanism *in vivo* based on the experimental data obtained *in vitro* by Remaut *et al.* (2006).

Zavialov *et al.* (2005) and Vitagliano *et al.* (2008) reported molecular dynamic characterizations of the *Y. pestis* Caf1 subunit in its monomeric-unbound and dimeric states. Data on the properties of the monomeric form show that it is highly reactive and tends to evolve toward compact states, which likely hamper the subunit–subunit association. The chaperone release and subunit–subunit association evidently take place in concert.

Molecular architecture of adhesive organelles

The final architecture and morphology of linear fibers depend on the subunit composition and the mode of subunit–subunit interactions. These factors determine the

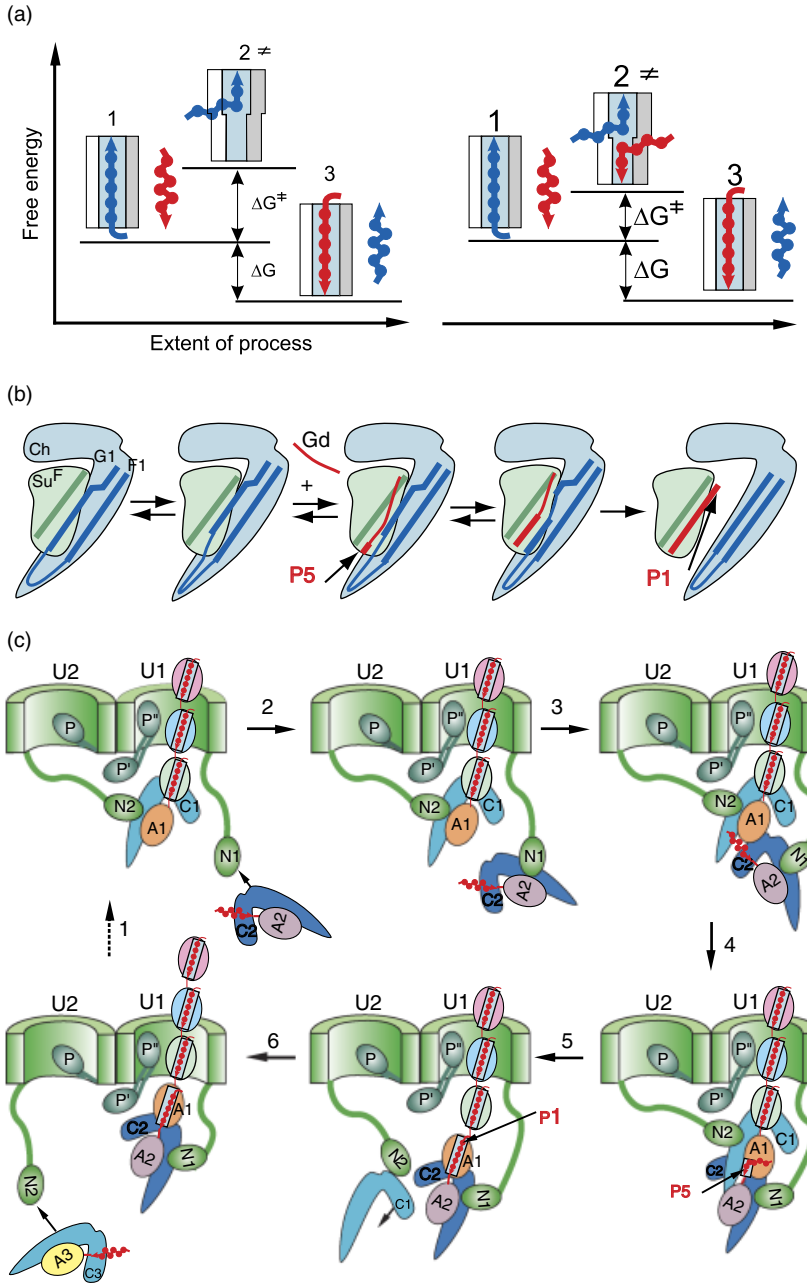

Fig. 7. Model for the mechanism of donor-strand exchange (DSE) *in vitro* and *in vivo*. (a) Models for usher-catalyzed assembly proposed by Zavialov *et al.* (2003). Left image: stepwise DSE in which the entire G1 donor strand is removed before the Gd strand is bound. Right image: sequential concerted DSE in which G1 is gradually replaced by Gd in a zip-in–zip-out mechanism. (1 and 3) Crystallographically observed chaperone–subunit and subunit–subunit structures, respectively. (2) Imaginary structures. DG corresponds to the free energy for fiber formation from chaperone–subunit assembly complex and must necessarily be 0. Values for the different free energy terms are not known, and the figure is not meant to indicate even relative sizes of these terms. (b) Schematic presentation of DSE *in vitro* based on the experimental data (Remaut *et al.*, 2006). Chaperone (Ch) and subunit (Su) are labeled in light blue and light green, respectively. In the chaperone, strands G1 and F1 are presented as solid dark blue lines. In the subunit, strand F, which directly interacts with the G1 donor strand, is depicted in dark green. An incoming N-terminal Gd donor strand (depicted in red) forms a ternary complex with the chaperone–subunit complex at the P5 pocket (indicated by a thicker line). DSE then proceeds and terminates by dissociation of the chaperone–subunit complex and insertion of the P1 residue in the P1 pocket. (c) Schematic representation of a single incorporation cycle at the usher. Chaperone and usher are shown light blue and light orange, respectively. For clarity, subunits are differentiated by color with the incoming subunit in light cyan. The N-terminal and C-terminal domains of the usher are indicated. Redrawing based on Zavialov *et al.* (2003), Remaut *et al.* (2006, 2008) and Fronzes *et al.* (2008).

coiling of secreted linear fibers into different structures such as FGS chaperone-assembled thick rigid monoadhesive pili with a diameter of 7–8 nm (Fig. 8a) (reviewed in Thanassi *et al.*, 1998; Soto & Hultgren, 1999; Knight *et al.*, 2000; Sauer *et al.*, 2000, 2004), FGS chaperone-assembled thin flexible hetero-polyadhesins with a diameter of 2–4 nm (Fig. 8b) (reviewed in van den Broeck *et al.*, 2000), FGS chaperone-assembled homo-polyadhesins with a diameter of about 2 nm (Fig. 8c) (Chessa *et al.*, 2008) and FGL chaperone-assembled polyadhesins with a diameter of about 2 nm (Fig. 8d) (Zavialov *et al.*, 2007). The latter polyadhesins can aggregate to form amorphous masses or capsules, for example the F1 capsular antigen (Chen & Elberg, 1977), NFA-I (Ahrens *et al.*, 1993), NFA-I-like Dr-II (Pham *et al.*, 1997) or afimbrial adhesins III, VII and VIII (Jouve *et al.*, 1997; Lalioui *et al.*, 1999).

In the case of FGS chaperone-assembled monoadhesive fimbriae/pili, the specialized adhesive subunit always occurs at the tip of fimbriae, either as the distal end of thin (~2.5 nm) and flexible fimbriae (e.g. F17G from F17 fimbriae) or at the edge of a thin (~2.5 nm) tip fibrillum that is stuck onto a relatively rigid, 1–2-mm-long and ~7.5-nm-wide

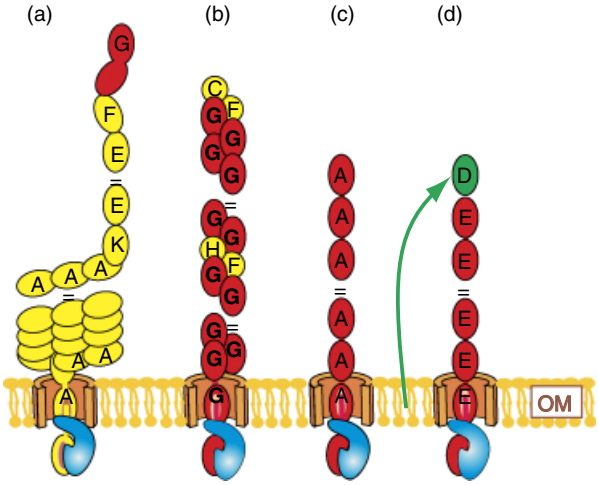

Fig. 8. (a) Schematic presentation (elaborated by the authors) of the structure of FGS chaperone-assembled thick rigid monoadhesive fimbriae/pili (P pili as example) (Sauer *et al.*, 2000, 2004), (b) FGS chaperone-assembled hetero-polyadhesins (F4, K88 pili as example) (van den Broeck *et al.*, 2000), (c) FGS chaperone-assembled homo-polyadhesins (PE fimbriae as example) (Chessa *et al.*, 2008) and (d) FGL chaperone-assembled polyadhesins (AfaE polyadhesin as example) (Anderson *et al.*, 2004a). Periplasmic chaperones and outer membrane ushers are in blue and light orange, respectively. Adhesin subunits are in red. Structural subunits are in yellow. Green arrow shows chaperone/usher-independent secretion of AfaD subunit (shown in green) via type II secretion system (Zalewska-Piątek *et al.*, 2008) and its potential display on the tip of the AfaE fimbrial polyadhesin (Anderson *et al.*, 2004a).

right-handed helical pilus rod (e.g. PapG of P pili and FimH of type I pili) (Fig. 8a) (de Greve *et al.*, 2007). This specialized subunit is called an adhesin.

All adhesive subunits of monoadhesive fimbriae/pili are two-domain adhesins (Choudhury *et al.*, 1999; Bouckaert *et al.*, 2005, 2006; Westerlund-Wikström & Korhonen, 2005; de Greve *et al.*, 2007; Li *et al.*, 2007). A two-domain adhesin consists of an N-terminal receptor-binding domain that can be stably expressed on its own and a rather conserved C-terminal pilin domain. Both domains have an immunoglobulin-like fold and are joined via a short interdomain linker. The few known crystal structures of tip-located receptor-binding N-terminal adhesin domains of monoadhesive fimbriae/pili, PapGII, FimH and F17G/GafD, show that, despite little or no sequence identity, common to them all is an elongated β-barrel jelly-roll fold that contains the receptor-binding groove (Fig. 9) (Choudhury *et al.*, 1999; Bouckaert *et al.*, 2005, 2006; Westerlund-Wikström & Korhonen, 2005; de Greve *et al.*, 2007; Li *et al.*, 2007). The adhesin domains differ in disulfide patterns, the size and location of the ligand-binding groove, as well as in the mechanism of receptor binding. In particular, their glycan-binding sites have evolved in different locations onto this similar scaffold, and with distinct, highly specific binding properties.

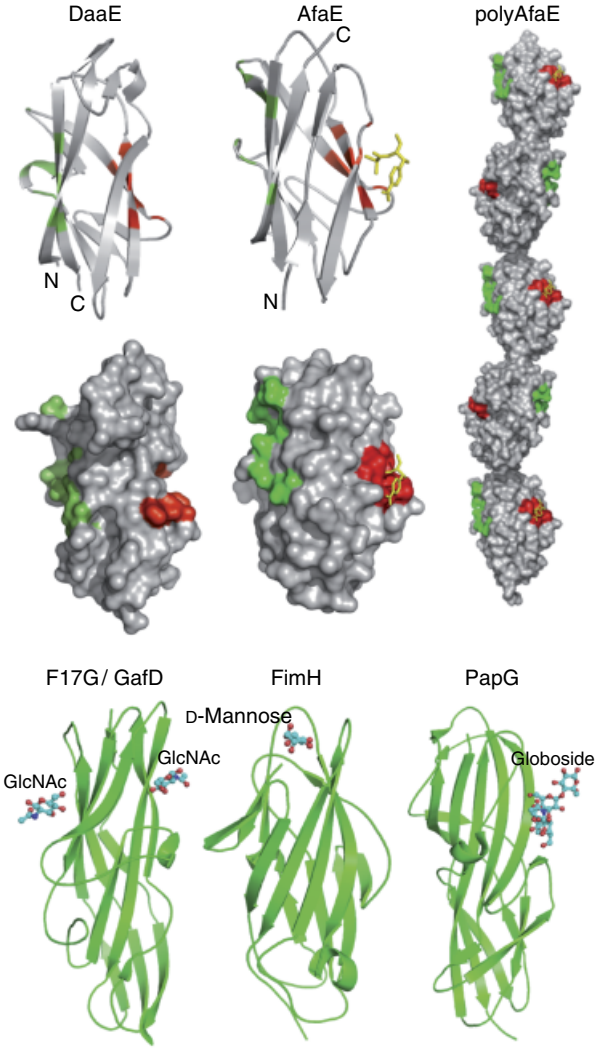

Fig. 9. Binding sites of FGL chaperone-assembled polyadhesins (DaaE and AfaE) and FGS chaperone-assembled monoadhesive fimbriae/pili (GafD/F17G, FimH and PapG). Ribbon diagrams and solvent-accessible surface presentations of the DaaE subunit of a strand-swapped trimer of wild-type DaaE of F1845 adhesin and a self-complemented AfaE subunit of AFA-III adhesin with chloramphenicol as a yellow stick presentation. CD55/DAF- and CEACAMS-binding sites derived from DraE and DaaE mutagenesis are shown in green and red, respectively. Molecular surface rendering of a model for the AfaE fiber was generated by assuming the same orientation between successive subunits as observed for Caf1′ and Caf1″ in the F1 fiber (Zavialov *et al.*, 2003). The residues involved in binding with CD55/DAF and CEACAMS are in green and red, respectively. Ribbon presentations are also given for adhesin domains of GafD/F17G (PDB accession number 1OIO), FimH (PDB accession number 1KLF) and PapG (PDB accession number 1J8R). Bound ligands, determined crystallographically, for GafD/F17G, FimH and PapG are also shown and labeled. The redrawing is based on the data and coordinates of atoms of the structures published by Anderson *et al.* (2004a, b), Korotkova *et al.* (2006a, b), Pettigrew *et al.* (2004) and Li *et al.* (2007).

Subunits of monoadhesive fimbriae are called pilins. In particular, P fimbriae are composed of ~1000 copies of the major subunit protein PapA, which polymerize to form a

rigid stalk connected to a flexible tip consisting of limited copies of the minor subunit proteins PapE and PapF and receptor-binding adhesin PapG at the distal end (Lindberg *et al.*, 1987; Kuehn *et al.*, 1992). Type I pili are composed of up to 3000 copies of the subunit FimA, which form a stiff, helical pilus rod, and subunits FimF, FimG and FimH, which form the linear tip fibrillum. All subunits in the pilus interact via the donor-strand complementation, in which the incomplete immunoglobulin-like fold of each subunit is complemented by insertion of an N-terminal extension from the following subunit. Gossert *et al.* (2008) determined the NMR structure of a monomeric, self-complemented variant of FimF, FimFF, which has a second FimF donor-strand segment fused to its C-terminus, enabling intramolecular complementation of the FimF fold. NMR studies on bimolecular complexes between FimFF and donor strand-depleted variants of FimF and FimG support the intrinsic flexibility of the tip fibrillum and indicate that this flexibility would significantly increase the probability that the adhesin at the distal end of the fibrillum successfully targets host-cell receptors. To determine whether the mechanical properties of the fimbrial rod regulate the stability of the FimH–mannose bond, Forero *et al.* (2006) pulled the fimbriae via a mannosylated tip of an atomic force microscope. Individual fimbriae rapidly elongate for up to 10 μm at forces > 60 pN and rapidly contract again at forces < 25 pN. At intermediate forces, fimbriae change length more slowly, and discrete 5.0 ± 0.3 nm changes in length can be observed, consistent with uncoiling and coiling of the helical quaternary structure of one FimA subunit at a time. The force range at which fimbriae are relatively stable in length is the same as the optimal force range at which FimH–mannose bonds live longest. Higher or lower forces, which cause shorter bond lifetimes, cause rapid length changes in the fimbria, which help maintain force at the optimal range to sustain the FimH–mannose interaction. The modulation of force and the rate at which it is transmitted from the bacterial cell to the adhesive catch bond present a novel physiological role for the fimbrial rod in bacterial host-cell adhesion. This suggests that the mechanical properties of the fimbrial shaft have codeveloped to optimize the stability of the terminal adhesion under flow.

In the case of FGL chaperone-assembled polyadhesins, all subunits may possess two independent binding sites specific to different host-cell receptors (Fig. 9; Anderson *et al.*, 2004a, b; Pettigrew *et al.*, 2004; Korotkova *et al.*, 2006a, b, 2008a, b). Dimensions of the bacterial polyadhesive fibers Dr, whose assembly is assisted by the FGL chaperone, were investigated with negative-stain electron microscopy (Anderson *et al.*, 2004a). Thin flexible fibers (2 nm diameter) were observed. The results are entirely consistent with the model with end-to-end contact between each subunit (Fig. 9) (Anderson *et al.*, 2004a) and are reminiscent of the model of capsular F1 antigen from *Y. pestis*, Caf1 (Zavialov *et al.*, 2003). Similar thin fibers have been observed for the pH6 antigen (Lindler & Tall, 1993). In addition to the predominance of thin fibers Dr, the electron microscopy also revealed a thicker morphology with overall dimensions larger than the linear model suggested (Anderson *et al.*, 2004a). Thick fibers are not consistent with end-to-end contact and imply that more extensive intersubunit interactions also exist. This would rigidify the resulting rod by the tighter coiling of a single fiber or formation of a trimeric coiled-coil arrangement of fibers.

Recently, Runco *et al.* (2008) examined the ultrastructure of the *Y. pestis* capsule with whole bacteria and negative-stain transmission electron microscopy. Bacteria were grown to the logarithmic phase at 37 °C, pH 7.4. The appearance of the capsule was more clearly visible than reported in previous studies, in which the capsule generally appeared as an amorphous haze or as a dense mass surrounding the bacteria (Chen & Elberg, 1977; Du *et al.*, 2002; Liu *et al.*, 2006). The *Y. pestis* KIM6$^+$ strain consistently produced an extended halo composed of thin fibrils and denser aggregates. This denser capsular material, likely composed of aggregates of the thin fibrils, sometimes extended out from the bacterial surface in long strands. The thin, fibrillar appearance of the F1 capsule resembles structures previously reported for other members of the FGL family of chaperone/usher pathways, including the pH6 antigen of *Yersinia* (Iriarte *et al.*, 1993; Lindler & Tall, 1993) and the CS3 and CS6 pili of ETEC (Levine *et al.*, 1984; Knutton *et al.*, 1989). This supports a common structure and assembly mechanism for members of the FGL family.

Salih *et al.* (2008) used negative-stain electron microscopy and single-particle image analysis to determine the 3D structure of the *S. typhimurium* Saf polyadhesin. The Saf polyadhesin comprises highly flexible linear multisubunit fibers that are formed by globular subunits connected to each other by short links, giving a 'beads on a string'-like appearance. Quantitative fitting of the atomic structure of the SafA polyadhesin subunit into the electron density maps, in combination with linker modeling and energy minimization, has enabled analysis of subunit arrangement and intersubunit interactions in the Saf polyadhesin. Short intersubunit linker regions provide the means for flexibility of the Saf polyadhesin by acting as molecular hinges that allow a large range of movement between consecutive subunits in the fiber.

Structure of outer membrane molecular usher proteins

3D structure of the outer membrane molecular usher protein

Recently, the 3.4 Å crystal structure of the 130–640-amino acid fragment of the PapC usher was solved. The results help

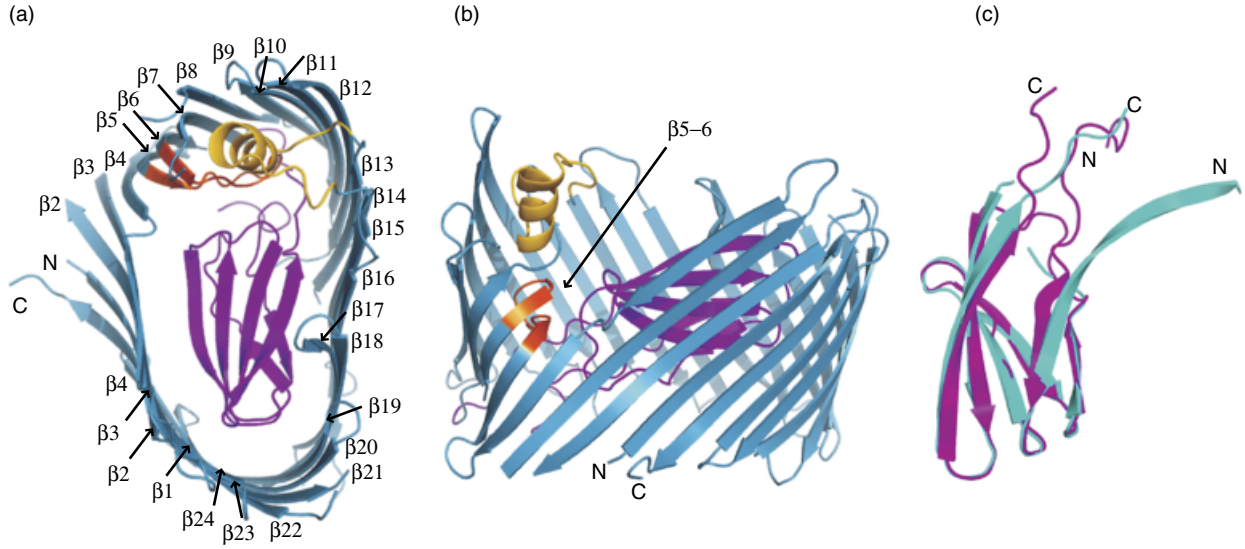

Fig. 10. (a) Ribbon presentation of the $PapC_{130–640}$ translocation channel (PDB accession number 2VQI) viewed from the extracellular side. The β-barrel, plug domain, β5–6 hairpin and helix α1 are colored blue, magenta, orange and yellow, respectively. β strands are labeled β1 through β24; the labels N and C indicate the N- and C-termini of the translocation channel. (b) Ribbon presentation of $PapC_{130–640}$ viewed from the side. Structural elements are colored as in (a). The N- and C-termini, helix α1, strand β4 and the β5–6 hairpin are labeled. (c) Structural superposition of the Caf1A plug domain (232–320-amino acid fragment of Caf1A; PDB accession number 3FCG) and the PapC plug domain (252–330-amino acid fragment of PapC; PDB accession number 2VQI). $Caf1A_{232-320}$ and $PapC_{252-330}$ are in magenta and cyan, respectively. β strands are labeled according to the immunoglobulin fold classification. N- and C-terminal ends of structured fragments are indicated. The structures are redrawn based on the coordinates of atoms published by Remaut *et al*. (2008) and Yu *et al*. (2009).

to understand adhesive fiber biogenesis at the outer membrane (Fronzes *et al*., 2008; Remaut *et al*., 2008). This fragment encompasses the full translocation pore consisting of a kidney-shaped, 24-stranded β-barrel (residues 146–635), 45 Å in height and with outer and inner dimensions of 65–45 and 45–25 Å, respectively (Fig. 10a and b). The β-barrel closes in an end-to-end fashion and positions the N- and C-termini on the periplasmic side of the outer membrane. The N- and C-terminal globular domains will thus be juxtaposed and reside in the periplasm, consistent with their role in chaperone–subunit recruitment and adhesin-induced pore activation (Saulino *et al*., 1998; Thanassi *et al*., 2002; Nishiyama *et al*., 2003; Ng *et al*., 2004). The predicted middle domain (residues 257–332) (Capitani *et al*. 2006) is formed by a long sequence between strands β6 and β7 and consists of a six-stranded, β sandwich fold (strands βA–βF). The domain is positioned laterally inside the β-barrel pore (Fig. 10a and b). As a result, the middle domain, referred to as the plug domain, completely occludes the luminal volume of the translocation pore, preventing passage of solutes or periplasmic proteins across the channel in its nonactivated form. The PapC plug domain is inserted into the loop connecting two β strands (strands 6 and 7). The plug domain is held in place by a β-hairpin (strands β5 and β6, hereafter referred to as the β5–6 hairpin), which is folded from the barrel wall into the channel lumen. The inward curvature of the β5–6 hairpin creates a large gap in the side of the β-barrel extending well into the part submerged in the outer membrane bilayer (Fig. 10a and b). The luminal part of the β5–6 hairpin is capped from the extracellular side by the only helix in the structure, the α1 helix (residues 448–465). Inside the β-barrel, the β5–6 hairpin interacts with the inner surface of the channel and helix α1 through a patch of hydrophobic interactions. In addition, the β5–6 hairpin forms two electrostatic interaction networks that bridge the plug domain with the channel wall and α1 helix and help position the plug domain laterally inside the translocation channel (Fig. 10a and b).

Mechanism of channel gating

In its nonactivated form, the PapC channel is obstructed by the plug domain (Figs 2 and 10). Therefore, the adhesive subunit-induced activation of the usher (Saulino *et al*., 1998) must include the displacement of the plug domain from the translocation channel. A rotation of the plug domain out of the pore lumen and into the periplasm would create a channel of 37×25 or 45×25 Å when the β5–6 hairpin and α1 helix are displaced from the channel as well (Fig. 2, position P′). Alternatively, a conformational change in the β5–6 hairpin and α1 helix could allow an upward rotation of the plug domain inside the pore, thereby

releasing a translocation channel of approximately 27 × 25 Å (Fig. 2, position P″). The outer membrane ushers function independent of a hydrolyzable energy source or a proton gradient (Jacob-Dubuisson *et al.*, 1994). Gating of the plug domain in the usher therefore relies solely on conformational changes induced by the binding of the chaperone–adhesin complex. Power for the large conformational rotation of the plug domain must therefore come from the energy emanating from the binding of the chaperone–adhesive subunit complex and/or must be stored as structural strains in the nonactivated PapC channel. One such area of apparent structural strain is seen in the β5–6 hairpin that breaks out of the β-barrel lining. The exposed part of the adjacent strand β4 represents a large open-edged β-sheet structure. Such exposed edges form highly aggregative surfaces for the edge-to-edge docking of β strands or β sheets (Richardson & Richardson, 2002). As part of the activation process, the β5–6 hairpin could line up with β4 in the barrel wall. This would break the interaction with the plug domain and allow its upward rotation or displacement out of the barrel lumen. Another area of structural strain could be the interaction of the plug domain with the barrel lumen, which includes a number of like-charge residues. It seems plausible that during activation, these repulsive forces will aid in expelling the plug domain from the barrel lumen.

Comparison of the isolated Caf1A plug domain with the structure of the corresponding domain of the PapC usher

Yu *et al.* (2009) reported the isolation and structural–functional characterization of the plug domain of Caf1A usher from *Y. pestis*. The isolated Caf1A plug domain is a highly soluble monomeric protein capable of autonomous folding. The 2.8 Å resolution crystal structure of the Caf1A plug domain reveals that this domain has an immunoglobulin-like fold similar to that of the donor-strand-complemented Caf1 fiber subunit. Moreover, these proteins display significant structural similarity. Although the Caf1A plug domain is in the middle of the predicted amphipathic β-barrel of Caf1A, the usher is still assembled in the membrane in the absence of this domain. The Caf1A plug domain does not bind Caf1M–Caf1 complexes, but its presence shows it to be essential for Caf1-fiber secretion. The study suggests that the Caf1A plug domain may play the role of a subunit-substituting protein (dummy subunit), plugging or priming secretion through the channel in the Caf1A usher. Comparison of the isolated Caf1A plug domain with the structure of the corresponding domain of the PapC usher (Fig. 10c) shows a high similarity of the core structures, suggesting a universal adaptation of FGL and FGS chaperone/usher pathways for the secretion of different types of fibers.

Mechanism of function of the chaperone–usher machinery

The N-terminal periplasmic domain of the usher protein binds the chaperone–subunit complex

Nishiyama *et al.* (2003) identified the N-terminal periplasmic domain of the FimD usher protein ($FimD_N$) comprising the N-terminal 139 residues of mature FimD. The purified $FimD_N$ usher domain is a monomeric, soluble protein that specifically recognizes complexes between the FimC chaperone and individual type I pilus subunits, but does not bind the isolated FimC chaperone or isolated subunits. In addition, the $FimD_N$ usher domain retains the ability of FimD usher protein to recognize different chaperone–subunit complexes with different affinities, and has the highest affinity toward the chaperone FimC–FimH adhesion complex. Overexpression of the $FimD_N$ usher domain in the periplasm of wild-type *E. coli* cells diminished incorporation of FimH adhesion at the tip of type I pili, whereas the pilus assembly itself was not affected. Nishiyama *et al.* (2003) reported NMR and X-ray protein structures of the $FimD_N$ usher domain before and after binding of a chaperone FimC–$FimH_P$ pilin domain complex. The $FimD_N$ usher domain consists of a flexible N-terminal segment of 24 residues (N-terminal 'tail'), a structured core with a novel fold and a C-terminal hinge segment (Fig. 11). In the ternary complex, residues 1–24 of the $FimD_N$ usher domain specifically interact with both the FimC chaperone and the $FimH_P$ pilin domain. The structures of the FimC chaperone and the $FimH_P$ pilin domain in the ternary complex closely resemble those in the previously published chaperone FimC–FimH adhesion binary complex (Choudhury *et al.*, 1999). Residues 1–24 of the N-terminal tail, which are completely unstructured in the free $FimD_N$ usher domain, become ordered upon complex formation and specifically interact with both the FimC chaperone and the bound $FimH_P$ pilin domain (Fig. 11; Nishiyama *et al.*, 2005). The interactions formed by the N-terminal $FimD_N$ usher domain tail constitute 60% of the total interface area of 1260 $Å^2$ between the $FimD_N$ (1–125) usher domain and the chaperone FimC–$FimH_P$ pilin domain complex. The other 40% of the contact area is contributed by the folded core $FimD_N$ (25–125) usher domain, which exhibits a complementary surface to the FimC chaperone. The N-terminal tail 1–24 of the $FimD_N$ usher domain thus serves as a sensor that selectively detects loaded FimC chaperone molecules. As the tail is the only $FimD_N$ usher domain region that forms contacts with the chaperone-bound subunit, it may be exclusively responsible for the discrimination of the different chaperone FimC–subunit complexes by the assembly platform (Saulino *et al.*, 1998). The FimD usher protein binds to different chaperone FimC–subunit complexes with

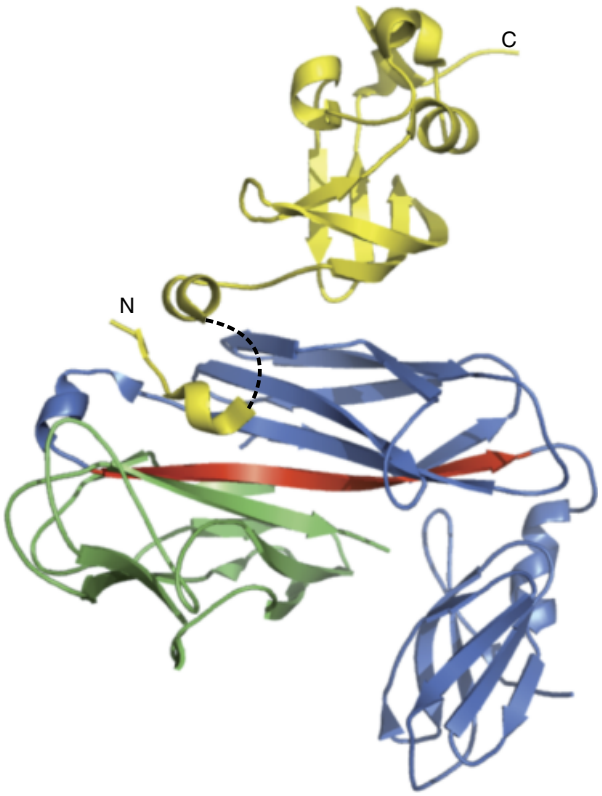

Fig. 11. X-ray structure of the ternary N-terminal usher domain $FimD_N$(1–125)–FimC chaperone–$FimH_P$ pilin complex. The ribbon diagram of the ternary complex is shown, with the $FimD_N$(1–125) N-terminal usher domain depicted in green, the FimC chaperone in cyan and the pilin domain $FimH_P$ in yellow. The G1 donor strand of the FimC chaperone is colored in blue. A black dashed line indicates residues 10–18 of the $FimD_N$ N-terminal usher domain, for which no electron density was observed. The N- and C-termini of the $FimD_N$ N-terminal usher domain are labeled in green. The structure is redrawn based on the coordinates of atoms published by Nishiyama *et al*. (2005) (PDB accession number 1ZE3).

different affinities, which is a key element for correct initiation of pilus assembly and for the correct ordering of the subunit incorporation into the pilus (Saulino *et al*., 1998; Nishiyama *et al*., 2003). In the case of the chaperone FimC–FimH adhesion complex, which is bound by the FimD usher protein with the highest affinity (Saulino *et al*., 1998), additional contacts between the FimH lectin domain and other FimD usher regions could contribute to binding, as the FimD usher protein has been shown to recognize the isolated FimH lectin domain (Barnhart *et al*., 2003), which is not bound by the $FimD_N$ usher domain (Nishiyama *et al*., 2003). The X-ray structure of the $FimD_N$ (1–125) usher domain–FimC chaperone–$FimH_P$ pilin domain complex thus predicts that the common element of the interactions of the $FimD_N$ usher domain with the four different chaperone FimC–subunit complexes is the contact area between the N-terminal FimC chaperone domain and the structured $FimD_N$ (25–125) usher domain. However, Nishiyama *et al*. (2005) assumed that this contact area by itself is sufficient neither for binding of the chaperone FimC–subunit complexes to the $FimD_N$ usher domain nor for stable binding of the free chaperone to the assembly platform (Saulino *et al*., 1998; Nishiyama *et al*., 2003). The fact that the FimC chaperone alone is not bound by the FimD usher ensures that the FimC chaperone is released into the periplasm for another reaction cycle as soon as the bound subunit dissociates from the ternary complex and is delivered to the translocation pore.

Twinned-pore model of the translocation machinery function

The type I pilus tip complex was analyzed by cryo-electron microscopy (Fronzes *et al*., 2008; Remaut *et al*., 2008). The available structural and biochemical data on the purified type I tip complex and PapC firmly establish that the outer membrane ushers function as dimers organized in twinned pores, which are the functional units for chaperone–usher pilus biogenesis (Li *et al*., 2004; So & Thanassi, 2006). The dimer interface in the 3D crystals is formed by the flat side of the kidney-shaped β-barrel, encompassing strands β11–β20 (residues 397–573; Fig. 10). The 3D cryo-electron microscopy reconstruction reveals that translocation of the polymerized subunits occurs asymmetrically and through only a single pore (usher 1; Fig. 2). The usher mediates the translocation of folded, polymerized protein units across the outer membrane (Sauer *et al*., 2002; Vetsch *et al*., 2004; Remaut *et al*., 2006). The width of the PapC translocation pore (inner diameter 45×25 Å) corresponds well with the passage of P pilus subunits in an upright orientation, along the length of the polymer (P pilus subunit dimensions are $55 \times 30 \times 25$, $57 \times 32 \times 23$ and $60 \times 27 \times 22$ Å for PapE [Protein Data Bank (PDB) accession number 1N12], PapK (PDB accession number 1PDK) and PapA (PDB accession number 2UY6), respectively (Sauer *et al*., 1999, 2002; Verger *et al*., 2007).

Integrated model for fiber assembly at the outer membrane molecular usher protein

Based on the cryo-electron microscopy data, Remaut *et al*. (2008) proposed a mechanism where the two ushers in the twinned pores cooperate in pilus polymerization by alternately recruiting new chaperone–subunit complexes through their N-terminal domains (Fig. 2). This mechanism provides a rationale for the known requirement of a dimeric usher complex: one usher provides the secretion channel, but two ushers are needed for successive rounds of subunit binding and fiber assembly. The structural information presented and the available biochemical background can be

combined into an integrated model for subunit recruitment, subunit polymerization and fiber translocation during pilus biogenesis at the outer membrane usher (Fig. 2). The structure of the Fim(D × 2)–C–F–G–H tip complex captures the fiber assembly process after FimH, FimG and FimF have assembled into a pilus tip. In this complex, the last incorporated chaperone–subunit complex (FimC–F) is bound to the N-terminal domain of usher pore 1. In the model, the next subunit to be incorporated into the fiber is recruited to the twinned pores through the N-terminal domain of usher 2 (step 1; Fig. 2). The N-terminal domain of the usher resides in the periplasm, tethered by a 20-residue flexible linker to the translocation pore. This spacer between the usher translocation pore and its N-terminal domain allows reorientation of the chaperone–subunit complex to a position where the N-terminal donor strand Gd of the newly recruited subunit is in proximity to the pilin domain of the previously recruited chaperone–subunit complex (bound to usher 1). This strand exchange reaction results in the release of the chaperone from the previously recruited chaperone–subunit complex and its dissociation from the N-terminal domain of usher 1; the usher lacks any detectable affinity for the chaperone when not in complex with the adhesin or a pilus subunit; Dodson *et al.*, 1993; Saulino *et al.*, 1998; Nishiyama *et al.*, 2003) (step 3; Fig. 2). Upon release of the chaperone, the subunit can enter the translocating pore of usher 1 and the N-terminal domain of usher 1 is free to bind a new chaperone–subunit complex from the periplasmic pool and bring it in proximity to the previously recruited chaperone–subunit complex for donor-strand exchange (steps 4 and 5; Fig. 2). In this way, iterations of the alternating recruitments of new chaperone–subunit complexes at the N-terminal domain of either usher, followed by donor-strand exchange with the previously assembled subunit, allow the stepwise polymerization and translocation of the pilus fiber (steps 5 and 6; Fig. 2).

The model for the chaperone–usher pilus assembly presented above incorporates all available biochemical data into the new structural framework. However, it does lack the usher C-terminal domain. Earlier studies in the P pilus system showed that the C-terminal domain of PapC is involved in the activation of the usher (So & Thanassi, 2006). From studies in type I pili, it is known that FimH recruitment triggers a conformational change in the usher required for its activation (Saulino *et al.*, 1998). This activation step depends on the presence of the FimH adhesin domain (Munera *et al.*, 2007). Remaut *et al.* (2008) proposed that, in its inactive state, the C-terminal domain (not shown in Fig. 2) is positioned at least partially under the PapC or the FimD channel and is in contact with the β5–6 hairpin and plug domain. This is consistent with cryo-electron microscopy data showing that in the absence of the C-terminal domain, the electron density within the channel is weaker (Li *et al.*, 2004). When the chaperone–adhesive subunit complex is recruited to the usher via the usher's N-terminal domain, a putative additional interaction between the adhesive subunit and the usher's C-terminal domain may relay a conformational change to the plug domain and the β5–6 hairpin and result in opening of the channel. Such an interaction has been observed between the PapC C-terminal domain and the PapD–G chaperone–adhesive subunit complex (So & Thanassi, 2006). As the FimD–tip complex captures a later stage of pilus biogenesis, a stage at which the twinned pores are already activated and the C-terminal domains may no longer be involved, it is not surprising that the C-terminal domains should not be seen. The C-terminal domains may lay idle, possibly tethered to a long linker (as for the N-terminal domain). However, further functional and structural work is needed to elucidate the role of the usher C-terminal domain and the mechanism of channel gating.

Functions of adhesive organelles assembled with the chaperone–usher machinery

Binding of bacterial adhesive organelles to host-cell receptors and serum proteins

Binding of polyadhesins to host-cell receptors and serum proteins

Afa/Dr polyadhesins

Dr, F1845 (DaaE), NFA-I and AfaE-III adhesins allow binding to the Dr^a blood-group antigen presented on the CD55/decay-accelerating factor (DAF), a complement-regulatory and signaling molecule (Nowicki *et al.*, 1988). Under physiological conditions, CD55/DAF plays a central role in preventing the amplification of the complement cascade on host-cell surfaces (Fujita *et al.*, 1987; Lublin & Atkinson, 1989). CD55/DAF interacts directly with membrane-bound C3b or C4b and prevents the subsequent uptake of C2 and factor B.

Human CD55/DAF is a cell-associated protein with an M_r of 55 000–70 000 depending on its glycosylation level. Membrane-bound CD55/DAF is attached to the cell surface membrane by a glycosylphosphatidylinositol anchor (Davitz *et al.*, 1986; Caras *et al.*, 1987) attached to a serine–threonine–proline-rich region, followed by four repeating domains (Carroll *et al.*, 1988; Rey-Campos *et al.*, 1988). They are currently known as complement control protein repeat (CCP) domains, and were originally known as short consensus repeats (Servin, 2005; Le Bouguénec & Servin, 2006). Removal of CCP-1 has no effect on CD55/DAF function, but individual deletion of CCP-2 and CCP-3 or

CCP-4 totally abolished it (Coyne *et al.*, 1992; Brodbeck *et al.*, 1996). Afa/Dr adhesins recognize CCP-3 on CD55/DAF (Nowicki *et al.*, 1993). Indeed, a single-point substitution in CCP-3 (Ser155 to Leu) causes complete abolition of adhesin binding to CD55/DAF (Nowicki *et al.*, 1993). Dr adhesin-binding and complement-regulating epitopes of CD55/DAF appear to be distinct and are approximately 20 Å apart (Hasan *et al.*, 2002). The amino acids Gly159, Tyr160 and Leu162 also aid in binding adhesin Dr, while residues Phe123 and Phe148 at the interface of CCP-2 and CCP-3, and also Phe154 in the CCP-3 cavity, are important in complement regulation.

An atomic resolution model for functions of AfaE-III adhesin revealed the pivotal role of CCP-2 and CCP-3 in binding of adhesins onto CD55/DAF (Anderson *et al.*, 2004a). At the same time, the residues of AfaE-III adhesin involved in CD55/DAF binding were localized (Fig. 9; Anderson *et al.*, 2004a). Like DraE, AfaE-III binds to CCP-2 and CCP-3, but CCP-3 contributes most to the free energy of binding. The binding regions for AfaE-III and the complement pathway convertases lie in close proximity to each other on CD55/DAF.

Binding of adhesin Dr to CD55/DAF is inhibited by chloramphenicol, whereas binding of AfaE-III is unaffected (Nowicki *et al.*, 1988; Westerlund *et al.*, 1989). This was used to locate the DraE adhesive site. The 3D structure of the strand-swapped trimer of wild-type DraE in complex with chloramphenicol was solved. NMR data supported the binding position of chloramphenicol within the crystal (Anderson *et al.*, 2004b; Pettigrew *et al.*, 2004). Chloramphenicol binds to a surface pocket between the N-terminal portion of strand B and the C-terminal portion of strand E and lies within the recently identified CD55/DAF-binding site (Fig. 9; Anderson *et al.*, 2004a). Recently, Pettigrew *et al.* (2009) reported X-ray structures of DraE bound to two chloramphenicol derivatives: chloramphenicol succinate (CLS) and bromamphenicol. The CLS structure demonstrates that acylation of the 3-hydroxyl group of CLM with succinyl does not significantly perturb the mode of binding, while the bromamphenicol structure implies that the binding pocket is able to accommodate bulkier substituents on the *N*-acyl group. It is concluded that modifications of the 3-hydroxyl group would generate a potent hemagglutinin Dr inhibitor that would not cause the toxic side effects that are associated with the normal bacteriostatic activity of CLM. Korotkova *et al.* (2006b) solved the 3D structure of DaaE at resolution 1.48 Å. Trimers of the protein were found in the crystal, as has been the case for other adhesins Dr. Naturally occurring variants and directed mutations in DaaE have been generated and analyzed for their ability to bind CD55/DAF. Mapping of the mutation sites onto the DaaE molecular structure shows that several of them contribute to a contiguous surface that is likely the primary CD55/DAF-binding site (Fig. 9).

Dr, F1845 (DaaE) and AfaE-III adhesins also interact with carcinoembryonic antigen (CEA)-related cellular adhesion molecules CEACAM1, CEACAM5 and CEACAM6 (Berger *et al.*, 2004). This recognition is followed by activation of CEACAMS-associated signaling by pathogens triggering the cellular events. CEACAM1, CEACAM5 and CEACAM6 belong to the immunoglobulin superfamily of adhesion molecules (Thompson *et al.*, 1991; Öbrink, 1997; Grunert & Kuroki, 1998; Hammarstrom, 1999). They share a conserved N-terminal immunoglobulin variable-like domain that is followed by three, six and two immunoglobulin constant-like domains, respectively. CEACAM1 is inserted into the cellular membrane via C-terminal transmembrane and cytoplasmic domains, whereas CEACAM5 and CEACAM6 have a glycosylphosphatidylinositol anchor. The CEACAMS family generally functions as intercellular adhesion molecules (Benchimol *et al.*, 1989), and could play a role in innate immunity (Fahlgren *et al.*, 2003). CEACAM1 has been shown to be expressed in leukocytes, including granulocytes, activated T cells, B cells and natural killer cells (Grunert & Kuroki, 1998). CEACAM1 acts as a novel class of immunoreceptor tyrosine-based inhibition motif-bearing regulatory molecules on T cells that are active during the early phases of the immune response in mice (Benchimol *et al.*, 1989; Kammerer *et al.*, 1998, 2001; Nakajima *et al.*, 2002; Fahlgren *et al.*, 2003). The intracytoplasmic domain, which contains two immunoreceptor tyrosine-based inhibition motif-like domains, is required for activation of a fraction of T cells in *Lamina propria* that express CEACAM1 by interleukin (IL)-7 and IL-15, indicating that CEACAM1 amplifies T-cell activation and thus could facilitate crosstalk between epithelial cells and T lymphocytes in the intestinal immune response (Donda *et al.*, 2000). The particular role of CEACAM1 in *Neisseria* pathogenicity has been documented. *Neisseria gonorrhoeae* evades host immunity by switching off T lymphocytes (Bradbury, 2002). In *N. gonorrhoeae*, the Opa_{52} protein is able to bind CEACAM1 expressed by primary $CD4^+$ T lymphocytes and to suppress their activation and proliferation after the Opa gonococcal protein associates with the tyrosine phosphatases SHP-1 and SHP-2 in the ITIM of CEACAM1 (Chen *et al.*, 2001; Boulton & Gray-Owen, 2002). Rougeaux *et al.* (2008) found that, as Opa, the adhesin Dr induces the Tyr-phosphorylation of ITIM and ITSM and the recruitment of Shp-2. The recent review by Nouvion & Beauchemin (2009) summarized multiple functions of CEACAM1. It was shown that this multifunctional protein plays a role in intercellular adhesion, as an inhibitor of tumor development, as a bacterial adhesin and as a receptor for the mouse hepatitis virus. Moreover, CEACAM1 is an active regulator of cell signaling, modulating the insulin or EGF receptor pathways in epithelial cells or the Zap-70 pathway in hematopoietic cells. The recent development of genetically modified mouse models

altering the *Ceacam1* gene corroborates most of these data, but also highlights the functional complexity of CEACAM1. Thus, in addition to the functions identified previously, CEACAM1 is an important regulator of lipid metabolism, of tumor progression as a regulator of the Wnt signaling pathway, of normal and tumor neo-angiogenesis and of immunity (Nouvion & Beauchemin, 2009).

Random mutagenesis with functional analysis and chemical shift mapping by NMR show a clear-cut CEACAMS-binding site located primarily in the A, B, E and D strands of the adhesin Dr subunit (Fig. 9; Korotkova *et al.*, 2006a). This site is located opposite the β-sheet encompassing the previously determined binding site for CD55/DAF, which implies that the polyadhesin Dr can bind simultaneously to both receptors on the epithelial cell surface. Recently, the structure of the CEA/Dr adhesin complex was proposed based on NMR spectroscopy and mutagenesis data in combination with biochemical characterization (Korotkova *et al.*, 2008a, b). The Dr adhesin/CEA interface overlaps appreciably with the region responsible for CEA dimerization. Binding kinetics, mutational analysis and spectroscopic examination of CEA dimers suggest that adhesins Dr can dissociate CEA dimers before the binding of monomeric forms (Korotkova *et al.*, 2008a, b).

Hemagglutinin Dr is unique in the Afa/Dr adhesin family because it binds specifically to the 7S domain (tetramer) of the basement membrane protein type IV collagen that is inhibited by the presence of chloramphenicol (Nowicki *et al.*, 1988; Westerlund *et al.*, 1989; Westerlund & Korhonen, 1993). Site-directed mutagenesis has been used to show that a negatively charged amino acid is required at position 54 of adhesive subunit Dr to confer chloramphenicol sensitivity of binding and that mutations at positions 32, 40, 54, 90 and 113 have different effects on type IV collagen binding and the chloramphenicol sensitivity of binding (Carnoy & Moseley, 1997). In particular, replacement of a single amino acid at position 113 of the DraE subunit results in loss of type IV collagen binding. Moreover, the two conserved Cys of the Afa/Dr family structural subunits form a disulfide bond, and mutations of these residues abolish both hemagglutination and binding to type IV collagen. Together with fibronectin, laminin, tenascin and heparin sulfate proteoglycans, type IV collagen is a component of the basement membrane, which is involved in complex interactions at the epithelial–mesenchymal interface. In particular, type IV collagen interacts with integrins expressed at the basal domain of polarized cells (Beaulieu, 1999) to form a link between the basement membrane and epithelial cells (Louvard *et al.*, 1992). However, during inflammation, deregulated expression of membrane-bound molecules that are normally segregated in the basolateral domain of polarized intestinal cells occurs, and it is possible that in this context, type IV collagen binding may contribute to the pathogenic action of Afa/Dr adhesins (Selvarangan *et al.*, 2004; Servin, 2005).

pH6 antigen

It was found that the pH6 antigen of *Y. pestis* is a novel bacterial immunoglobulin G (IgG)-binding receptor (Zav'yalov *et al.*, 1996). A pseudoimmune complex with human IgG1, IgG2 and IgG3 was formed. No binding to human IgG4, rabbit, mouse or sheep IgG was found. Antigen pH6 binds the human IgG1 Fc subunit and does not bind Fab and pFc′ subunits. This finding may be explained by pH6 antigen binding to the β1-linked galactosyl residue (Payne *et al.*, 1998) in a carbohydrate moiety of human IgG1, IgG2 and IgG3 that is linked to C_H2 domains of their Fc subunit (Deisenhofer, 1981).

Binding of purified recombinant pH6 antigen to gangliotetraosylceramide, gangliotriaosylceramide and lactosylceramide was indicated by an enzyme-linked immunosorbent assay (ELISA) (Payne *et al.*, 1998). The binding was saturable, with 50% of maximal binding occurring at 498, 390 and 196 nM, respectively. Intact *E. coli* cells that expressed the pH6 antigen had a specificity similar to the purified pH6 antigen of *Y. pestis* on thin-layer chromatography, except that non-hydroxylated galactosylceramide was also bound. The binding pattern indicates that the presence of the β1-linked galactosyl residue in glycosphingolipids is the minimum requirement for binding of the pH6 antigen.

Purified pH6 antigen selectively binds to apolipoprotein B-containing lipoproteins (low-density lipoproteins) in human plasma (Makoveichuk *et al.*, 2003). Low-density lipoproteins at a normal physiological concentration in human blood (equal to $\sim$250 μg mL^{-1}) nearly abolish the interaction of purified pH6 antigen with macrophages. This process could prevent the recognition of a pathogen by the host immune defense system (Makoveichuk *et al.*, 2003). Such immune masking could be important for the ability of the pathogen to cause disease (Makoveichuk *et al.*, 2003).

Liu *et al.* (2006) found by flow cytometry that individual *Y. pestis* cells can express the capsular F1 antigen concomitant with the pH6 antigen (Psa) on their surface when analyzed. To better evaluate the separate effects of F1 and Psa on the adhesive and invasive properties of *Y. pestis*, isogenic Δ*caf* (F1 genes), Δ*psa* and Δ*caf*Δ*psa* mutants were constructed and studied with the three respiratory tract epithelial cells. The Δ*psa* mutant bound significantly less to all three epithelial cells compared with the parental wild-type strain and the Δ*caf* and Δ*caf*Δ*psa* mutants, indicating that the pH6 antigen acts as an adhesin for respiratory tract epithelial cells. An antiadhesive effect of the F1 antigen was clearly detectable only in the absence of the pH6 antigen, underlining the dominance of the Psa$^+$ phenotype. Both F1 and pH6 antigens inhibited the intracellular uptake of *Y. pestis*. Thus, F1 inhibits bacterial uptake by inhibiting

bacterial adhesion to epithelial cells, whereas the pH6 antigen seems to block bacterial uptake by interacting with a host receptor that controls the direct internalization. The Δ*caf*Δ*psa* double-mutant bound and invaded all three epithelial cell types well, indicating the presence of undefined adhesin(s) and invasin(s).

It was found that pH6 antigen (Psa) fimbriae mediate bacterial binding to human alveolar epithelial cells (Galván *et al.*, 2006). The pH6 fimbriae bound mostly to one component present in the total lipid extract from type II alveolar epithelial cells A549. The receptor of the pH6 antigen was identified as phosphatidylcholine by thin-layer chromatography, molybdenium blue staining and pH6 antigen overlays. The pH6 antigen fimbriae bound to phosphatidylcholine in a dose-dependent manner, whereas the binding was inhibited by phosphorylcholine and choline. Antigen pH6 also bound to the pulmonary surfactant, which covers the alveolar surface as a product of type II alveolar epithelial cells and includes phosphatidylcholine as the major component. The observed dose-dependent interaction of the pH6 antigen with the pulmonary surfactant was blocked by phosphorylcholine. Interestingly, the surfactant did not inhibit pH6 antigen-mediated bacterial binding to alveolar cells, suggesting that both the surfactant and cell membrane phosphatidylcholine retain pH6 antigen-fimbriated bacteria on the alveolar surface. Altogether, the results indicate that the pH6 antigen uses the phosphorylcholine moiety of phosphatidylcholine as a receptor to mediate bacterial binding to pulmonary surfactant and alveolar epithelial cells.

F1 antigen

It was found that human IL-1β specifically binds to a protein of the *caf* operon, expressed on the surface of the recombinant *E. coli* strain (Zav'yalov *et al.*, 1995a). The binding was specifically inhibited by the Caf1M–Caf1 complex, but not by the free Caf1M chaperone. Partially purified Caf1A also demonstrated binding with human IL-1β. The contradiction between the results can be explained by the presence of an admixture of the Caf1M–Caf1 complex in the Caf1A sample. Indeed, it has been demonstrated that the chaperone–subunit complex is copurifying in complex with usher protein (Nishiyama *et al.*, 2005). It is surprising that there is an absence of IL-1β binding with the fragments of the F1 antigen that are scattering in cultural media (Chen & Elberg, 1977). This implies that only short nonaggregated F1 fibers, expressed during the early stages of cultivation/infection, possess the IL-1β-binding activity.

Binding of monoadhesins to host-cell receptors and serum host proteins

FGS chaperone-assembled monoadhesive fimbriae or pili are cell-surface fibers that project a specialized bacterial lectin, or adhesin subunit, away from the bacterial surface, to reach out to specific glycan receptors on the host cell (De Greve *et al.*, 2007). Monoadhesive fimbriae/pili can also mediate interbacterial interactions, thereby facilitating biofilm formation (De Greve *et al.*, 2007). Monoadhesins are important virulence factors that exploit the diversity and virtually unlimited combinatorial potential of their carbohydrate receptors to ensure selective and fine-tuned pathogen–host interactions (De Greve *et al.*, 2007). In recent years, it was shown that monoadhesive fimbriae/pili allow bacterial pathogens to colonize, multiply, disseminate and, in some cases, persist for weeks to months within their animal hosts (Bower *et al.*, 2005). Among these invasive bacteria, there are strains of uropathogenic *E. coli* (UPEC) that were previously characterized as strictly extracellular microorganisms, but have now been shown to behave as opportunistic intracellular pathogens. Worldwide, UPEC account for the majority of urinary tract infections (UTIs), including cystitis (bladder infection) and pyelonephritis (kidney infection) (Foxman & Brown, 2003). These infections are exceedingly common in females, and are suffered by 11% of women each year (Foxman *et al.*, 2000).

FimH adhesin

UPEC typically expresses filamentous adhesive organelles, called type I pili, which mediate both bacterial attachment to and invasion of bladder urothelial cells. Type I pili or fimbriae possess a lectin-like component, FimH, which is commonly thought to cause binding to mannose-containing oligosaccharides of host receptors. As adhesion of type I fimbriated organisms is inhibited by mannose, the reactions are described as mannose-sensitive (MS).

Sokurenko *et al.* (1992) studied the adhesion of the type I fimbriated CSH-50 strain of *E. coli* (which expresses only type I fimbriae) to fibronectin (FN). *Escherichia coli* CSH-50 does not bind detectable amounts of soluble FN, but adheres well to immobilized plasma or cellular FN. This adhesion was inhibited by mannose-containing saccharides. Using purified domains of FN, it was found that *E. coil* CSH-50 adheres primarily to the N-terminal and gelatin-binding domains, only one of which is glycosylated, in a MS way. Binding of the mannose-specific lectin concanavalin A to FN and ovalbumin was eliminated or reduced, respectively, by incubation with periodate or endoglycosidase. Adhesion of *E. coli* CSH-50 to ovalbumin was reduced by these treatments, but adhesion to FN was unaffected. *Escherichia coli* CSH-50 also adheres in an MS way to a synthetic peptide copying a portion of the amino-terminal FN domain (FNspl). Purified CSH-50 fimbriae bound to immobilized FN and FNspl in an MS way and inhibited adhesion of intact organisms. However, fimbriae purified from HB101(pPKL4), a recombinant strain harboring the entire type I *fim* gene locus

and expressing functional type I fimbriae, did not bind to FN or to FNspl, nor did they inhibit *E. coli* adhesion to immobilized FN or FNspl. These findings suggest that there are two forms of type I MS fimbriae. One form exhibits only the well-known MS lectin-like activity that requires mannose-containing glycoproteins. The other form exhibits not only the MS lectin-like activity but also binds to nonglycosylated regions of proteins in an MS manner. Sokurenko *et al.* (1994) provided evidence that this functional heterogeneity is due to variations in the *fimH* genes. They also investigated functional heterogeneity among clinical isolates and whether variation in *fimH* genes accounts for differences in receptor specificity. Twelve isolates obtained from human urine were tested for their ability to adhere to mannan, fibronectin, periodate-treated fibronectin and a synthetic peptide copying 30 amino-terminal residues of fibronectin. CSH-50 and HB101 (pPKLA) were tested for comparison. Selected isolates were also tested for adhesion to purified fragments spanning the entire fibronectin molecule. Three distinct functional classes, designated M, MF and MFP, were observed. The *fimH* genes were amplified by PCR from chromosomal DNA obtained from representative strains and expressed in a *fim*$^-$ strain (AAEC191A) transformed with a recombinant plasmid containing the entire *fim* gene cluster, but with a translational stop-linker inserted into the *fimH* gene (pPKL114). Cloned *fimH* genes conferred on AAEC191A (pPKL114) receptor specificities mimicking those of the parent strains from which the *fimH* genes were obtained, demonstrating that the FimH subunits are responsible for the functional heterogeneity. Representative *fimH* genes were sequenced and the deduced amino acid sequences were compared with the previously published FimH sequence. Allelic variants exhibiting $>$ 98% homology and encoding proteins differing by as little as a single amino acid substitution confer distinct adhesive phenotypes. This unexpected adhesive diversity within the FimH family broadens the scope of potential receptors for enterobacterial adhesion and may lead to a fundamental change in the understanding of the role(s) that type I fimbriae may play in enterobacterial ecology or pathogenesis.

To further study the relationship between allelic variation of the *fimH* gene and adhesive properties of type I fimbriae, Sokurenko *et al.* (1995) cloned the *fimH* genes from five strains and used them to complement the FimH deletion in *E. coli* KB18. The parental and recombinant strains showed a wide quantitative range in the ability of bacteria to adhere to immobilized mannan. The differences in adhesion are due to differences in the levels of fimbriation or relative levels of incorporation of FimH because these parameters were similar in low- and high-adhesion strains. The nucleotide sequence for each of the *fimH* genes was determined. Analysis of deduced FimH sequences showed two sequence homology groups, based on the presence of Asn70 and Ser78 or Ser70 and Asn78 residues. The consensus sequences for each group conferred very low adhesion activity, and this low-adhesion phenotype predominated among a group of 43 fecal isolates. Strains isolated from different host niches in the urinary tract expressed type I fimbriae that conferred an increased level of adhesion. The results suggest that the quantitative variations in MS adhesion are primarily due to structural differences in the FimH adhesin.

The differences in MS adhesion among *E. coli* isolates suggest that phenotypic variants of FimH may play a functional role in population dynamics. Sokurenko *et al.* (1997) analyzed in more detail the ability of isogenic, recombinant strains of *E. coli* expressing *fimH* genes of the predominant fecal and UTI phenotypes to adhere to glycoproteins and uroepithelial cells. Type I fimbriae differ in their ability to recognize various mannosides by utilizing at least two different mechanisms. All FimH subunits studied to date are capable of mediating adhesion via trimannosyl residues, but only certain variants are capable of mediating high levels of adhesion via monomannosyl residues. The ability of the FimH lectins to interact with monomannosyl residues strongly correlates with their ability to mediate *E. coli* adhesion to uroepithelial cells. It would be possible for certain phenotypic variants of type I fimbriae to contribute more than others to the virulence of *E. coli* in the urinary tract. Sokurenko *et al.* (1998) showed that genetic variation in the FimH lectin of type I fimbriae can change the tropism of *E. coli*, shifting it toward the urovirulent phenotype.

Random point mutations in *fimH* genes that increase binding of an adhesin to monomannose residues, structures abundant in the oligosaccharide moieties of urothelial glycoproteins, confer increased virulence. These mutant FimH variants, however, owe their increased sensitivity to soluble inhibitors bathing the oropharyngeal mucosa, the physiological portal of *E. coli*. This functional trade-off seems to be detrimental to the intestinal ecology of the urovirulent *E. coli*. Thus, bacterial virulence can be increased by random functional mutations in a commensal trait that are adaptive for a pathologic environment, even at the cost of reduced physiological fitness in the nonpathologic habitat. Schembri *et al.* (2000) used random mutagenesis to identify specifically the nonselective mutations in the FimH adhesin that modify its binding phenotype. Isogenic *E. coli* clones expressing FimH variants were tested for their ability to bind yeast cells and model glycoproteins that contain oligosaccharide moieties rich in terminal monomannose, oligomannose or nonmannose residues. Type I fimbriae were altered for amino acids in the FimH protein. The monomannose-binding phenotype was particularly sensitive to the changes, with extensive differences in binding being observed in comparison with wild-type FimH levels. Different structural alterations caused similar functional changes in FimH, suggesting a high degree of flexibility to target recognition by this adhesin. Alteration of residue

Pro49 of the carbohydrate-binding pocket of FimH completely abolished its function. Amino acid changes that increased the binding capacity of FimH were located outside receptor-interacting residues, indicating that functional changes relevant to pathogenicity are likely to be due to conformational changes of the adhesin.

Weissman *et al.* (2006) analyzed the variability of *fimA* and *fimH* in strains of *E. coli* O1:K1, O2:K1 and O18:K1 serotypes. Multiple locus sequence typing (MLST) of this group revealed that the strains are identical at eight housekeeping loci around the genome and belong to the ST95 complex. Multiple highly diverse *fimA* alleles have been introduced into the ST95 clonal complex via horizontal transfer at a frequency comparable to that of genes defining the major O- and H-antigens. However, no further significant FimA diversification occurred via point mutation after the transfers. In contrast, although *fimH* alleles also move horizontally (along with the *fimA* loci), they acquire point amino acid replacements at a higher rate than either housekeeping genes or *fimA*. These FimH mutations enhance binding to monomannose receptors and bacterial tropism for human vaginal epithelium. A similar pattern of rapid within-clonal structural evolution of the adhesive, but not pilin, subunit is also seen, respectively, in *papG* and *papA* alleles of the digalactose-specific P-fimbriae. Thus, while structurally diverse pilin subunits of *E. coli* fimbriae are under selective pressure for frequent horizontal transfer between clones, the adhesive subunits of extraintestinal *E. coli* are under strong positive selection (Dn/Ds $>$ 1 for *fimH* and *papG*) for functionally adaptive amino acid replacements. Thomas *et al.* (2002) showed that bacterial attachment to target cells switches from loose to firm with a 10-fold increase when a shear stress is applied. Steered molecular dynamics simulations of tertiary structure of the FimH receptor-binding domain and subsequent site-directed mutagenesis studies indicate that shear enhancement of the FimH-receptor interactions involves extension of the interdomain linker chain under mechanical force. The ability of FimH to function as a force sensor provides a molecular mechanism for the discrimination between surface-exposed and soluble receptor molecules. Thomas *et al.* (2004) demonstrated that increasing the shear stress (within the physiologically relevant range) increased accumulation of type I fimbriated bacteria on monomannose surfaces by up to two orders of magnitude and reduced the shear stress, causing them to detach. In contrast, bacterial binding to anti-FimH antibody-coated surfaces showed essentially the opposite behavior, the bacteria detaching when the shear stress was increased. These results can be explained if FimH is force-activated, that is, that FimH mediates 'catch-bonds' with mannose that are strengthened by tensile mechanical force. As a result, on monomannose-coated surfaces, bacteria displayed a complex 'stick-and-roll' adhesion in which they tend to roll over the surface at low shear, but increasingly halted to stick firmly as the shear was increased. Mutations in FimH that were predicted earlier to increase or decrease force-induced conformational changes in FimH were furthermore shown to increase or decrease the probability that bacteria exhibited the stationary vs. the rolling mode of adhesion. This 'stick-and-roll' adhesion could allow type I fimbriated bacteria to move along mannosylated surfaces under relatively low-flow conditions and to accumulate preferentially in high-shear regions.

Nilsson *et al.* (2008) described two distinctively different conformations of the mannose-bound FimH-binding site. Force-induced dissociation was slowed when the mannose ring rotated so that additional force-bearing hydrogen bonds formed with the base of the FimH-binding pocket. The lifetime of the complex was further significantly enhanced by rigidifying this base. It was shown how even sub-Å spatial alterations of the hydrogen-bonding pattern within the base can lead to significantly decreased bond lifetimes (Nilsson *et al.*, 2008). Pereverzev *et al.* (2005) developed a physical model that explains how the ligand escapes the receptor-binding site via two alternative routes: a catch pathway that is opposed by the applied force and a slip pathway that is promoted by force. The model predicts under what conditions and at what critical force the catch-to-slip transition would be observed, as well as the degree to which the bond lifetime is enhanced at the critical force. Nilsson *et al.* (2006a, b) discovered that when surface adhesion is mediated by catch bonds, whose bond life increases with increased applied force, shear stress may dramatically increase the ability of bacteria to withstand detachment by soluble competitive inhibitors. This shear stress-induced protection against inhibitor-mediated detachment was shown for the fimbrial FimH-mannose-mediated surface adhesion of *E. coli*. Shear stress-enhanced reduction of bacterial detachment has major physiological and therapeutic implications and should be considered when developing and screening drugs.

Nilsson *et al.* (2006a, b) showed that the oligosaccharide-specific interaction of FimH with trimannose (3M) lacks a shear threshold for binding, as the number of bacteria bind under static conditions stronger than under any flow. However, similar to 1M, the binding strength of surface-interacting bacteria is enhanced by shear. Bacteria change from rolling to firm stationary surface adhesion as shear increases. The shear-enhanced bacterial binding on 3M is mediated by catch bond properties of the 1M-binding subsite within the extended oligosaccharide-binding pocket of FimH, as structural mutations in the putative force-responsive region and in the binding site affect 1M- and 3M-specific binding in an identical manner. A shear-dependent conversion of the adhesion mode is also exhibited by P-fimbriated *E. coli* adhering to digalactose surfaces.

Anderson *et al.* (2007) compared the levels of surface colonization by *E. coli* strains that differ in the strength of adhesion as a result of flow conditions or point mutations in FimH. They showed that the weak rolling mode of surface adhesion allows a more rapid spreading during growth on a surface in the presence of fluid flow. An attempt to inhibit the adhesion of strongly adherent bacteria by blocking mannose receptors with a soluble inhibitor actually increased the rate of surface colonization by allowing the bacteria to roll. This work suggests that (1) an advantage of a weak adhesion is a rapid surface colonization and (2) antiadhesive therapies intended to prevent biofilm formation can have the unintended effect of enhancing the rate of surface colonization.

Nilsson *et al.* (2007) showed that removal of the cysteine bond in the mannose-binding domain of FimH did not affect FimH-mannose binding under static or low shear conditions (≤ 0.2 dynes cm^{-2}). However, the adhesion level was substantially decreased under increased fluid flow. Under intermediate shear (2 dynes cm^{-2}), the ON rate of bacterial attachment was significantly decreased for disulfide-free mutants. Molecular dynamic simulations demonstrated that the lower ON rate of cysteine bond-free FimH could be due to destabilization of the mannose-free binding pocket of FimH. In contrast, mutant and wild-type FimH had similar conformations when bound to mannose, explaining their similar binding strength to mannose under intermediate shear. The stabilizing effect of mannose on disulfide-free FimH was also confirmed by protection of the FimH from thermal and chemical inactivation in the presence of mannose. However, this stabilizing effect could not protect the integrity of the FimH structure under high shear (> 20 dynes cm^{-2}), where lack of the disulfide significantly increased adhesion OFF rates. Thus, the cysteine bonds in bacterial adhesins could be adapted to enable bacteria to bind target surfaces under increased shear conditions.

Yakovenko *et al.* (2008) applied force to single isolated FimH bonds with an atomic force microscope to test this directly. If force was loaded slowly, most of the bonds broke up at a low force (< 60 pN of rupture force). However, when force was loaded rapidly, all bonds survived until a much higher force (140–180 pN of rupture force), behavior that indicates a catch bond. Structural mutations or pretreatment with a monoclonal antibody, both of which allosterically stabilize a high-affinity conformation of FimH, cause all bonds to survive until high forces, regardless of the rate at which force is applied. Pretreatment of FimH bonds with intermediate force has the same strengthening effect on the bonds. This demonstrates that FimH forms catch bonds and that tensile force induces an allosteric switch to the high-affinity, strong binding conformation of the adhesin. The catch bond behavior of FimH, the amount of force needed to regulate FimH and the allosteric mechanism all provide insights into how bacteria bind and form biofilms in fluid flow. Additionally, these observations may provide a means for designing antiadhesive mechanisms.

Thomas *et al.* (2008) reviewed experimental data and biophysical theory to analyze why mechanical force prolongs the lifetime of these bonds rather than shorten the lifetime by pulling the ligand out of the binding pocket. Although many mathematical models can explain catch bonds, experiments using structural variants have been more helpful in determining how catch bonds work. So far, the underlying mechanism has been worked out only for the bacterial adhesive protein FimH. This protein forms catch bonds because it is allosterically activated when mechanical force pulls an inhibitory domain away from the ligand-binding domain. Other catch bond-forming proteins, including blood cell adhesion proteins called selectins and the motor protein myosin, show evidence of allosteric regulation between two domains, but it remains unclear as to whether this is related to their catch bond behavior.

FimH adhesin consists of a fimbria-associated pilin domain and a mannose-binding lectin or adhesin domain, with the binding pocket positioned opposite the interdomain interface (Fig. 9; Choudhury *et al.*, 1999). Using the yeast two-hybrid system, purified lectin and pilin domains and docking simulations, it was shown that the FimH domains interact with one another (Aprikian *et al.*, 2007). The affinity for mannose is greatly enhanced (up to 300-fold) in FimH variants in which the interdomain interaction is disrupted by structural mutations in either the pilin or the lectin domains. Also, affinity to mannose is dramatically enhanced in isolated lectin domains or in FimH complexed with the chaperone molecule that is wedged between the domains. Furthermore, FimH with a native structure mediates weak binding at low shear stress, but shifts to strong binding at high shear, whereas FimH with disrupted interdomain contacts (or the isolated lectin domain) mediates strong binding to mannose-coated surfaces even under low shear. Interactions between lectin and pilin domains decrease the affinity of the mannose-binding pocket via an allosteric mechanism (Choudhury *et al.*, 1999). Mechanical force at high shear separates the two domains, allowing the lectin domain to switch from a low-affinity to a high-affinity state. This shift provides a mechanism for FimH-mediated shear-enhanced adhesion by enabling the adhesin to form catch bond-like interactions that are longer lived at high tensile force. The FimH lectin domain possesses a ligand-induced binding site – a type of allosterically regulated epitope characterized in integrins (Tchesnokova *et al.*, 2008). Analogous to integrins, in FimH, the ligand-induced binding site epitope becomes exposed in the presence of the ligand (or 'activating' mutations) and is located far from the ligand-binding site, close to the interdomain interface. Also, the antibody binding to the ligand-induced binding site shifts adhesin from the low- to the high-affinity state.

Binding of streptavidin to the biotinylated residue within the ligand-induced binding site also locks FimH in the high-affinity state, suggesting that the allosteric perturbations in FimH are sustained by the interdomain wedging. In the presence of antibodies, the strength of bacterial adhesion to mannose is increased similar to the increase observed under shear force, suggesting the same allosteric mechanism – a shift in the interdomain configuration. Thus, an integrin-like allosteric link between the binding pocket and the interdomain conformation can serve as the basis for the catch bond property of FimH and, possibly, of other adhesive proteins. Pereverzev *et al.* (2009) found that the type I fimbrial adhesive protein (FimH)/mannose bond is governed by the interface between the lectin and pilin domains of FimH. Catch binding occurs in these systems when the external force stretches the receptor proteins and increases the interdomain distance. The proposed model accurately describes the experimentally observed anomalous behavior of the lifetimes of the FimH/mannose complexes as a function of applied force and provides valuable insights into the mechanism of catch binding.

Recently, Pereverzev *et al.* (2009) reviewed the proposed model that demonstrates the allosteric role of the two-domain region of the receptor protein in the increased lifetimes of biological receptor/ligand bonds subjected to an external force. The interaction between the domains is represented by a bounded potential, containing two minima corresponding to the attached and separated conformations of the two protein domains. The dissociative potential with a single minimum, describing receptor/ligand binding, fluctuates between deep and shallow states, depending on whether the domains are attached or separated. A number of valuable analytic expressions are derived and are used to interpret experimental data for two catch bonds.

Using overlay assays with FimH, the purified type I pilus adhesin and mass spectroscopy, β1 and α3 integrins were identified as key host receptors for UPEC (Eto *et al.*, 2007). FimH recognizes *N*-linked oligosaccharides on these receptors, which are expressed throughout the urothelium. In a bladder cell culture system, β1 and α3 integrin receptors colocalize with invading type I-piliated bacteria and F-actin. FimH-mediated bacterial invasion of host bladder cells is inhibited by β1 and α3 integrin-specific antibodies and by disruption of the β1 integrin gene in the GD25 fibroblast cell line. Phosphorylation site mutations within the cytoplasmic tail of β1 integrin alter integrin signaling. They also variably affect UPEC entry into host cells, by either attenuating or boosting invasion frequencies (Eto *et al.*, 2007). Furthermore, focal adhesion and Src family kinases, which propagate integrin-linked signaling and downstream cytoskeletal rearrangements, are shown to be required for FimH-dependent bacterial invasion of target host cells. Together, these results indicate that β1 and α3 integrins are functionally important receptors for type I pili-expressing bacterium within the urinary tract and possibly at other sites within the host (Eto *et al.*, 2007).

GP2 is the major membrane protein present in the pancreatic zymogen granule, and is cleaved and released into the pancreatic duct along with exocrine secretions. The function of GP2 is unknown. The closest homologue to GP2 is uromodulin, a protein expressed by the kidney that shows 52% identity and 67% conservation in amino acid sequence. Uromodulin is secreted into the urine and binds *E. coli* with type I fimbriae. A role in host defense has been proposed in which uromodulin serves as a molecular decoy that prevents bacteria from binding to uroplakin, the host receptor in uroepithelia (Mo *et al.*, 2004; Pak *et al.*, 2001). In addition, two independent laboratories (Mo *et al.*, 2004; Pak *et al.*, 2001) have produced uromodulin *null* mice that showed increased sensitivity to UTIs. Yu & Lowe (2009) examined whether GP2 also shares similar binding properties to bacteria with type I fimbria. Commensal and pathogenic bacteria, including *E. coli* and *Salmonella*, express type I fimbria. An *in vitro* binding assay was used to assay the binding of recombinant GP2 to defined strains of *E. coli* that differ in their expression of type I fimbria or its subunit protein, FimH. Studies were also performed to determine whether GP2 binding is dependent on the presence of mannose residues, which is a known determinant for FimH binding. It was demonstrated that GP2 binds *E. coli* that expresses type I fimbria. Binding is dependent on GP2 glycosylation and specifically the presence of mannose residues. Thus, GP2 binds to type I fimbria, a bacterial adhesin that is commonly expressed by members of the *Enterobacteriacae* family.

PapG adhesin

The most extensively studied adhesin, and also the first virulence-associated factor identified for UPEC, is P fimbria (Lane & Mobley, 2007), encoded by the *pap* (pyelonephritis-associated pili) genes. P fimbria are prevalent among strains of UPEC causing pyelonephritis 4 and are characterized by their mannose-resistant adherence to Gal(a1–4)Galb moieties present in the globoseries of membrane glycolipids on human erythrocytes of the P blood group and on uroepithelial cells (Leffler & Svanborg-Edén, 1980, 1981; Johnson, 1991; Jones *et al.*, 1996). Three major and well-studied classes of *papG* alleles exist, which encode the molecular variants of adhesin PapGI, -II and -III. Each PapG variant is known to have a distinct isoreceptor specificity, which in turn results in altered host tissue tropism. PapGII, which is clinically associated with acute pyelonephritis in humans, binds preferentially globoside, or GbO4, the predominant glycolipid isoreceptor of the human kidney.

Both the solution structure of the PapGII adhesin domain and the crystal structure of the PapGII receptor bound to

GbO4 as well as the unbound form of the adhesin have been determined using NMR and the multiwavelength anomalous dispersion phasing method (Fig. 9; Dodson *et al.*, 2001; Sung *et al.*, 2001).

F17G/GafD adhesin

Bacterial adhesion to intestinal surfaces is important for successful colonization, and a number of fimbrial adhesins expressing differing receptor-binding specificities and serological properties have been detected on ETEC from different hosts (Nataro & Kaper, 1998). The G fimbria is most closely related to the F17c fimbriae that are common on bovine septicemic and diarrhea-associated *E. coli* (Saarela *et al.*, 1995) and they occur in human *E. coli* infections as well (Le Bouguénec & Bertin, 1999). The G fimbriae bind to the terminal *N*-acetyl-D-glucosamine (GlcNAc) residues of glycoproteins at calf intestinal brush borders as well as the mammalian basement membrane (Sanchez *et al.*, 1993; Saarela *et al.*, 1996). The latter is thought to potentiate translocation of the ETEC into circulation. G fimbrial binding to GlcNAc receptors is mediated by the 321-amino acid residue GafD lectin subunit (Saarela *et al.*, 1995) present mainly at the G-fimbrial tip (Saarela, 1999). The structure of the ligand-binding domain, GafD1-178, has been determined at 1.7 Å resolution in the presence of the receptor sugar GlcNAc (Fig. 9; Merckel *et al.*, 2003). As in N-terminal adhesin PapG and FimH domains, the overall fold of GafD1-178 is a β-barrel jelly-roll fold. The ligand-binding site was identified and localized to the side of the molecule. Receptor binding is mediated by side-chain as well main-chain interactions. Ala43-Asn44 and Ser116-Thr117 form the sugar acetamide specificity pocket, Asp88 confers tight binding and Trp109 appears to position the ligand. There is a disulfide bond that rigidifies the acetamide specificity pocket.

MrkD adhesin

Li *et al.* (2009a, b) expressed the recombinant adhesin MrkD of *K. pneumoniae* in *E. coli* and purified it to homogeneity. The adhesive activity of MrkD was examined and the binding site was studied with laser confocal microscopy. The adherent activity of *K. pneumoniae* was significantly inhibited by MrkD, showing that MrkD putative adhesin contains adhesion epitopes.

Anti-immune and proinflammatory activities of adhesive organelles

Features of anti-immune and proinflammatory activities of poly- and monoadhesive organelles

In contrast to monoadhesive pili, which possess only one binding domain on the tip of the pilus (Fig. 12a), each polyadhesive fiber potentially might (Fig. 12b):

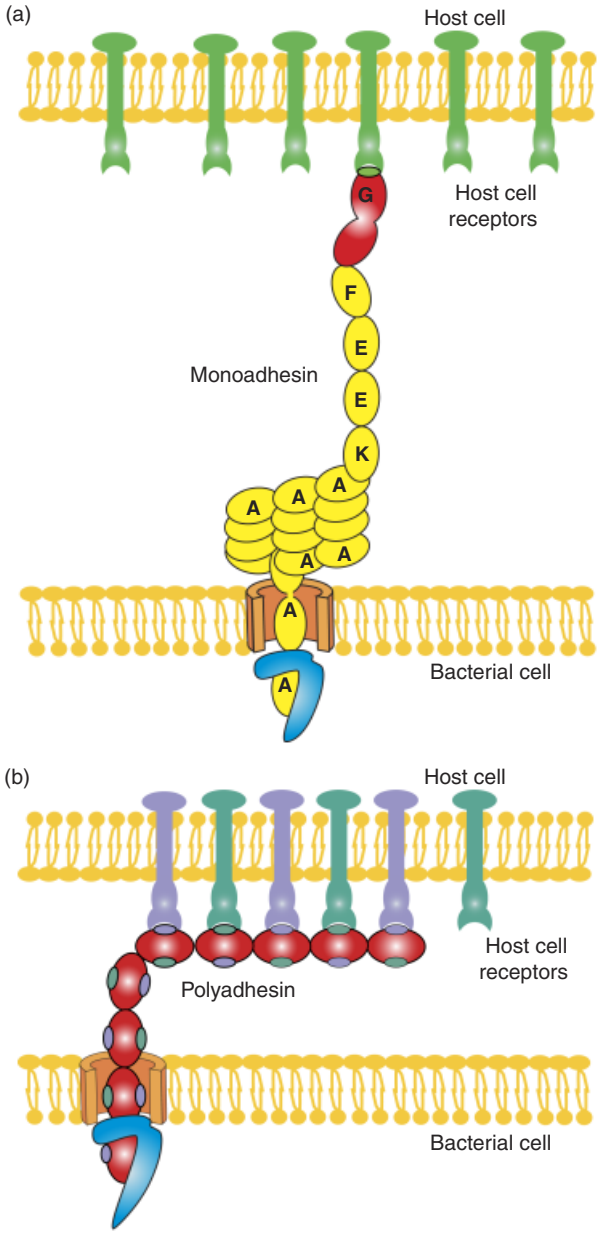

Fig. 12. Schematic illustration (elaborated by the authors) of a binding of monoadhesive (a) and polyadhesive (b) organelles to host-cell receptors. Periplasmic chaperones and outer membrane ushers are in blue and orange, respectively. Adhesin and pilin subunits are in red and yellow, respectively. Host receptors for monoadhesins are shown in green. Two different types of host receptors for polyadhesins are shown by violet and greencyan.

(1) ensure a powerful polyvalent fastening of a bacterial pathogen to a host target cell (Galván *et al.*, 2006);
(2) aggregate host-cell receptors and trigger transduction of signals, causing immunosuppressive and proinflammatory responses (Sodhi *et al.*, 2004; Sharma *et al.*, 2005a, b; Galván *et al.*, 2006);

(3) pull a bacterium to a host cell by a zipper-like mechanism that increases tightness of the contact.

It was directly demonstrated that Psa fimbriae (pH6 antigen) of *Y. pestis* function as polyadhesins (Galván *et al.*, 2006). The Psa fimbriae bound to phosphatidylcholine in a dose-dependent manner and binding was inhibited by phosphorylcholine and choline. Binding inhibition was dose-dependent, although only high concentrations of phosphorylcholine completely blocked Psa binding to phosphatidylcholine. In contrast, less than 1 μM of a phosphorylcholine–polylysine polymer inhibited specifically the adhesion of Psa-fimbriated *E. coli* to phosphatidylcholine, type I (WI-26 VA4) and type II alveolar epithelial cells.

A tight contact between interacting cells hampers diffusion of Ca^{2+} in the site of contact and consequently triggers the Ca^{2+}-dependent type III secretion system (encoded by the pCD1 virulence plasmid) that destroys the defense activity of the host cell (Cornelis & Wolf-Watz, 1997; Viboud & Bliska, 2005). This is extremely important for bacterial virulence. In particular, *Y. pestis* appears to utilize the type III secretion pathway to destroy cells with innate immune functions (macrophages, dendritic cells and neutrophils), which represent the first line of defense, thereby preventing adaptive responses and precipitating the fatal outcome of plague (Marketon *et al.*, 2005). It was found that dendritic cells infected with *Y. pestis* failed to adhere to solid surfaces and to migrate toward the chemokine CCL19 in an *in vitro* transmembrane assay. Both effects were dependent on the presence of a pCD1 plasmid, and on bacterial growth shift to 37 °C, before infection (Velan *et al.*, 2006). Moreover, although instillation of a pCD1-cured *Y. pestis* strain into mice airways triggered effective transport of alveolar dendritic cells to the mediastinal lymph node, instillation of *Y. pestis* harboring the plasmid failed to do so. Taken together, these results suggest that pCD1 virulence-plasmid-dependent impairment of dendritic cell migration is the major mechanism utilized by *Y. pestis* to subvert dendritic cell function.

Contribution of polyadhesins to virulence and anti-immune activity of bacteria

Afa/Dr adhesins

Most important structure–function information by now has been obtained for the Afa/Dr adhesins. Nowicki *et al.* (1994) found a gestational age-dependent distribution of *E. coli* fimbriae in pregnant patients with pyelonephritis. Later, Hart *et al.* (1996) indicated that it is likely that *E. coli* associated with acute pyelonephritis during different trimesters of pregnancy represent nonrandom closely related isolates, and some of these strains may be characteristic in pregnant patients only. Nowicki *et al.* (1997) demonstrated that the rate of uterine infection in pregnant rats was about 10-fold higher than that in nonpregnant animals. It was proposed that infectious complications of pregnancy may be related to gestation-dependent sensitivity to the pathogenic microorganism and the host nitric oxide (NO) status. Fang *et al.* (1999) indicated with immunofluorescence studies that macrophages and natural killer cells, located in the endometrial layer clustering around epithelial cells, expressed type II protein. They suggested that a localized increase in type II NO synthase (NOS) expression and NO production occurs in response to intrauterine infection, while the NO system may play a role in host response to restrict the infection. Moreover, Fang *et al.* (2001) demonstrated that intrauterine infection induced an elevated expression of tumor necrosis factor (TNF)-α in both nonpregnant and pregnant rats. The sequential stimulation of NOS expression, especially the inducible isoform, and generation of uterine NO may be lacking during pregnancy despite an elevated TNF-α after infection. Fang *et al.* (2001) indicated that NO synthesis response may be maximal at pregnancy, and infection may not further induce the NO system. These studies, together with the previous report (Fang *et al.*, 1999), suggest that intrauterine infection-induced lethality in pregnant rats is amplified by the inhibition of NO and that pregnancy is a state predisposed to increased complications associated with intrauterine infection. The constitutively elevated uterine NO during pregnancy may help reduce the risk of infection-related complications.

Kaul *et al.* (1999) reported that expression of the CD55/DAF protein, recognized by adhesin Dr of diffusially adhering *E. coli* as the host tissue receptor, is increased during pregnancy. Induction of pathogenesis is a cumulative process of the host–pathogen relationship involving specific host factors and virulence characteristics of the invading organism. Kaul *et al.* (1999) developed an experimental model of chronic pyelonephritis with *E. coli*-bearing adhesin Dr (*E. coli* Dr1) in nonpregnant lipopolysaccharide-hyporesponder C3H/HeJ mice. This model was used to investigate the role of *E. coli* Dr1 in the outcome of pregnancy in C3H/HeJ mice. Groups of pregnant mice were infected with *E. coli* Dr1 or its isogenic mutant, which does not bear the adhesin Dr (*E. coli* Dr2) by urethral catheterization. Nearly 90% of pregnant mice infected with *E. coli* Dr1 delivered preterm (before 90% gestation) compared with 10% of mice infected with *E. coli* Dr2, but none of the mice treated with phosphate-buffered saline (PBS). There was a significant reduction in fetal birth weight in the *E. coli* Dr1-infected group compared with the *E. coli* Dr2- and PBS-treated groups ($P = 0.003$) (Kaul *et al.*, 1999). Goluszko *et al.* (2001) used a gentamycin protection assay to assess the ability of gestational pyelonephritis isolates of *E. coli* to invade HeLa cells. The ability to enter HeLa cells was

strongly associated with the presence of *dra* gene clusters coding adhesins Dr. In contrast, the noninvasive isolates predominantly expressed *papG*, coding P fimbriae. Hart *et al.* (2001) found a significant increase of ampicillin resistance among gestational pyelonephritis *E. coli* and an association with the *dra* gene cluster encoding colonization and invasive capacity.

It was found that the family of adhesins Dr, like type I fimbriae, mediated concentration-dependent adherence to human neutrophils [polymorphonuclear leukocytes (PMNs)] (Johnson *et al.*, 1995). Adherence to human neutrophils was MS for type I fimbriae, but mannose-resistant for Dr family adhesins. Chloramphenicol inhibited PMN adherence for the hemagglutinin Dr with the same potency with which it inhibited hemagglutination, but it was inactive against PMN adherence and hemagglutination mediated by other members of the adhesin Dr family. In contrast to PMN adherence, mediated by type I fimbriae, the adherence mediated by the hemagglutinin Dr did not lead to significantly increased bacterial killing. These data suggest that the family of adhesins Dr mediates a novel pattern of adherence to PMNs, probably by recognizing CD55/DAF, with minimal consequent bacterial killing.

Peiffer *et al.* (1998) studied F-actin rearrangements in the host cells expressing CD55/DAF protein as a result of attachment of *E. coli* strain bearing adhesin Dr. Infection of INT407 cells by the diffusely adhering strain *E. coli* C1845 (DAEC C1845) can induce dramatic F-actin rearrangements without cell entry. Clustering of phosphotyrosines was observed, revealing that the DAEC C1845–CD55/DAF F interaction involves recruitment of signal transduction molecules. DAEC C1845-induced F-actin rearrangements can be blocked dose dependently by protein tyrosine kinase, phospholipase Cg, phosphatidylinositol 3-kinase (PI3K), protein kinase C and Ca21 inhibitors. F-actin rearrangements and blocking by inhibitors were observed after infection of the cells with two *E. coli* recombinants carrying the plasmids containing the fimbrial adhesin F1845 or the fimbrial hemagglutinin Dr, belonging to the same family of adhesins. Thus, the DAEC Dr family of pathogens promotes alterations in the intestinal cell cytoskeleton by piracy of the CD55/DAF-GPI signal cascade without bacterial cell entry. Later, Peiffer *et al.* (2000a, b) provided evidence that infection of the polarized human intestinal cell line Caco-2/TC7 by strain C1845 is followed by an increase in the paracellular permeability for [^{3}H]-mannitol without a decrease of the transepithelial resistance of the monolayers. Alterations in the distribution of tight-junction-associated occludin and ZO-1 protein were observed, whereas the distribution of the zonula adherens-associated E-cadherin was not affected. Using the recombinant *E. coli* strains HB101-(pSSS1) and -(pSSS1C) expressing the F1845 fimbrial adhesin, it was demonstrated that the adhesion–CD55/DAF interaction is not sufficient for the induction of structural and functional tight-junction lesions (Peiffer *et al.*, 2000b). Moreover, using the actin filament-stabilizing agent Jasplakinolide, Peiffer *et al.*, 2000b demonstrated that the C1845-induced functional alterations in tight junctions are independent of the C1845-induced apical cytoskeleton rearrangements. The results indicated that pathogenic factor(s) other than the F1845 adhesin may be operant in Afa/Dr DAEC C1845. Infection of human intestinal Caco-2/TC7 cells by the Afa/Dr DAEC strains C1845 and IH11128 causes clustering of CD55/DAF around adhering bacteria (Guignot *et al.*, 2000). Mapping of CD55/DAF epitopes involved in CD55/DAF clustering by Afa/Dr DAEC was conducted with CD55/DAF deletion mutants expressed by stable transfection in CHO cells. Deletion in the short consensus repeat 1 (SCR1) domain abolished Afa/Dr DAEC-induced CD55/DAF clustering. In contrast, deletion in the SCR4 domain did not modify Afa/Dr DAEC-induced CD55/DAF clustering. It was shown that the brush border-associated glycosylphosphatidylinositol (GPI)-anchored protein CD66e/CEA is recruited by the Afa/Dr DAEC strains C1845 and IH11128. This conclusion is based on the observations that (i) infection of Caco-2/TC7 cells by Afa/Dr DAEC strains is followed by clustering of CD66e/CEA around adhering bacteria and (ii) Afa/Dr DAEC strains bound efficiently to stably transfected HeLa cells expressing CD66e/CEA, accompanied by CD66e/CEA clustering around adhering bacteria.

Inhibition assays with monoclonal antibodies directed against CD55/DAF SCR domains and polyclonal anti-CD55/DAF and anti-CD66e/CEA antibodies demonstrate that CD55/DAF and CD66e/CEA function as receptors for the C1845 and IH11128 bacteria. Moreover, using structural *draE* gene mutants, Guignot *et al.* (2000) found that a mutant in which cysteine replaces aspartic acid at position 54 conserved the binding capacity, but failed to induce CD55/DAF and CD66e/CEA clustering. Peiffer *et al.* (2000b) further characterized cell injuries following the interaction of wild-type Afa/Dr DAEC strains C1845 and IH11128 expressing fimbrial F1845 adhesin and hemagglutinin Dr, respectively, with polarized, fully differentiated Caco-2/TC7 cells. In both cases, bacterium–cell interaction was followed by rearrangement of the major brush border-associated cytoskeletal proteins F-actin, villin and fimbrin, proteins that play a pivotal role in brushborder assembly. In contrast, the distribution of G-actin, actin-depolymerizing factor and tubulin was not modified. Peiffer *et al.* (2000b) found that a mutant in which cysteine replaces aspartic acid at position 54 conserved the binding capacity, but failed to induce F-actin disassembly. The distribution of brushborder-associated functional proteins sucrase-isomaltase, dipeptidylpeptidase IV, glucose transporter SGLT1 and fructose transporter GLUT5 was dramatically altered. In parallel, sucrase-isomaltase and dipeptidylpeptidase IV enzyme activity decreased.

Selvarangan *et al.* (2004) constructed an isogenic mutant in the DraE adhesin subunit that was unable to bind type IV collagen, but retained binding to CD55/DAF, and examined its virulence in the mouse model. The collagen-binding mutant DrI113T was eliminated from the mouse renal tissues in 6–8 weeks, whereas the parent strain caused persistent renal infection that lasted for at least 14 weeks. *Trans*-complementation with the intact operon *dra* restored collagen-binding activity, interstitial tropism and the ability to cause persistent renal infection. It was concluded that type IV collagen binding mediated by DraE adhesin is a critical step for the development of the infection in a murine model of *E. coli* pyelonephritis.

Brest *et al.* (2004) found that infection of PMNs by Afa/Dr DAEC strains induced PMN apoptosis, characterized by morphological nuclear changes, DNA fragmentation, caspase activation and a high level of annexin V expression. PMN apoptosis depended on their agglutination, induced by Afa/Dr DAEC, and was still observed after preincubation of PMNs with anti-CD55/DAF and/or anti-CD66e/CEA antibodies. Low levels of phagocytosis of Afa/Dr DAEC strains were observed in both non-transmigrated and transmigrated PMNs compared with that observed with the control *E. coli* DH5α strain. The interaction of Afa/Dr DAEC with PMNs may increase the bacterial virulence both by inducing apoptosis of PMNs through an agglutination process and by diminishing their phagocytic capacity.

Wroblewska-Seniuk *et al.* (2005) investigated the role of the *afaE* and *afaD* genes in the mortality of pregnant rats from intrauterine infection using *afaE* and/or *afaD* mutants. The highest maternal mortality was observed in the group infected with the $afaE^+$ $afaD^+$ strain, followed by the group infected with the $afaE^+$ *afaD* strain. The *afaE afaD* double mutant did not cause maternal mortality, even with the highest infection dose. The *in vivo* studies corresponded to the invasion assay, where the $afaE^+$ strains were the most invasive ($afaE^+$ *afaD* strain > $afaE^+$ $afaD^+$ strain), whereas the *afaE* mutant strains (*afaE* $afaD^+$ and *afaE afaD* strains) seemed to be noninvasive. This study shows for the first time that the *afaE* gene coding the AfaE subunit of Dr/Afa adhesin is involved in the lethal outcome of gestational infection in rats. This lethal effect associated with AfaE correlates with the invasiveness of $afaE^+$ *E. coli* strains *in vitro*.

Korotkova *et al.* (2008b) demonstrated that CD55/DAF or CEACAM receptors independently promote DraE-mediated internalization of *E. coli* by CHO cell transfectants expressing these receptors. They also found that DraE-positive recombinant bacteria adhere to and are internalized by primary human bladder epithelial cells that express CD55/DAF and CEACAMs. DraE-mediated bacterial internalization by bladder cells was inhibited by agents that disrupt lipid rafts, microtubules and PI3K activity. Immunofluorescence confocal microscopic examination of epithelial cells detected considerable caveolin, β1 integrin, phosphorylated ezrin, phosphorylated PI3K and tubulin, but not F-actin, in cell-associated bacteria. The DraD subunit, previously implicated as an 'invasin,' is not required for β1 integrin recruitment or bacterial internalization. Guignot *et al.* (2009) also provided evidence that AfaD or DraD putative invasin subunits do not participate in the cell association and cell entry of bacteria, whereas DraE or AfaE-III adhesin subunits are necessary and sufficient to promote the receptor-mediated bacterial internalization into epithelial cells expressing CD55/DAF, CEACAM1, CD66e/CEA or CEACAM6. They confirmed independently data of Korotkova *et al.* (2008b) that internalization of Dr fimbriae-positive *E. coli* within CHO-CD55/DAF, -CEACAM1, -CD66e/CEA or -CEACAM6 cells occurs through a microtubule- and lipid raft-dependent mechanism. Wild-type Dr fimbriae-positive bacteria survived more in cells expressing CD55/DAF than bacteria internalized in CHO-CEACAM1, -CD66e/CEA or -EACAM6 cells (Guignot *et al.*, 2009).

Korotkova *et al.* (2007) posited that immune escape may be the driving force behind the structural variability of major antigens on the surface of bacterial pathogens, such as fimbriae. In the family Dr of *E. coli* adhesins, structural and adhesive functions are carried out by the same subunit. Adhesins Dr have been shown to bind CD55/DAF, collagen IV and CEACAMs. They showed that genes encoding adhesins Dr from 100 *E. coli* strains form eight structural groups with a high level of amino acid sequence diversity between them. However, genes constituting each group differ from each other by only a small number of point mutations. Of 66 polymorphisms identified within the groups, only three were synonymous mutations, indicating a strong positive selection for amino acid replacements. Functional analysis of intragroup variants making up the hemagglutinin Dr (DraE) group revealed that the point mutations result in distinctly different binding phenotypes, with a tendency toward increased affinity to CD55/DAF, decreased sensitivity of CD55/DAF binding to inhibition by chloramphenicol and loss of binding capability to collagen, CEACAM3 and CEACAM6. Thus, variability by point mutation of major antigenic proteins on the bacterial surface could be an indication of selection for functional modification.

F1 antigen

Yersinia pestis is the etiologic agent of bubonic and pneumonic plague, one of the most deadly diseases known to humans (Cleri *et al.*, 1997; Perry & Fetherston, 1997; Smiley, 2008a, b; Li *et al.*, 2009a, b). Electron micrographs of *Y. pestis* demonstrate that the F1 antigen-forming capsule is maximally expressed at 37 °C after 72 h of cultivation *in vitro* (Chen & Elberg, 1977). The expression of F1 antigen at

22 °C is negligible (Chen & Elberg, 1977). During the early stages of infection, when the F1 capsule is not yet formed, the type III secretion system protects *Y. pestis* from phagocytosis (Cornelis & Wolf-Watz, 1997; Viboud & Bliska, 2005). This system is encoded on a virulence plasmid 70 kb in size that is common to *Y. pestis*, *Y. pseudotuberculosis* and *Y. enterocolitica*. After 24 h of cultivation *in vitro* at 37 °C, *Y. pestis* expresses a large capsule-like structure composed of an aggregating F1 antigen (Chen & Elberg, 1977). The capsule material is readily soluble and dissociates from the bacterium during *in vitro* cultivation. The association of the F1 antigen with virulence is evident from recent studies, as all F1$^-$ mutants were of low virulence to mice compared with the wild types (Welkos *et al.*, 2004). Similar to other capsules or capsule-like antigens, F1 seems to be involved in the antiphagocytic activity reported for *Y. pestis*, but the contribution of F1 to this activity was not understood until recently. *Yersinia pestis* strain EV76 is highly resistant to uptake by J774 cells (Du *et al.*, 2002). *Yersinia pestis* strain EV76 with an in-frame deletion of the *caf1M* gene failed to express the F1 polymer on the bacterial surface. This strain had a somewhat reduced ability to prevent uptake by J774 cells. Strain EV76C, cured with the virulence plasmids, was much reduced in its ability to resist uptake. A strain lacking both the virulence plasmid and *caf1M* was almost totally phagocytosed (95%; Du *et al.*, 2002). It was concluded that F1 and the type III secretion system act in concert to make *Y. pestis* highly resistant to phagocytosis. The type III secretion system of *Y. pestis* may function optimally only during the early stages of infection, when the contact-dependent delivery of Yop effector proteins is the highest. Later on, when the surface of *Y. pestis* is covered with the F1 capsule, the delivery of Yop effector proteins may be lower. Although the expression of F1 capsule reduces the number of bacteria that interact with the macrophages, it does not influence the general phagocytic ability of J774 cells (Du *et al.*, 2002). This suggests that the F1 capsule prevents uptake by interfering at the level of receptor interaction in the phagocytosis process. Sebbane *et al.* (2009) found that a *caf*$^-$ *Y. pestis* mutant was not impaired either in flea colonization or in virulence in mice after intradermal inoculation of cultured bacteria. In contrast, absence of the *caf* operon decreased bubonic plague incidence after fleabite. Successful development of plague in mice infected by fleabite with the *caf*$^-$ mutant required a higher number of infective bites per challenge. In addition, the mutant displayed a highly autoaggregative phenotype in infected liver and spleen. The results suggest that acquisition of the *caf* locus via horizontal transfer by an ancestral *Y. pestis* increased transmissibility and the potential for epidemic spread. Sebbane *et al.* (2009) suggested a model in which atypical *caf*$^-$ strains could emerge during climatic conditions that favor a high flea burden. Human infection with such strains would not be diagnosed by the standard clinical tests that detect F1 antibody or antigen, suggesting that more comprehensive surveillance for atypical *Y. pestis* strains in plague foci may be necessary.

Yersinia pestis survives and replicates in phagosomes of murine macrophages. *Yersinia pestis*-containing vacuoles (YCVs) acquire markers of late endosomes or lysosomes in naïve macrophages and these bacteria can survive in macrophages activated with interferon-γ. An autophagic process known as xenophagy, which destroys pathogens in acidic autophagolysosomes, can occur in naïve macrophages and is upregulated in activated macrophages. Studies on the mechanism of *Y. pestis* survival in phagosomes of naïve and activated macrophages were undertaken to determine whether the pathogen avoids or co-opts autophagy. Colocalization of the YCV with markers of autophagosomes or acidic lysosomes and the pH of the YCV were determined by microscopic imaging of infected macrophages (Pujol *et al.*, 2009). Some YCVs contained double membranes characteristic of autophagosomes, as determined by electron microscopy. Fluorescence microscopy showed that approximately 40% of YCVs colocalized with green fluorescent protein (GFP)-LC3, a marker of autophagic membranes, and that YCVs failed to acidify below pH 7 in naïve macrophages. Replication of *Y. pestis* in naïve macrophages caused accumulation of LC3-II, as determined by immunoblotting. Whereas activation of infected macrophages increased LC3-II accumulation, it decreased the percentage of GFP-LC3-positive YCVs (approximately 30%). A viable count assay showed that *Y. pestis* survived equally well in macrophages proficient for autophagy and macrophages rendered deficient for this process by Cre-mediated deletion of ATG5, showing that this pathogen does not require autophagy for intracellular replication. Pujol *et al.* (2009) concluded that although YCVs can acquire an autophagic membrane and accumulate LC3-II, the pathogen avoids xenophagy by preventing vacuole acidification.

pH6 antigen

The pH6 antigen was first described > 40 years ago and was initially identified as an antigen expressed only at a pH below 6 at 37 °C (Ben-Efraim *et al.*, 1961). The electron micrographs of highly virulent phenotype *Y. pestis* grown at 37 °C, pH 6, indicate the expression of both the F1 capsule and thin filaments of the pH6 (PsaA) antigen on the bacterial surface (Lindler & Tall, 1993). The pH6 antigen is essential for full virulence of *Y. pestis* (Lindler *et al.*, 1990; Lindler & Tall, 1993). A Δ*psaA* mutant had a significant dissemination defect after subcutaneous infection, but only slight attenuation by the pneumonic-disease model, indicating different roles of the pH6 antigen in bubonic and pneumonic plague (Cathelyn *et al.*, 2006). The expression of the pH6 antigen adds to the antiphagocytic armament of the bacterium (Huang & Lindler, 2004). *Yersinia pestis psaA*

isogenic strains do not show any significant difference in their association with mouse macrophage cells. However, expression of *psaA* appeared to reduce significantly phagocytosis of both *Y. pestis* and *E. coli* by mouse macrophages ($P < 0.05$). Furthermore, complementation of the *psaA* mutant of *Y. pestis* strains could completely restore the bacterial resistance to phagocytosis. Fluorescence microscopy following differential labeling of intracellular and extracellular portions of *Y. pestis* revealed that significantly lower numbers of *psaA*-expressing bacteria were located inside the macrophages. Enhanced phagocytosis resistance was specific for bacteria expressing *psaA* and did not influence the ability of the macrophages to engulf other bacteria. This shows that *Y. pestis* pH6 antigen does not enhance adhesion to macrophages, but rather promotes resistance to phagocytosis, helping the bacteria to escape host immune defense mechanisms (Huang & Lindler, 2004). Recently, Anisimov *et al.* (2009), by site-directed mutagenesis of the *psa* operon and subsequent complementation *in trans*, generated two isogenic sets of *Y. pestis* strains, composed of wild-type strains 231 and I-1996, their nonpolar pH6$^-$ mutants with deletions in the *psaA* gene or the whole operon, as well as strains with restored ability for temperature- and pH-dependent synthesis of adhesion fimbriae or constitutive production of the pH6 antigen. It was shown that the loss of synthesis or constitutive production of the pH6 antigen did not influence *Y. pestis* virulence or the average survival time of subcutaneously inoculated BALB/c naïve mice or animals immunized with this antigen.

SefD putative invasin

The translocation of the minor putative invasin SefD subunit is a prerequisite for the export of the major structural SefA subunit across the outer membrane and formation of the SEF14 fimbriae (R.A. Edwards, B.C. Matlock & S.R. Maloy, unpublished data); thus, SefD is probably located at the tip of the fimbrial shaft (Edwards *et al.*, 2000). The lethal dose 50% (LD_{50}) values for the wild-type strain and mutants lacking SefA are comparable, but both the oral and the intraperitoneal virulence of mutants lacking SefD are considerably reduced. This means that major SEF14 subunit SefA is not required for the virulence of *S. enteritidis*, indicating that the tip of the fimbrial structure composed of SefD subunits is probably sufficient for successful interactions with phagocytes (Edwards *et al.*, 2000). SefD may bind to a receptor on the macrophage surface and alter the uptake of *S. enteritidis* into the phagocyte, enabling *S. enteritidis* to survive in the intracellular environment.

Polyadhesin Ral

Hart *et al.* (2009) investigated the contribution of a fimbrial polyadhesin, Ral, of REPEC to host specificity by introducing Ral into derivatives of human-specific EPEC (hEPEC) strain, E2348/69, in which expression of the fimbrial adhesin, Bfp, had been interrupted. Although unable to cause diarrheal disease in rabbits, Ral-bearing hEPEC strains colonized rabbit intestine more efficiently and showed altered intestinal localization when compared with an isogenic Ral$^-$ strain. These findings suggest that Ral enhances the initial interaction between a Δ*bfpA* mutant of hEPEC and rabbit intestine and may influence tissue specificity, but is not sufficient on its own to transform hEPEC into a rabbit pathogen.

Contribution of monoadhesins to virulence

Type I fimbriae

UTI is the second most common infectious disease and is caused predominantly by type I-fimbriated UPEC. UPEC initiates infection by attaching to uroplakin (UP) Ia, its urothelial surface receptor, via the FimH adhesins capping the distal end of its fimbriae. UP Ia, together with UP Ib, UP II and UP IIIa, forms a 16-nm receptor complex that is assembled into hexagonally packed, 2D crystals (urothelial plaques) covering $> 90\%$ of the urothelial apical surface. Recent studies indicate that FimH is the invasin of UPEC, as its attachment to the urothelial surface can induce cellular signaling events including calcium elevation and the phosphorylation of the UP IIIa cytoplasmic tail, leading to cytoskeletal rearrangements and bacterial invasion. However, it remains unknown how the binding of FimH to the UP receptor triggers a signal that can be transmitted through the highly impermeable urothelial apical membrane. Wang et al. (2009) showed by cryo-electron microscopy that FimH binding to the extracellular domain of UP Ia induces global conformational changes in the entire UP receptor complex, including a coordinated movement of the tightly bundled transmembrane helices. This movement of the transmembrane helix bundles can cause a corresponding lateral translocation of the UP cytoplasmic tails, which can be sufficient to trigger downstream signaling events. The results suggest a novel pathogen-induced transmembrane signal transduction mechanism that plays a key role in the initial stages of UPEC invasion and receptor-mediated bacterial invasion in general.

EPEC produce attaching/effacing lesions on eukaryotic cells mediated by the outer membrane adhesin intimin. EPECs are subgrouped into typical EPEC (tEPEC) and atypical EPEC (aEPEC). aEPEC strain 1551-2 (serotype O nontypable, nonmotile) invades HeLa cells by a process dependent on the expression of intimin subtype omicron. Yamamoto *et al.* (2009) showed that invasion of HeLa cells by aEPEC 1551-2 depends on actin filaments, but not on microtubules. In addition, disruption of tight junctions

enhanced its invasion efficiency in T84 cells, suggesting preferential invasion via a nondifferentiated surface. It was concluded that some aEPEC strains may invade intestinal cells *in vitro* with varying efficiencies and independent of the intimin subtype.

FimH, the mannose-specific, type I fimbrial adhesin of *E. coli*, acquires amino acid replacements that are adaptive in extraintestinal niches (the genitourinary tract), but detrimental in the main habitat (the large intestine). This microevolutionary dynamics is reminiscent of an ecological 'source-sink' model of continuous species spread from a stable primary habitat (source) into transient secondary niches (sink), with eventual extinction of the sink-evolved populations. Chattopadhyay *et al.* (2007) adapted two ecological analytical tools – diversity indexes DS and α – to compare the size and frequency distributions of *fimH* haplotypes between evolutionarily conserved FimH variants ('source' haplotypes) and FimH variants with adaptive mutations (putative 'sink' haplotypes). Both indexes show two- to threefold increased diversity of the sink fimH haplotypes relative to the source haplotypes, a pattern that was in contrast to those seen with nonstructural fimbrial genes (*fimC* and *fimI*) and housekeeping loci (*adk* and *fumC*), but similar to that seen with another fimbrial adhesin of *E. coli*, papG-II, also implicated in extraintestinal infections. The increased diversity of the sink pool of adhesin genes is due to the increased richness of the number of unique haplotypes, rather than their extent of similarity in relative abundances. Taken together, this pattern supports a continuous emergence and extinction of the gene alleles adaptive to virulence sink habitats of *E. coli*, rather than a one-time change in the habitat conditions. Thus, ecological methods of species diversity analysis can be successfully adapted to characterize the emergence of microbial virulence in bacterial pathogens subject to source–sink dynamics.

The enteric bacterium *K. pneumoniae* is an environmental organism that is also a frequent cause of sepsis, UTI and liver abscess. Type I fimbriae have been shown to be critical for the ability of *K. pneumoniae* to cause UTI in a murine model. Stahlhut *et al.* (2009) showed that the *K. pneumoniae fimH* gene is found in 90% of strains from various environmental and clinical sources. The *fimH* alleles exhibit relatively low nucleotide and structural diversity, but are prone to frequent horizontal transfer events between different bacterial clones. Addition of the *fimH* locus to MLST significantly improved the resolution of the clonal structure of pathogenic strains, including the K1-encapsulated liver isolates. In addition, the *K. pneumoniae* FimH protein is targeted by adaptive point mutations, although not to the same extent as FimH from UPEC or TonB from the same *K. pneumoniae* strains. Such adaptive mutations include a single amino acid deletion from the signal peptide that might affect the length of the fimbrial rod by affecting FimH translocation into the periplasm. Another FimH mutation (S62A) occurred in the course of endemic circulation of a nosocomial uropathogenic clone of *K. pneumoniae*. This mutation is identical to the one found in a highly virulent UPEC, suggesting that the FimH mutations are pathoadaptive in nature. Considering the abundance of type I fimbriae in *Enterobacteriaceae*, the finding, presented by Stahlhut *et al.* (2009), suggests that *fimH* genes are subject to adaptive microevolution, and substantiates the importance of type I fimbriae-mediated adhesion in *K. pneumoniae*.

Long polar fimbriae

The long polar fimbriae (Lpf) are one of a few adhesive factors of enterohemorrhagic *E. coli* O157:H7 associated with colonization of the intestine. *Escherichia coli* O157:H7 strains possess two *lpf* loci encoding highly regulated fimbrial structures. Database analysis of the genes encoding the major fimbrial subunits demonstrated that they are present in pathogenic *E. coli* (including commensal as well as intestinal and extraintestinal pathogenic *E. coli* isolates) and *Salmonella* strains, and that the *lpfA1* and *lpfA2* genes are highly prevalent among LEE-positive *E. coli* strains associated with severe and/or epidemic disease (Torres *et al.*, 2009). Further DNA sequence analysis of the *lpfA1* and *lpfA2* genes from different 'attaching and effacing' *E. coli* strains has led to the identification of several polymorphisms and the classification of the major fimbrial subunits into distinct variants (Torres *et al.*, 2009). Using collections of pathogenic *E. coli* isolates from Europe and Latin America, Torres *et al.* (2009) demonstrated that the different *lpfA* types are associated with the presence of specific intimin (eae) adhesin variants and that, most importantly, they are found in specific *E. coli* pathotypes. Their results showed that the use of these fimbrial genes as markers, in combination with the different intimin types, resulted in a specific test to identify *E. coli* O157:H7 from other pathogenic *E. coli* strains.

Induction of proinflammatory responses by polyadhesins

Afa/Dr polyadhesins

Afa/Dr diffusely adhering *E. coli* strains in polarized monolayers of intestinal T84 cells were able to promote the basolateral secretion of IL-8 through the activation of the mitogen-activated protein kinases (MAPK), including ERK1/2, p38 and SAPK/JNK (stress-activated protein kinase/c-Jun NH2-terminal kinases) kinases (Betis *et al.*, 2003a). IL-8 in turn induced the transmigration of PMNs across the epithelial monolayer (Betis *et al.*, 2003a). The PMNs' transepithelial migration induced epithelial synthesis of TNF-α and IL-1β, which in turn promoted the

upregulation of DAF, increasing the adhesion of Afa/Dr diffusely adhering *E. coli* bacteria (Betis *et al.*, 2003b). Moreover, upregulation of the inflammation-associated molecule, MICA, has been found in intestinal Caco-2 cells infected by AfaE-III-positive bacteria, an effect mediated by the specific interaction between bacterial adhesin and DAF (Tieng *et al.*, 2002).

Angiogenesis has been recently described as a novel component of inflammatory bowel disease pathogenesis. The level of vascular endothelial growth factor has been found to be increased in Crohn's disease and ulcerative colitis mucosa. To test whether a proinflammatory *E. coli* could regulate the expression of vascular endothelial growth factor in human intestinal epithelial cells, Cane *et al.* (2007) examined the response of cultured human colonic T84 cells to infection by *E. coli* strain C1845, which belongs to the typical Afa/Dr diffusely adhering *E. coli* family (Afa/Dr DAEC). Vascular endothelial growth factor mRNA expression was examined by Northern blotting and q-PCR. VEGF protein levels were assayed by ELISA and its bioactivity was analyzed in endothelial cells. The bacterial factor involved in vascular endothelial growth factor induction was identified by recombinant *E. coli* expressing adhesin Dr, purified adhesin Dr and lipopolysaccharide. The signaling pathway activated for the upregulation of vascular endothelial growth factor was identified by a blocking monoclonal anti-DAF antibody, Western blot analysis and specific pharmacological inhibitors. C1845 bacteria induced the production of vascular endothelial growth factor protein, which is bioactive. Vascular endothelial growth factor was induced by adhering C1845 in both a time- and bacteria concentration-dependent manner. This phenomenon was not cell line-dependent, as Cane *et al.* (2007) reproduced this observation in intestinal LS174, Caco2/TC7 and INT407 cells. Upregulation of vascular endothelial growth factor production requires:

(1) the interaction of the bacterial F1845 adhesin with the brushborder-associated CD55/DAF acting as a bacterial receptor;

(2) the activation of an Src protein kinase upstream of the activation of the Erk and Akt signaling pathways.

Results demonstrate that Afa/Dr diffusely adhering *E. coli* strain induces an adhesin-dependent activation of CD55/DAF signaling that leads to the upregulation of bioactive vascular endothelial growth factor in cultured human intestinal cells. Thus, these results suggest a link between an enteroadherent, proinflammatory *E. coli* strain and angiogenesis, which appeared recently as a novel component of inflammatory bowel disease pathogenesis.

Diard *et al.* (2006) showed that fragments of polyadhesin Dr are released in response to multiple environmental signals. Production and secretion of fragments of polyadhesin Dr are clearly regulated by temperature. Secretion of fragments of polyadhesin Dr is drastically increased during anaerobic growth in minimal medium. The secretion was maximal during the logarithmic-phase growth and corresponded to 27% and 57% of the total fimbriae Dr produced by bacteria grown in mineral medium with glucose and Luria–Bertani broth, respectively. Controlled release of fragments of polyadhesin Dr, which is carried out in the absence of cellular lysis, appears to be independent of the action of proteases or the process of maturation. The fragments of polyadhesin Dr secreted into the environmental medium by diffusely adhering *E. coli* strains can induce unproductive proinflammatory responses like the fragments of the F1 capsule scattered into cultural media by *Y. pestis* (see following section).

F1 antigen

Fragments of the recombinant F1 capsule of *Y. pestis* scattered into cultural media activate mice peritoneal macrophages *in vitro* (Sodhi *et al.*, 2004). The fragments of the F1 capsule induce the production of proinflammatory cytokines, TNF-α, IL-1 and IL-6. The activation suggests the involvement of nuclear factor (NF)-κB and MAPK pathways (Sodhi *et al.*, 2004; Sharma *et al.*, 2005a, b). Whereas IL-1β and F1 stimulate macrophages to produce various proinflammatory mediators via the same pathway (Kida *et al.*, 2005), *Yersinia* virulence factor, YopJ, which is essential for the death of infected macrophages, can block host proinflammatory responses by inhibiting both NF-κB and MAPK pathways (Zhou *et al.*, 2005). Lemaitre *et al.* (2006) confirmed that YopJ suppresses TNF-α induction and contributes to apoptosis of immune cells in the lymph node, but is not required for virulence in a rat model of bubonic plague.

Thus, during the early stage of infection, the type III secretion system and short nonaggregated F1 Ag act in concert: the former inhibits the production of proinflammatory cytokines and the latter inhibits binding of IL-1β to the host cell receptors. However, at the final stage of systemic infection, fragments of the F1 capsule from the disseminated bacteria can induce an unproductive proinflammatory response, contributing to toxic shock and death of the host. Sebbane *et al.* (2006) demonstrated that high NO levels induced during plague may also influence the developing adaptive immune response and contribute to septic shock.

Induction of proinflammatory responses by monoadhesins

P pili

Bergsten *et al.* (2005) uncovered a molecular cross-talk between innate immune Toll-like receptor (TLR) 4 binding bacterial lipopolysaccharide signaling and P-fimbrial-mediated attachment, which is lipopolysaccharide-independent.

Upon P-fimbrial attachment to its glycosphingolipid receptor, ceramide is released from the lipid part of the receptor; in particular, it has recently been shown that ceramide acts as an agonist of TLR4 and potentially acts as a signaling intermediate between TLR4 and the glycosphingolipid receptor (Fischer *et al.*, 2007). Activation of the TLR4 receptor by P-fimbrial attachment subsequently leads to the production of proinflammatory cytokines and chemokines (IL-6 and CXCL8, respectively) and recruitment of neutrophils (Bergsten *et al.*, 2005). Although this proinflammatory response is beneficial in initiating bacterial clearance, it also causes damage to the surrounding tissue and is associated with renal complications. As P fimbriae are implicated in triggering inflammation, it can be deduced that they may also contribute to the pathology and symptoms of acute pyelonephritis.

Function–structure classification of adhesive organelles assembled with the chaperone–usher machinery

The first classification of periplasmic chaperones and the organelles assembled by them was suggested by Zav'yalov *et al.* (1995b). For this, the 3D structure of the CaflM chaperone was reconstructed by computer modeling, using a primary structure homology between CaflM and PapD proteins, and the atomic coordinates obtained by the X-ray crystallography for PapD (Holmgren & Branden, 1989). In the 3D model of CaflM, an accessory sequence between Fl and Gl β-strands (as compared with PapD) was recognized. The sequences of 17 periplasmic chaperones known at that time were aligned and two families with specific structural properties were identified. It was found that the characteristic structural feature of the family of periplasmic chaperones with the accessory sequence (CaflM family) is the existence of solvent-exposed Cys residues in Fl and Gl β-strands that can form a disulfide bond in the putative binding site for organelle subunits. The specific functional property of the CaflM family is that it aids in the assembly of nonfimbrial surface structures or thin fibrillae of a simple composition (i.e. F1 and pH6 antigens of *Y. pestis* consist of only one subunit) in comparison with the chaperones of the PapD family, which aid in assembling of more complex thick fimbriae/pili (i.e. P pili are composed of seven different subunits).

Hung *et al.* (1996) studied 26 chaperones and defined proteins containing a relatively long F1–G1 loop as the FGL chaperone family and proteins with a short F1–G1 loop as the FGS chaperone family. These authors also revealed that the FGL chaperone family assembles nonfimbrial surface structures or thin fibrillae, composed of one to two subunits, whereas the FGS chaperone family assembles thick fimbriae/pili, composed of up to seven subunits.

Sequence comparison of 31 chaperones by the neighbor-joining method suggests that the classical chaperone/usher superfamily can be divided into several clades, each including members that apparently share a common ancestor not shared by proteins outside of the clade (Bonci *et al.*, 1997). This phylogenetic tree suggests that members of the FGL chaperone family (i.e. MyfB, PsaB, Caf1M, CS3-1, AggD, AfaB, NfaE, SefB and CssC) share a common ancestor. However, this analysis also shows that the FGS chaperone subfamily cannot be defined by a single node or branch on the phylogenetic tree, suggesting that further subdivision is needed to categorize explicitly the respective fimbriae into clades on the basis of common ancestry.

The next principal step in the development of a function/structure nomenclature of adhesive fimbrial organelles, assembled with the classical chaperone/usher machinery, was the discovery that FGL chaperone-assembled organelles possess a polyadhesive function (Zavialov *et al.*, 2007) in contrast to FGS chaperone-assembled monoadhesive thick fimbriae/pili, with one adhesive domain on the tip of the fiber.

Analysis of the currently available data suggests that the classical chaperone/usher machinery involves three distinct families and a few subfamilies of surface-exposed adhesive organelles that have unique functional and structural properties (Table 2).

The FGL chaperone-assembled adhesive organelles represent linear polymers of one or, in some cases, two distinct types of protein subunits. The characteristic feature of the organelles is that each protein subunit in the fiber possesses two independent binding sites, which are specific to different receptors on cells of the host. This architecture enables a single fiber to establish polyvalent contacts with receptors on the host cells. The FGL chaperone-assembled polyadhesins may be subdivided into three subfamilies (Table 2):

(1) FGL chaperone-assembled polyadhesins-1-1, where the first numeral shows that organelles of this subfamily are homopolymers composed of only one subunit. The second numeral indicates that assembly of the organelles is assisted by one chaperone.

(2) FGL chaperone-assembled polyadhesins-(1+1)-1, where the numerals in parentheses indicate that organelles of this subfamily are heteropolymers composed of two distinct subunits secreted via different pathways. One subunit is secreted via the classical chaperone/usher machinery, and another subunit is displayed on the tip of the fiber with the type II secretion system. The numeral outside the parentheses indicates that assembly of the organelles is assisted by one chaperone.

(3) FGL chaperone-assembled polyadhesins-2-1, where the first numeral shows that organelles of this subfamily are heteropolymers composed of two distinct subunits, both of which are secreted with the chaperone/usher machinery.

The second numeral shows that assembly of the organelles is assisted by one chaperone.

The majority of FGS chaperone-assembled adhesive fimbriae/pili are monoadhesins, which display only one adhesin domain on the tip of the pilus. The FGS chaperone-assembled monoadhesins may be subdivided into six subfamilies (Table 2):

(1) The subfamily of FGS chaperone-assembled monoadhesins-2-1 collects the structurally simplest monoadhesive organelles composed of two subunits, one of which is structural and another that contains the adhesive domain exposed on the tip of pili. Assembly of the organelles is assisted by one chaperone.

(2) The subfamily of FGS chaperone-assembled monoadhesins-3-1 includes the monoadhesive organelles composed of three subunits, two of which are structural and one contains the adhesive domain exposed on the tip of pili. Assembly of the organelles is also assisted by one chaperone.

(3) The subfamily of FGS chaperone-assembled monoadhesins-3-3 also represents the monoadhesive organelles composed of three subunits, two of which are structural and one of which is a specific adhesin exposed on the tip of pili. However, assembly of these organelles is assisted by three distinct chaperones.

(4) The subfamily of FGS chaperone-assembled monoadhesins-4-1 collects the monoadhesive organelles composed of four subunits, three of which are structural and one of which contains an adhesive domain exposed on the tip of pili. Assembly of the organelles is assisted by one chaperone.

(5) The subfamily of FGS chaperone-assembled monoadhesins-5-1 represents the monoadhesive organelles composed of five subunits, four of which are structural and one of which is a specialized adhesin exposed on the tip of pili. Assembly of the organelles is assisted by one chaperone.

(6) The subfamily of FGS chaperone-assembled monoadhesins-7-1 is the most complex subfamily of monoadhesive organelles, composed of seven subunits, six of which are structural and one of which is a specialized adhesin exposed on the tip of pili. Assembly of the organelles is assisted by one chaperone.

However, the FGS chaperone-assembled thin flexible pili F4 (K88), F5 (K99) and Lda of *E. coli*, PE fimbriae of *S. typhimurium*, atypical fimbriae ACIAD of *Acinetobacter* sp. and ATF of *P. mirabilis* are an exception, as they do not display specialized adhesive domains on the tip of the pilus, but carry a binding site on their main structural subunit (FaeH, FanH and LdaH) or are composed of only one structural subunit functioning as an adhesin subunit (ACIAD122, AtfA and PefA). This architecture enables a single fiber to establish polyvalent contacts with receptors on the host cells. We have therefore called this family FGS chaperone-assembled polyadhesins. These polyadhesins may be subdivided into five subfamilies (Table 2):

(1) The subfamily of FGS chaperone-assembled polyadhesins-1-1 collects the polyadhesive homopolymers. Assembly of the organelles is assisted by one chaperone.

(2) The subfamily of FGS chaperone-assembled polyadhesins-1-2 also represents the polyadhesive homopolymer. However, assembly of the fiber is assisted by two distinct chaperones.

(3) The subfamily of FGS chaperone-assembled polyadhesins-3-1 includes the heteropolymer composed of three distinct subunits. The organelle carries a binding site on its main structural subunit. Assembly of the polyadhesin is assisted by one chaperone.

(4) The subfamily of FGS chaperone-assembled polyadhesins-4-1 includes the heteropolymer composed of four distinct subunits. The organelle carries a binding site on its main structural subunit. Assembly of the polyadhesin is assisted by one chaperone.

(5) The subfamily of FGS chaperone-assembled polyadhesins-5-1 includes the heteropolymers composed of five distinct subunits. The organelles carry a binding site on their main structural subunit. Assembly of the polyadhesins is assisted by one chaperone.

Phylogenesis of the classical chaperone/usher gene clusters

It is very interesting to compare the suggested functional–structural nomenclature of adhesive organelles, assembled with the classical chaperone/usher machinery, and their phylogenetic classification.

Sequence comparison of chaperones (Bonci *et al.*, 1997) may not be ideally suited for developing a phylogenetic subdivision because some fimbrial operons encode more than one chaperone, thus raising the question as to which protein should be used to assign the respective operon to a phylogenetic group. Therefore, comparison of usher sequences has been used to derive phylogenetic trees of members of the chaperone/usher assembly class (Yen *et al.*, 2002; Anantha *et al.*, 2004). This approach has the advantage that the resulting definition of phylogenetic groups is unambiguous because all fimbrial operons belonging to the chaperone/usher assembly class contain only a single usher gene. An initial comparison of 58 members of the fimbrial usher protein (FUP) superfamily distinguished 10 clusters on the basis of common ancestry (Yen *et al.*, 2002). A revised phylogenetic tree of the FUP superfamily constructed by comparing 189 proteins is shown in Fig. 13 (Nuccio & Bäumler, 2007). The phylogenetic analysis of 189 usher proteins suggests a classification into clades, which is similar, but not identical to that proposed based on the analysis of 58 usher proteins (Yen *et al.*, 2002). Nuccio & Bäumler (2007) proposed a nomenclature using Greek letters to refer to individual clades. Using a node-based

Table 2. Function–structure classification of superfamily of adhesive fimbrial organelles assembled on the Gram-negative pathogen cell surface via classical chaperone/usher pathway.

Subfamilies	Function	Morphology	Chaperones	No. of subunits	Adhesin subunits
Family 1: Polyadhesins					
Subfamily 1.1: FGL chaperone-assembled polyadhesins-1*-1†	Polyadhesive binding	From thin flexible fibers (2 nm diameter) observed for Psa fimbriae to amorphous or capsule-like morphology for F1 antigen (by electron microscopy)	Caf1M, CS3-E, MyfB, NfaE, PsaB	1	The main structural subunit: Caf1, CS3, MyfA, NfaA, PsaA.
Subfamily 1.2: FGL chaperone-assembled polyadhesins-(1+1‡)-1	Polyadhesive binding	Thin flexible fibers (2 nm diameter) were observed for Dr adhesin by electron microscopy	AafD, Afa-3B, Afa-8B, AggD, Agg-3D, DaaB, DafaB, DraB	2	The main structural subunit: AafA, Afa-3E, Afa-8E, AggA, Agg-3A, DaaE, DafaE, DraE. Additional subunit (AafD, Afa-3D, Afa-8D, AggD, Agg-3D, DaaD, DafaD, DraD) is displayed on the tip of the fiber with Type II secretion system.
Subfamily 1.3: FGL chaperone-assembled polyadhesins-2-1	Polyadhesive binding	Atypical fimbrial structures	SafB, SefB, CssC	2	The main structural subunits: CssA, CssB; SafA, SefA. SafD and SefD subunits might be displayed on the tip of the fiber.
Subfamily 1.4: FGS chaperone-assembled polyadhesins-1-1	Polyadhesive binding	Thin flexible pili with a poorly defined diameter (2–4 nm, Pef pili) or atypical fimbria (Atf)	AtfB, PefD	1	The main structural subunit: AtfA, PefA.
Subfamily 1.5: FGS chaperone-assembled polyadhesins-1-2	Polyadhesive binding	ND§	ACIAD0120, ACIAD0123	1	The main structural subunit ACIAD0122.
Subfamily 1.6: FGS chaperone-assembled polyadhesins-3-1	Polyadhesive binding§	AF/R1 pili	AfrC	3	The main structural subunit AfrE§.
Subfamily 1.7: FGS chaperone-assembled polyadhesins-4-1	Polyadhesive binding	Thin flexible pili with a poorly defined diameter (2–4 nm, K88 pili)	FanE	4	The main structural subunit FanH.
Subfamily 1.8: FGS chaperone-assembled polyadhesins-5-1	Polyadhesive binding	Thin flexible pili with a poorly defined diameter (2–4 nm, K99 pili)	FaeE, LdaE, RalE	5	The main structural subunit FaeH, LdaH, RalG§.
Family 2: Monoadhesins					
Subfamily 2.1: FGS chaperone-assembled monoadhesins-2-1	Monoadhesive binding	Thin pili	AcuD, F17D, FimB	2	One domain (adhesin) on the tip: AcuG, F17G, FimD.
Subfamily 2.2: FGS chaperone-assembled monoadhesins-3-1	Monoadhesive binding	Fimbriae/pili	HifB, HafB, MrkB, LpfB, PmfD	3	One domain (adhesin) on the tip: AfrE, HifE, HafE, MrkD, LpfE, PmfE.
Subfamily 2.3: FGS chaperone-assembled monoadhesins-3-3	Monoadhesive binding	Fimbriae/pili	FasB, FasC, FasE; CswB, CswC, CswE; FotB, FotC, FotE	3	One domain (adhesin) on the tip: FasG, CswG, FotG.
Subfamily 2.4: FGS chaperone-assembled monoadhesins-4-1	Monoadhesive binding	Fimbriae/pili	FocC, StfD	4	One domain (adhesin) on the tip: FocH, StfG.
Subfamily 2.5: FGS chaperone-assembled monoadhesins-5-1	Monoadhesive binding	Fimbriae/pili	FimC, SfpD, SfaE, MrpD	5	One domain (adhesin) on the tip: FimH, SfpG, SfaH, MrpH.
Subfamily 2.6: FGS chaperone-assembled monoadhesins-7-1	Monoadhesive binding	Fimbriae/pili	MrfD, PapD	7	One domain (adhesin) on the tip: MrfH, PapG.

*Number of different types of subunits secreted via the classical chaperone/usher pathway.
†Number of periplasmic chaperones assisting assembly of fiber.
‡Additional subunit displayed on the tip of the fiber with the type II secretion system.
§Based on high homology of the *ral* and *afr* gene clusters with the *fae* cluster.

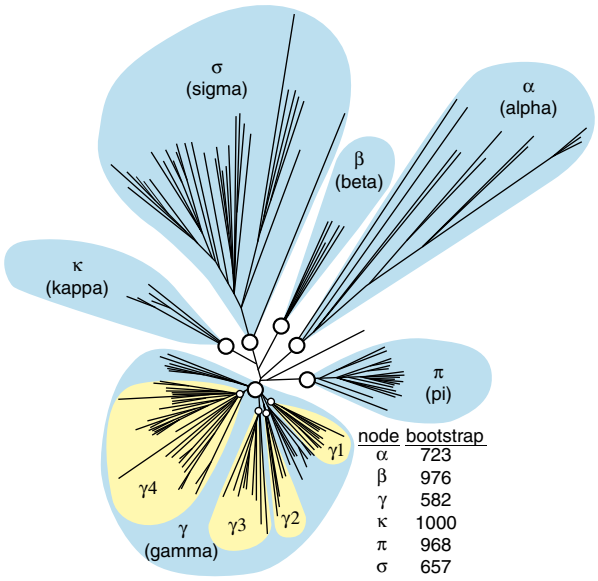

Fig. 13. Phylogenetic tree of the FUP family (the redrawing is based on Nuccio & Bäumler, 2007). The graph shows an unrooted phenogram generated using analysis of amino acid sequences of 189 ushers (Nuccio & Bäumler, 2007). Ushers are grouped into six fimbrial clades (highlighted in light blue) termed α-, β-, γ-, κ-, π- and σ-fimbriae. Ushers of the γ-clade are subdivided into four clades (highlighted in yellow) termed γ1-, γ2-, γ3- and γ4- fimbriae. Bootstrap values of nodes defining these clades (indicated by open circles at the base of each fimbrial clade) are shown. For details of generation of the phylogenetic tree and bootstrap values, see Nuccio & Bäumler (2007).

definition, the FUP superfamily can be divided into six clades, designated α-, β-, γ-, κ-, π- and σ-fimbriae, each stemming from a common ancestor represented by a node in the phylogenetic tree (Fig. 13). The γ-fimbrial clade is further subdivided into four clades, termed γ1-, γ2-, γ3- and γ4-fimbriae. Nuccio & Bäumler (2007) arbitrarily assigned α-, β-, γ-, κ-, π- and σ-fimbrial clade names to denote a particular characteristic of the clade or a prominent member as follows: α-fimbriae, alternate chaperone/usher family; κ-fimbriae, K88 (F4) fimbriae; π-fimbriae, pyelonephritis-associated fimbriae (P fimbriae); and σ-fimbriae, spore coat protein U from *Myxococcus xanthus*. The β- and γ-fimbriae were assigned names alphabetically. This subdivision of the FUP superfamily largely confirms the subdivisions proposed initially (Yen *et al.*, 2002), but former FUP clusters 4 and 5 now form a single clade (γ3-fimbriae). The subdivision of the chaperone/usher class into six FUP clades confirms that the alternate chaperone/usher family (α-fimbriae) (Anantha *et al.*, 2004) contains operons that stem from a common ancestor (Fig. 13; Nuccio & Bäumler, 2007). The FGL chaperone-assembled family of polyadhesins forms a monophyletic group (γ3-fimbriae) within the classical chaperone/usher family (Zav'yalov *et al.*, 1995b; Hung *et al.*, 1996). However, the FGS chaperone-assembled family of adhesive organelles is composed of several clades (β-, γ1-, γ2-, γ4-, κ- and π-fimbriae) that are not more closely related to each other than to the FGL chaperone-assembled family of polyadhesins (γ3-fimbriae). The analysis also reveals the existence of a major FUP clade (σ-fimbriae) that was represented only by two usher proteins in a previous analysis (Yen *et al.*, 2002) and whose members share limited or no sequence homology to members of the alternate chaperone/usher family (α-fimbriae) or the classical chaperone/usher family (β-, γ-, κ- and π-fimbriae).

The utility of delineating the genealogy of gene clusters that encode fimbrial adhesins lies in its value for predicting their evolutionary relationship. For instance, gene clusters of the γ3- and κ-fimbrial clades, identified by Nuccio & Bäumler (2007), encode exclusively FGL and FGS chaperone-assembled polyadhesins, respectively, whereas gene clusters belonging to the α-, γ1-, γ2-, γ4- and π-fimbrial clades exclusively encode monoadhesins. When the most common gene clusters within each clade are placed at the end of each of the corresponding branches on the FUP tree, an evolutionary scenario explaining the divergence of gene clusters from a common precursor can be derived. The exact relationship between major clusters in the FUP tree (Fig. 13; Nuccio & Bäumler, 2007) is not clear at present, as the nodes connecting α-, β-, γ-, κ-, π- and σ-fimbrial clades are supported by low bootstrapping values. However, the gene clusters of κ- and π-fimbriae are related to each other, as both share a core structure composed of genes encoding a major subunit, an usher and a chaperone. Furthermore, a close relationship of the γ-fimbriae with the κ- and π-fimbriae is indicated by the presence of a PFAM00419 domain exclusively in subunits of gene clusters belonging to these three clades (Nuccio & Bäumler, 2007). These data suggest that members of the γ-, κ- and π-fimbrial clades form a monophyletic group, which will be referred to as the γκπ cluster from here on. The γκπ cluster and the β-fimbriae together constitute the previously defined classical chaperone/usher superfamily.

The FGL chaperone-assembled polyadhesins that correspond to γ3-fimbriae (Fig. 14; Nuccio & Bäumler, 2007) constitute the adhesive organelles, which consist of only one or two distinct types of subunits, and at a low resolution, typically have a nonpilus, amorphous or capsule-like morphology (Hung *et al.*, 1996; Soto & Hultgren, 1999; Zavialov *et al.*, 2003, 2005, 2007; Anderson *et al.*, 2004a, b; Pettigrew *et al.*, 2004; Westerlund-Wikström & Korhonen, 2005; Korotkova *et al.*, 2006a, b, 2008a, b; Remaut *et al.*, 2006; Li *et al.*, 2007; Verger *et al.*, 2007; Salih *et al.*, 2008). Their notable property is that all subunits possess two independent binding sites specific to different host-cell receptors. In particular, DraE/AfaE/DaaE subunits of the Dr/Afa polyadhesins have two independent binding sites to CD55/DAF

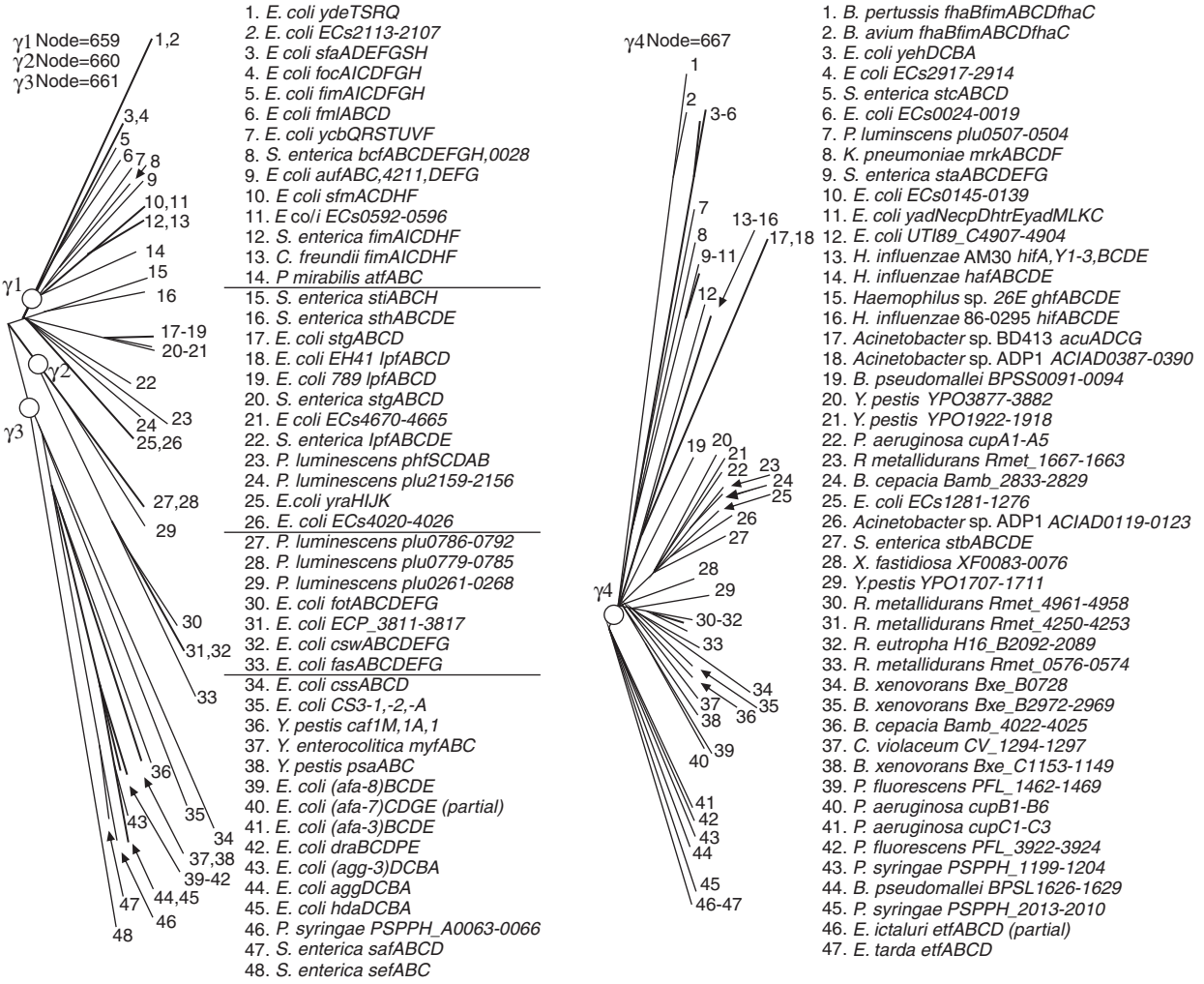

Fig. 14. Phylogenetic relationship of operons belonging to the γ1-, γ2-, γ3- and γ4-fimbriae (redrawing based on Nuccio & Bäumler, 2007). The branch of the FUP tree representing γ1-, γ2-, γ3- and γ4-fimbriae is shown on the left. The bootstrap value for the node defining each subclade is displayed at the top and was generated in the analysis performed for this figure. Numbers at the end of each branch of the phylogenetic tree correspond to the numbers given for each operon on the right.

and CEACAMs (Fig. 9; Anderson *et al.*, 2004a, b; Pettigrew *et al.*, 2004; Korotkova *et al.*, 2006a, b, 2008a). The PsaA subunit of the pH6 antigen binds to the β1-linked galactosyl residue of glycosphingolipids (Payne *et al.*, 1998) and to the phosphorylcholine moiety of phosphatidylcholine (Galván *et al.*, 2006) as the host-cell receptors.

The κ-clade (Fig. 15; Nuccio & Bäumler, 2007) comprises all subfamilies of the FGS chaperone-assembled polyadhesins, in particular, the FGS chaperone-assembled polyadhesins-1-1 (Pef pili), -3-1 (AF/R1 pili), -4-1 (K88 pili) and -5-1 (K99 pili, REPEC fimbriae and afimbrial adhesin, encoded by the locus for diffuse adherence, *lda*). Like the FGL polyadhesive fibers, the FGS polyadhesins carry a binding site on their main structural subunit (FaeH, FanH and LdaH) or are composed of only one structural subunit functioning as an adhesin subunit (ACIAD122 and PefA). In contrast to monoadhesive pili, which possess only one binding domain on the tip of the pilus (Fig. 12a), each polyadhesive fiber might potentially (Fig. 12b) ensure powerful polyvalent fastening of a bacterial pathogen to a host target cell (Galván *et al.*, 2006), as well as aggregate host-cell receptors by a zipper-like mechanism that triggers transduction of signals, causing immunosuppressive and proinflammatory responses (Sodhi *et al.*, 2004; Sharma *et al.*, 2005a, b; Galván *et al.*, 2006).

The γ2 clade (Fig. 14; Nuccio & Bäumler, 2007) corresponds to the FGS chaperone-assembled monoadhesins-3-3, which represent the monoadhesive organelles composed of three subunits, two of which are structural and one of which is a specific adhesin exposed on the tip of pili. Assembly of these organelles is assisted by three distinct chaperones. Although the FasB, CswB and FotB chaperones belong to

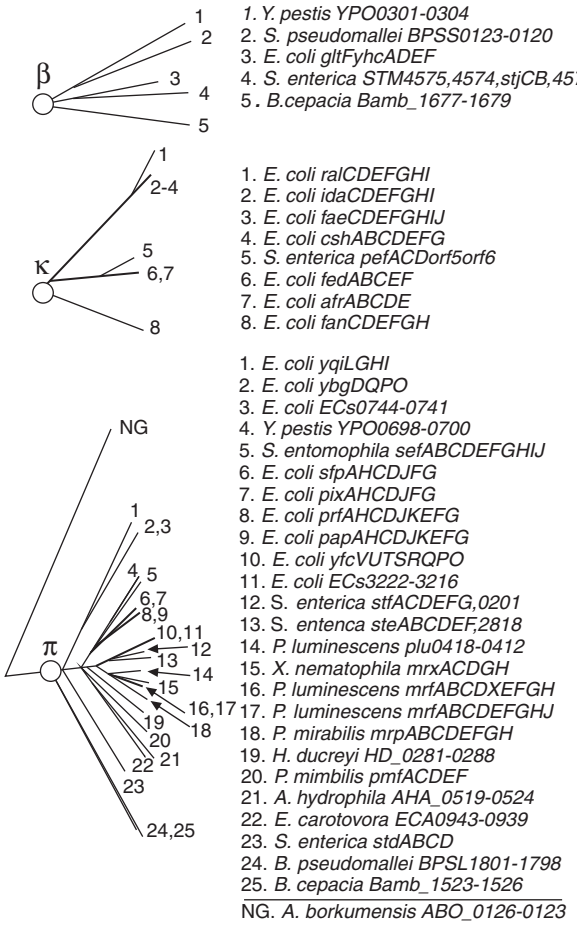

Fig. 15. Phylogenetic relationship of operons belonging to the β-, κ- and π-fimbriae (the redrawing is based on Nuccio & Bäumler, 2007). The branch of the FUP tree representing β-, κ- and π-fimbriae is shown on the left. The bootstrap value for the node defining each subclade is displayed at the top and was generated in the analysis performed for Fig. 14. Numbers at the end of each branch of the phylogenetic tree correspond to the numbers given for each operon on the right.

the FGS family, they have the same length of the F1–G1 loop as the CssC1 and CssC2 chaperones of the FGL family (see Fig. 4).

The γ1-clade (Fig. 14; Nuccio & Bäumler, 2007) comprises some of the members of the FGS chaperone-assembled monoadhesins-3-1, 4-1 and 5-1; however, the ambient-temperature fimbriae (Atf) of *P. Mirabilis*, related to the FGS chaperone-assembled polyadhesins-1-1, are the exception. Like most of the FGL chaperone-assembled polyadhesins, Atf fimbriae are polyadhesive homopolymers.

The γ4-clade (Fig. 14; Nuccio & Bäumler, 2007) includes some of the members of the FGS chaperone-assembled monoadhesins-2-1, -3-1, -4-1 and -5-1.

The π-clade (Fig. 15; Nuccio & Bäumler, 2007) consists of some of the members of the FGS chaperone-assembled monoadhesins-3-1, -4-1, -5-1 and -7-1.

The remarkable feature of the κ- and π-gene clusters is the location of the gene encoding the chaperone after the gene encoding the usher, whereas in the γ-cluster the gene encoding the chaperone precedes the gene encoding the usher. This finding underlines closer phylogenetic relationships between κ- and π-clusters of genes than with the γ-clusters.

Applications of adhesive organelles assembled with the chaperone–usher machinery

Applications of polyadhesins

Applications of polyadhesins for vaccine design

Antiplague vaccines based on the recombinant F1 antigen or on peptides from the F1 antigen

Yersinia pestis, the causative agent of pneumonic plague, is a rapidly progressing and exceptionally virulent disease (reviewed by Cleri *et al.*, 1997; Perry & Fetherston, 1997; Smiley, 2008a, b). Extensively antibiotic-resistant strains of *Y. pestis* exist and a safe and effective pneumonic plague vaccine is currently lacking (Smiley, 2008a, b). This raises concerns that *Y. pestis* may be exploited as a biological weapon.

F1 antigen is the major or single protective component of the current human whole-cell vaccines against plague (Li *et al.*, 2005; Li & Yang, 2008; Smiley, 2008a, b). However, this vaccine is ineffective against pneumonic plague caused by typical $F1^+$ strains of *Y. pestis* (Heath *et al.*, 1998). It is also ineffective against $F1^-$ *Y. pestis* strains, which have been isolated from one human patient and from several rodents. For these reasons, new recombinant plague vaccines comprising Caf1 and V antigens of *Y. pestis* are under development.

Heath *et al.* (1998) developed a recombinant vaccine composed of a fusion protein of F1 with a second protective immunogen, V antigen. V antigen is an essential virulence factor and mediator of immunity common for *Yersinia*. It plays a crucial role in the functioning of the type III secretion system. This protein forms a distinct structure at the tip of the injectisome needle (Mueller *et al.*, 2005). Derewenda *et al.* (2004) solved the 3D structure of V antigen with high-resolution X-ray analysis. The developed recombinant F1-V fusion vaccine protected mice against pneumonic as well as bubonic plague produced by either an $F1^+$ or $F1^-$ strain of *Y. pestis* and provided a better protection than recombinant F1 or recombinant V alone against the $F1^+$ strain. Therefore, the recombinant proteins serve as the basis of an improved human antiplague vaccine (Heath *et al.*, 1998).

Powell *et al.* (2005) re-engineered a two-component F1-V fusion protein antigen and tested it as a medical countermeasure against the possible biological threat of aerosolized

Y. pestis. As formulated with aluminum hydroxide adjuvant and administered in a single subcutaneous dose, this new F1-V fusion protein also protected mice from wild-type and nonencapsulated *Y. pestis* challenge strains, modeling prophylaxis against pneumonic and bubonic plague. Jones *et al.* (2006) found that the rF1–V antigen given intramuscularly with Alhydrogel adjuvant protects mice against the challenge, but is less effective in nonhuman primates against high-dose aerosolized *Y. pestis*, perhaps because the antigen fails to induce respiratory immunity. Mice immunized intranasally with rF1–V formulated with a proteosome-based adjuvant (ProtollinTM) were 100% protected against aerosol challenge with 170 LD_{50} of *Y. pestis* and 80% protected against 255 LD_{50} (Jones *et al.*, 2006). Indeed, the examination of different prime-boost regimens with rF1–V demonstrated that inclusion of an appropriate adjuvant is critical for nonparenteral immunization (Glynn *et al.*, 2005). In view of the extraordinary potency of flagellin as an inducer of innate immunity and the contribution of innate responses to the development of adaptive immunity, Honko *et al.* (2006) evaluated the efficacy of recombinant *Salmonella* flagellin as an adjuvant in subunit antiplague vaccine. Mice immunized intranasally or intratracheally with the F1 antigen and flagellin exhibited dramatic increases in anti-F1 plasma IgG titers that remained stable over time. Importantly, intranasal immunization with flagellin and the F1 antigen was protective against intranasal challenge with virulent *Y. pestis* CO92, with 93–100% survival of immunized mice. Vaccination of *Cynomolgus* monkeys with flagellin and the rF1–V fusion protein induced a robust antigen-specific IgG antibody response. Alvarez *et al.* (2006) developed a novel production and delivery system for an antiplague vaccine of the rF1–V fusion protein expressed in tomato. The immunogenicity of the rF1–V transgenic tomatoes was confirmed in mice that were primed subcutaneously with bacterially produced rF1–V and boosted orally with transgenic tomato fruit. Expression of the plague antigens in fruit made it possible to produce an oral vaccine candidate without protein purification and with minimal processing technology. The recombinant plague antigens F1, V and fusion protein F1-V were produced by transient expression in *Nicotiana benthamiana* using a reconstructed tobacco mosaic virus-based system that allowed very rapid and extremely high levels of expression (Santi *et al.*, 2006). All of the plant-derived purified antigens administered subcutaneously to guinea pigs generated systemic immune responses and provided protection against an aerosol challenge of virulent *Y. pestis*. Chichester *et al.* (2009) reported a plague vaccine consisting of the F1 and LcrV antigens fused to a single carrier molecule, the thermostable enzyme lichenase from *Clostridium thermocellum*, and expressed in and purified from *N. benthamiana* plants. When administered to *Cynomolgus* Macaques, this purified plant-produced vaccine induced high titers of serum IgG, mainly of the IgG1 isotype, against both F1 and LcrV. These immunized animals were subsequently challenged and the LcrV-F1 plant-produced vaccine conferred complete protection against aerosolized *Y. pestis*. Del Prete *et al.* (2009) produced F1 and V antigens in *N. benthamiana* and F1-V fusion protein and administered them to guinea pigs; the result was immunity and protection against an aerosol challenge of virulent *Y. pestis*. They examined the effects of plant-derived F1, V and F1-V on human cells on the innate immunity. F1, V and F1-V proteins engaged TLR2 signaling and activated IL-6 and CXCL-8 production by monocytes, without affecting the expression of TNF-α, IL-12, IL-10, IL-1β or CXCL10. Native F1 antigen and plant-derived rF1 and rF1-V all induced similar specific T-cell responses, as shown by their recognition by T-cells from subjects who recovered from *Y. pestis* infection. Native F1 and rF1 were equally well recognized by serum antibodies of *Y. pestis*-primed donors, whereas serological reactivity to rF1-V hybrid was lower, and that to rV was virtually absent. In conclusion, plant-derived F1, V and F1-V antigens are weakly reactogenic for human monocytes and elicit cell-mediated and humoral responses similar to those raised by *Y. pestis* infection.

The subunit vaccine involving a mixture of recombinant F1 and V antigens protects mice against exposure to 4104 CFUs of virulent plague organisms (100 LD_{50} doses), whereas the whole cell vaccine provided only 50% protection against 1.8–103 CFU (Williamson *et al.*, 1997). The enhanced protective efficacy of this subunit vaccine over existing vaccines has been demonstrated in an animal model of pneumonic plague. Bronchopulmonary administration of the combined subunits (1 mg V plus 5 mg F1) entrapped within microspheres composed of a biodegradable polyester (poly-L-lactide) elicits a level of protective immunity against systemic plague infection similar to that evoked by injecting co-encapsulated subunits into the muscle (Eyles *et al.*, 2000). Such findings indicate that introduction of appropriately formulated F1 and V subunits into the respiratory tract may be an alternative to parenteral immunization schedules for protecting individuals from plague (Eyles *et al.*, 2000). Elvin *et al.* (2006) individually encapsulated the recombinant F1 and V antigens in polymeric microspheres; the same antigen was adsorbed to the surface of these microspheres. Virulent challenge experiments showed that noninvasive immunization by intranasal instillation can provide strong systemic and local immune responses and protect against high-level challenge. Recently, Thomas *et al.* (2009) reported that the pathogenesis patterns of plague infections caused by the deposition of 1- and 12-μm particle aerosols of *Y. pestis* in the lower and upper respiratory tracts (URTs) of mice are different. The median lethal dose for

12-μm particles was 4.9-fold higher than that for 1-μm particles. The 12-μm particle infection resulted in the degradation of the nasal mucosa and nasal-associated lymphoid tissue (NALT) plus cervical lymphadenopathy before bacteremic dissemination. Lung involvement was limited to secondary pneumonia. In contrast, the 1-μm particle infection resulted in primary pneumonia; in 40% of mice, the involvement of NALT and cervical lymphadenopathy were observed, indicating entry via both URT lymphoid tissues and lungs. Despite bacterial deposition in the gastrointestinal tract, the involvement of Peyer's patches was not observed in either infection. Although there were major differences in pathogenesis, the recombinant F1 and V antigen vaccine and ciprofloxacin protected against plague infections caused by small- and large-particle aerosols.

Human immune response to the recombinant plague vaccine comprising F1 and V antigens was assessed during a phase 1 safety and immunogenicity trial in healthy volunteers (Williamson *et al.*, 2005). All the subjects produced specific IgG in serum after the priming dose, which peaked in value after the booster dose (day 21). However, no significant vaccination-related change in activation of peripheral blood mononuclear cells was detected at any time. Thus, any evidence on the cell immune response to recombinant F1 and V antigens is missing. Williamson *et al.* (2005) suppose that it may be associated with the immunosuppressive action of these antigens. De Bord *et al.* (2006) therefore designed the recombinant V10 (rV10) variant lacking residues 271–300. This variant does not suppress the release of proinflammatory cytokines by immune cells. In contrast to *Y. pestis* LcrV, the immunization with rV10 generates robust antibody-induced protective responses against bubonic plague and pneumonic plague, suggesting that rV10 may serve as an improved component of antiplague vaccine.

The antigen structure may critically influence the protective immune responses (Watts, 2004). The data on the structural and thermodynamic properties of Caf1 (Zavialov *et al.*, 2003, 2005) can explain the failure to induce the cell immune response to this antigen. The structurally observed complete collapse of the donor-strand-complemented fiber Caf1 subunit results in a dramatic increase in the enthalpy and transition temperature for the melting of the fiber module (Zavialov *et al.*, 2005). The collapse of the hydrophobic core of subunits shifts the equilibrium toward fiber formation (Zavialov *et al.*, 2003, 2005). As a result, the temperature of melting of the fiber subunit increases to as high as 90 °C (Zavialov *et al.*, 2005). The subunit preserves practically the same stability at pH 2.4 (Fooks *et al.*, pers. commun.). It can be deduced that such a high stability can reduce the processing of Caf1 antigen in macrophages to CD4 T cell epitopes and therefore abolish cellular immune responses. Indeed, Musson *et al.* (2006) found that optimal T-cell responses required significantly extended exposure of antigen-presenting cells to highly stable polymeric Caf1 compared with Caf1 that was depolymerized and destabilized by heating. Destabilization of Caf1 caused a shift toward presentation by mature major histocompatibility complex class II and toward independence of low pH and proteolytic processing. The unusually high thermodynamic and kinetic stability is probably universal to adhesive organelles assembled with the chaperone/usher machinery. Erilov *et al.* (2007) and Puorger *et al.* (2008) identified the most kinetically stable, non-covalent protein complex known to date. The complex between the pilus subunit FimG and the donor strand peptide of the subunit FimF of the adhesive Type 1 pili shows an extrapolated dissociation half-life of 3×109 years. The 15 residue peptide forms ideal intermolecular beta sheet H-bonds with FimG over 10 residues, and its hydrophobic side chains strongly interact with the hydrophobic core of FimG. The results show that kinetic stability and non-equilibrium behavior in protein folding confers infinite stability against dissociation in extracellular protein complexes.

An attempt to overcome low proteolytic processing of highly stable native Caf1 involved the development of an antiplague vaccine based on the peptide conjugates made between different B- and T-cell epitopes of F1 antigen of *Y. pestis* (Sabhnani & Rao, 2000; Sabhnani *et al.*, 2003; Tripathi *et al.*, 2006). Intranasal immunization generated consistently high titers and a long-lasting immune response for both IgG and IgA in sera and secreted IgA in washes, whereas the intramuscular route generated peak IgG levels in sera only. *In vivo* protective studies showed that B1–T1 and B2–T1 peptide conjugates protected mice till day 15.

Antiplague passive immunization with monoclonal antibodies against the F1 antigen

The newest antiplague vaccines based on the F1 and V antigens provide a high degree of protection. However, they must be administered several weeks before exposure to prevent plague. It is unlikely that vaccines will provide postexposure protection against plague. As an alternative to vaccines, passive immunization with monoclonal antibodies against the F1 protein, has been demonstrated to be effective in mice for protection from fatal bubonic and pneumonic plague (Anderson *et al.*, 1997). Moreover, Hill *et al.* (2003) showed that intraperitoneal injection of monoclonal antibodies that target the F1 and LcrV proteins protected mice in a synergistic manner used as either a pretreatment or a postexposure therapy. Recently, Hill *et al.* (2006) demonstrated that intratracheal delivery of aerosolized monoclonal antibodies with specificity for LcrV and F1 antigens protected mice in a model of pneumonic plague. These data support the utility of inhaled antibodies as a fast-acting

postexposure treatment for plague. The efficacy of passive immunization with monoclonal IgG antibodies specific for Caf1 suggests that opsonization is a major mechanism to overcome the resistance of *Y. pestis* to phagocytosis conferred by the Caf1 capsule.

Application of polyadhesin Saf for design of *Salmonella* vaccine

Typhoid fever caused by *S. enterica* serovar Typhi (*S.* Typhi), which is a predominantly human pathogen, remains a burdensome problem in India and worldwide (Crump *et al.*, 2004; Hamid & Jain, 2007). The mortality rates in untreated typhoid fever infections can be 10–15%. There are an estimated 20 million cases and 200 000 deaths resulting from this infection worldwide each year (Crump *et al.*, 2004). In some instances patients recover but remain carriers of the bacteria for many years. Another clinical syndrome associated with *Salmonella* infection is nontyphoidal salmonellosis – a gastrointestinal disease also known as enteritis. Components of the *Salmonella* atypical fimbriae (Saf) were investigated for inclusion in a vaccine (Strindelius *et al.*, 2004). A complex of recombinant SafB chaperone with SafD adhesin was expressed in *E. coli* and purified. Starch microparticles were used as the adjuvant. The recombinant cholera toxin B subunit (rCTB) was included as mucosal antigen-uptake enhancer. BALB/c mice were immunized orally or subcutaneously with SafB/D- and rCTB-conjugated microparticles and intranasally or subcutaneously with SafB/D mixed with rCTB. The systemic and mucosal immune responses were studied. An oral challenge with *S. enteritidis* was performed. All the immunized groups, except the group receiving oral immunization, responded with high IgM–IgG titers to SafB/D. Analysis of the subclass ratio (IgG1/IgG2a1IgG2b) indicated a mixed Th1 and Th2 response, with Th1 predominating. Only the group receiving intranasal immunization showed the mucosal response, measured as specific IgA/total IgA (from fecal samples), which was significantly higher than that in the untreated control group ($P < 0.05$). Spleens were removed 6 days after oral challenge and *Salmonella* CFU were counted. The group immunized subcutaneously with SafB/D- and rCTB-conjugated microparticles had significantly lower CFU counts than the untreated control group ($P < 0.05$).

Application of *sefA* gene for the design of a live recombinant *Salmonella* vaccine

Lopes *et al.* (2006) cloned the *sefA* gene, which encodes the main subunit of the SEF14 fimbrial protein, into a temperature-sensitive expression vector and transformed it into a nonpathogenic, avirulent strain of *E. coli*. The recombinant strain was used as a vaccine to elicit a specific immune response against the SefA protein of *S. enteritidis* in 1-day-old chickens. The recombinant strain was reisolated from the intestines of treated birds up to 21 days after treatment, demonstrating its ability to colonize the intestinal tracts of 1-day-old chickens. In addition, IgA against the SefA protein was detected by ELISA in intestinal secretions from treated birds 7 days after treatment and in bile samples 14–21 days after treatment. Nontreated birds did not show any evidence of intestinal colonization by the recombinant strain or anti-SefA IgA response in their bile or intestinal secretions. Thus, the preliminary evaluation of the recombinant strain showed a potential use of this strain to elicit protection against *S. enteritidis* infection in chickens.

Vaccination with *E. coli* polyadhesin Dr against chronic UTI

Escherichia coli expressing Dr fimbria and related adhesins are associated with UTI, including cystitis and/or pyelonephritis and diarrhea. Children and pregnant women are prone to recurrent or persistent infections caused by these organisms (Garcia *et al.*, 1996). Goluszko *et al.* (2005) used purified *E. coli* Dr fimbrial antigen to vaccinate C3H/HeJ mice against an experimental UTI due to a homologous strain bearing Dr polyadhesins. They demonstrated reduced mortality in the vaccinated animals. Immune sera with high titers of anti-Dr antibody inhibited bacterial binding to bladders and kidneys, but did not affect the rate of renal colonization.

Oral vaccination with *E. coli* F4 (K88) polyadhesive fimbriae against intestinal infection

ETEC is the leading cause of diarrhea in piglets and newborn calves. Massive efforts have therefore been made to develop a vaccine for the induction of protective mucosal immunity against ETEC. Verdonck *et al.* (2009) showed that as a result of oral immunization of piglets with F4 fimbriae purified from pathogenic ETEC, the fimbriae bind to the F4 receptor (F4R) in the intestine and induce a protective F4-specific immune response. F4 fimbriae are very stable polymeric structures composed of some minor subunits and a major subunit FaeG that is also the fimbrial adhesin. Verdonck *et al.* (2009) identified with the mutagenesis experiments FaeG amino acids 97 (N to K) and 201 (I to V) as determinants of F4 polymeric stability. The interaction between the FaeG subunits in mutant F4 fimbriae is reduced, but both mutant and wild-type fimbriae behaved identically in F4R binding and showed equal stability in the gastrointestinal lumen. Oral immunization experiments indicated that a higher degree of polymerization of the fimbriae in the intestine was correlated with a better F4-specific mucosal immunogenicity. Hu *et al.* (2009) developed recombinant *Lactococcus lactis* that expresses K88 (F4) fimbrial polyadhesin FaeG for oral vaccination. They demonstrated a protective immune response in mice to FaeG. Recently,

Remer *et al.* (2009) constructed the recombinant strain EcN pMut2-kanK88 (EcN-K88) stably expressing the determinant for the K88 fimbrial adhesin of ETEC on the bacterial surface. After oral application of EcN-K88 to mice for 1 week, EcN-K88 as well as wild-type EcN and EcN mock-transformed with the plasmid vector could only be detected in fecal samples a minimum of 7 days after the last feeding, indicating that EcN can transiently colonize the murine intestine. Oral application of EcN-K88 resulted in significant IgG serum titers against K88 as early as 7 days after the initial feeding with EcN-K88, but no significant IgA titers. In contrast, Remer *et al.* (2009) failed to detect any specific T-cell responses toward the K88 antigen either in the spleen or in mesenteric lymph nodes. Although dendritic cells readily upregulated maturation and activation markers in response to K88 stimulation, accompanied by secretion of IL-12, IL-6, IL-10 and TNF, restimulation of T cells from mice having received EcN-K88 with K88-loaded dendritic cells did not result in detectable T-cell proliferation and IL-2 secretion, but rather induced an IL-10 bias. Although the serum antibody responses clearly demonstrate that K88 is recognized by the humoral immune system, the findings of Remer *et al.* (2009) indicate that oral application of probiotic EcN expressing the K88 fimbrial adhesin does not induce a selective T-cell response toward the antigen.

Applications of polyadhesins for expression of heterologous proteins

Application of polyadhesins for the design of antiviral vaccines

The major structural subunit DraE of *E. coli* Dr fimbriae has been used to display a peptide of glycoprotein D derived from *Herpes simplex* virus (HSV) type I (Zalewska *et al.*, 2003). One copy of the heterologous sequence mimicking an epitope from glycoprotein D was inserted into the *draE* gene in place of a predicted 11-amino acid sequence in the N-terminal region of surface-exposed domain 2 within the conserved disulfide loop (from Cys21 to Cys53). The inserted epitope was displayed on the surface of the chimeric DraE protein, as shown by immunofluorescence, and was recognized by monoclonal antibodies to the target HSV glycoprotein D antigen. Conversely, immunization of rabbits with purified chimeric Dr-HSV fimbriae resulted in a serum that specifically recognized the 11-amino acid epitope of HSV glycoprotein D, indicating the utility of the strategy used (Zalewska *et al.*, 2003).

Application of polyadhesins for expression of cytokines

The ability of the Caf1M chaperone/Caf1A usher pathway to express large amounts of the F1 antigen (Caf1) in *E. coli* was investigated to facilitate secretion of full-length heterologous proteins fused to the Caf1 subunit (Zavialov *et al.*, 2001). Despite correct processing of chimeric protein composed of a modified Caf1 signal peptide, mature human IL-1β (hIL-1β) and mature Caf1, the processed product (hIL-1β–Caf1) remained insoluble. Coexpression of this chimera with a functional Caf1M chaperone led to the accumulation of soluble hIL-1β–Caf1 in the periplasm. Soluble hIL-1β–Caf1 reacted with monoclonal antibodies directed against structural epitopes of hIL-1β. The results indicate that the Caf1M-induced release of hIL-1 β–Caf1 from the inner membrane promotes folding of the hIL-1β domain. Similar results were obtained with the fusion of Caf1 to hIL-1ra or to human GM-CSF. Following coexpression of the hIL-1β–Caf1 precursor with the Caf1M chaperone and Caf1A outer membrane protein, hIL-1β–Caf1 could be detected on the cell surface of *E. coli* (Zavialov *et al.*, 2001). These results demonstrated for the first time the potential of the chaperone/usher secretion pathway in the transport of subunits with large heterogeneous N-terminal fusions. This represents a novel means for the delivery of correctly folded heterologous proteins to the periplasm and cell surface as either polymers or cleavable monomeric domains (Korpela *et al.*, 1999).

Applications of monoadhesins

Applications of monoadhesins for vaccine design

Vaccination with the FimH adhesin against infection by UPEC

Virtually all UPEC, the primary cause of cystitis, assemble adhesive surface organelles called type I pili that contain the FimH adhesin. Langermann et al. (1997) demonstrated that sera from animals vaccinated with candidate FimH vaccines inhibited UPEC from binding to human bladder cells *in vitro*. They found that immunization with FimH reduced *in vivo* colonization of the bladder mucosa by $> 99\%$ in a murine cystitis model, and IgG to FimH was detected in urinary samples from protected mice. Furthermore, passive systemic administration of immune sera to FimH also resulted in reduced bladder colonization by UPEC. Later, Langermann *et al.* (2000) studied four monkeys inoculated with 100 μg of the FimCH adhesion–chaperone complex mixed with an MF59 adjuvant, and four monkeys administered adjuvant only intramuscularly. After two doses (day 0 and week 4), a booster at 48 weeks elicited a strong IgG antibody response to FimH in the vaccinated monkeys. All eight monkeys were challenged with 1 mL of 108 *E. coli* cystitis isolate NU14. Three of the four vaccinated monkeys were protected from bacteruria and pyuria; all control monkeys were infected. These findings suggest that a vaccine based on the FimH adhesin of *E. coli* type I pili may have utility in preventing cystitis in humans.

Monoadhesins as targets for specific inhibition of adhesion

Mannose-binding type I pili are important virulence factors for the establishment of *E. coli* UTIs. These infections are initiated by adhesion of UPEC to uroplakin receptors in the uroepithelium via the FimH adhesin located at the tips of type I pili. By blocking bacterial adhesion, it is possible to prevent infection. Bouckaert *et al.* (2005) provided the binding data of the molecular events underlying type I fimbrial adherence, using crystallographic analyses of the FimH receptor-binding domains from a uropathogenic and a K-12 strain, and affinity measurements with mannose, common mono- and disaccharides and a series of alkyl and aryl mannosides. Their results illustrate that the lectin domain of the FimH adhesin is a stable and functional entity and that an exogenous butyl α-D-mannoside, bound in the crystal structures, exhibits a significantly better affinity for FimH ($K_d = 0.15\,\mu M$) compared with mannose ($K_d = 2.3\,\mu M$). Exploration of the binding affinities of α-D-mannosides with longer alkyl tails revealed affinities of up to 5 nM. Aryl mannosides and fructose can also bind with high affinities to the FimH lectin domain, with a 100-fold improvement and a 15-fold reduction in affinity, respectively, compared with mannose. Taken together, these relative FimH affinities correlate exceptionally well with the relative concentrations of the same glycans needed for the inhibition of adherence of type I piliated *E. coli*. Wellens *et al.* (2008) demonstrated that α-D-mannose-based inhibitors of FimH not only block bacterial adhesion on uroepithelial cells but also antagonize invasion and biofilm formation. Heptyl α-D-mannose prevents binding of type I-piliated *E. coli* to the human bladder cell line 5637 and reduces both adhesion and invasion of the UTI89 cystitis isolate instilled in mouse bladder via catheterization. Heptyl α-D-mannose also specifically inhibited biofilm formation at micromolar concentrations. The structural basis of the high inhibitory potential of alkyl and aryl α-D-mannosides was elucidated in the crystal structure of the FimH receptor-binding domain in complex with oligomannose-3. FimH interacts with Man1, 3Manβ1, 4GlcNAcβ1 and 4GlcNAc in an extended binding site. The interactions along the α-1,3 glycosidic bond and the first β-1,4 linkage to the chitobiose unit are conserved with those of FimH with butyl α-D-mannose. The strong stacking of the central mannose with the aromatic ring of Tyr48 is congruent with the high affinity found for synthetic inhibitors in which this mannose is substituted with an aromatic group.

Chaperone–usher assembly-translocation machinery as a target for a new generation of antimicrobials interrupting the assembly of adhesive organelles

Pinkner *et al.* (2006) rationally designed small compounds that specifically inhibit biogenesis of adhesive pili assembled by the chaperone–usher pathway in Gram-negative pathogens. The activity of a family of bicyclic 2-pyridones, termed pilicides, was evaluated in two different pilus biogenesis systems in UPEC. Hemagglutination mediated by either type I or P pili, adherence to bladder cells and biofilm formation mediated by type I pili were all reduced by ≈ 90% in laboratory and clinical *E. coli* strains. Figure 16 shows a stereoimage of the PapD–pilicide complex (Pinkner *et al.*, 2006) in overlay with the FimD1–125 N-terminal usher domain in complex with the FimC-FimH158–279 chaperone–adhesion complex (Fig. 16; Nishiyama *et al.*, 2005). The conserved hydrophobic patch across the back of the F1-C1-D1 β-sheet formed by residues I90/I93, L32/L32 and L54/V56 (FimC/PapD) forms part of both the usher-interaction site and the pilicide-binding site. In the chaperone–pilicide interaction, the plane of the 2-pyridone system and the R1-cyclopropyl and R2-CH2-naphthyl substituents coincides with and mimics the interactions of the F4, L19 and F22 side chains from the usher N-terminal domain. The overlay demonstrates the steric clash between the pilicide and the usher N-terminal domain. Point mutations in the pilicide-binding site dramatically reduced pilus formation, but did not block the ability of PapD to bind subunits and mediate their folding (Pinkner *et al.*, 2006). Surface plasmon resonance experiments confirmed that the pilicide interfered with the binding of chaperone–subunit complexes to the usher (Pinkner *et al.*, 2006). These pilicides thus target key virulence factors in pathogenic bacteria and represent a promising proof of concept for developing drugs that function by targeting virulence factors.

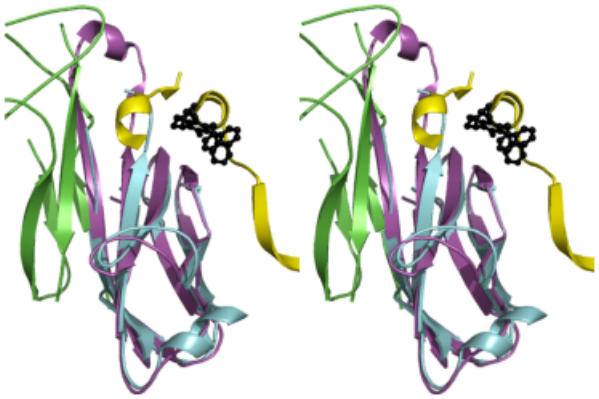

Fig. 16. Stereoimage of the $FimD_{1–125}$ N-terminal usher domain in complex with the FimC-$FimH_{158–279}$ chaperone–adhesion complex with the PapD–pilicide complex in overlay. PapD and pilicide are shown with a light blue ribbon and ball-and-stick, respectively. FimC and $FimH_{158–279}$ are shown in magenta and green, with the $FimD_{1–125}$ N-terminal domain shown in yellow. The redrawing is based on the coordinates of atoms of the structures published by Nishiyama *et al.* (2005) (PDB accession number 1ZE3).

Conclusions and future perspectives

Antibiotic-resistant strains of Gram-negative pathogens have emerged extensively in the last dozen years, whereas safe and effective vaccines against many of them are currently not available. There are now a growing number of reports of cases of infections caused by Gram-negative organisms for which no adequate therapeutic options exist (de Jong & Ekdahl, 2006; Giske *et al.*, 2008). This return to the preantibiotic era has become a reality in Europe as well as in other parts of the world. Targeting bacterial virulence is an alternative approach to antimicrobial therapy that offers promising opportunities to inhibit pathogenesis and its consequences without placing immediate life-or-death pressure on the target bacteria. Two general strategies exist to inhibit fimbrial adhesion-mediated functions (Cegelski *et al.*, 2008; Cusumano & Hultgren, 2009):

(1) the specific inhibition of adhesion, which involves physically precluding pathogen binding to host cells, for example with carbohydrate derivatives of host ligands;

(2) the interruption of fimbrial adhesion assembly, which also blocks adhesion, and invasion and intracellular biofilm formation.

The first strategy is most effective for specific inhibition of monoadhesins. It was demonstrated that α-D-mannose-based inhibitors of the FimH adhesin not only block bacterial adhesion on uroepithelial cells but also antagonize invasion and biofilm formation (Bouckaert *et al.*, 2005; Adinda *et al.*, 2008; Wellens *et al.*, 2008).

The second general strategy to inhibit fimbrial adhesion-mediated functions is targeted to the classical chaperone–usher assembly-translocation machinery (Pinkner *et al.*, 2006; Aberg & Almqvist, 2007). The recently solved structure of the usher translocator pore of the twinned-pore translocation machinery created a basis for the rational design of a new generation of antimicrobials interrupting the assembly of adhesive organelles. However, there are a few crucial details about the chaperone/usher machinery that have not been well studied. They are likely to be the major direction for future studies.

The strong correlation revealed between the number of residues in an F1–G1 loop of chaperones and the number of subunits operated by them is the basis for the novel functional–structural classification of fimbrial adhesins. The FGS chaperone-assembled polyadhesive fimbriae have been discovered, as well as the previously discovered family of the FGL chaperone-assembled polyadhesins. The FGL and FGS chaperone-assembled polyadhesins are encoded exclusively by the gene clusters of the γ3- and κ-monophyletic groups, respectively, whereas gene clusters belonging to the γ1-, γ2-, γ4- and π-fimbrial clades exclusively encode monoadhesins (Nuccio & Bäumler, 2007). Polyadhesive binding possesses an advantage over monoadhesive binding because it results in the formation of a more powerful and tighter contact between the pathogen and the host cell and it may lead to a massive aggregation of the receptors. This subsequently would trigger subversive signals directed to mislead functions of host cells, in particular, the cells of the immune system. Anti-immune function is likely to be common for all fimbrial polyadhesins, including FGS chaperone-assembled polyadhesive fimbriae/pili. Hence, a search for binding to immune system-associated receptors could be a starting point for the functional characterization of known and newly revealed members of both FGL and FGS chaperone-assembled families of polyadhesins.

The fimbrial polyadhesins that are represented by the linear homopolymers of hundreds to thousands of subunits have a huge potential for cross-linking of B-cell receptors and stimulation of antibody production. They are specific and very powerful surface antigens typical only for pathogenic strains. Therefore, they are promising candidates for the development of recombinant vaccines against Gram-negative infections and for their medical diagnosis. The exploitation of these extraordinary properties of fimbrial polyadhesins is of great importance because Gram-negative infections are a burdensome problem worldwide, with a considerable negative economic impact and health risk to people.

The outbreak of pneumonic plague in Surat in 1994 and its spread to other cities in India lasted for only slightly over 2 weeks, but it created an unprecedented panic that had global repercussions (Dutt *et al.*, 2006). At first, the Surat hospital doctors could not diagnose the disease, but when they did, immediate intervention, in the form of prevention and treatment (administration of antibodies), stopped the disease spreading beyond Surat, Delhi, Calcutta, Bombay and their vicinities. Fewer than 1200 people were diagnosed with plague. A DNA-based study in 2000 decisively concluded that the Surat episode was plague, but the Indian isolates were genetically more heterogeneous compared with others in the world. The last outbreak of primary pneumonic plague took place in the Shimla District of Himachal Pradesh State in northern India during February 2002 (Gupta & Sharma, 2007). Sixteen cases of plague were reported, with a case-fatality rate of 25%.

The infections caused by two other representatives of the *Yersinia* genus, *Y. enterocolitica* and *Y. pseudotuberculosis*, are also a significant health concern in India and worldwide. *Yersinia enterocolitica* is the important food-borne enteropathogen that causes a variety of syndromes (Virdi & Sachdeva, 2005). Most commonly, it causes gastroenteritis, terminal ileitis and mesenteric lymphadenitis. Postinfectious sequelae include reactive arthritis and erythema nodosum. *Yersinia pseudotuberculosis* also causes a variety of gastrointestinal and extraintestinal infections in humans (Kumar *et al.*, 2009). Encoded by the *caf* gene cluster

(Fig. 1), F1 capsular antigen from *Y. pestis* is the most specific and potent antigen for medical diagnostics of bubonic and pneumonic plague. The same *psa* gene clusters present in *Y. pestis* and *Y. pseudotuberculosis* (Fig. 1) encode for proteins for the expression and assembly of the fimbrial pH6 antigen. Positive detection of the pH6 antigen without any traces of the F1 antigen is an indicator of infection caused by *Y. pseudotuberculosis* or evidence of the $F1^{-}$ strain of *Y. pestis*. *Yersinia enterocolitica* contains a closely related *psa* gene cluster *myf* (Fig. 1) encoding the Myf fimbriae, which is built up of MyfA subunits. *Yersinia enterocolitica* is very heterogeneous (Virdi & Sachdeva, 2005). Therefore, specific medical diagnostics of pathogenic strains of *Y. enterocolitica* still remains an unsolved problem. The Myf polyadhesin is a promising conservative antigen for indication of infection caused by *Y. enterocolitica*.

Salmonella spp. is an extremely heterogeneous species (Layton & Galyov, 2007). There are over 2500 serotypes of *Salmonella* spp. Specific medical diagnostics of pathogenic strains from *Salmonella* still remains an unsolved problem. The *Salmonella* spp. gene clusters *saf* and *sef* (Fig. 1) encode for proteins for expression and assembly of the atypical fimbriae Saf and the filamentous fimbriae-like structures SEF14/18. These gene clusters encode two distinct adhesin subunits: the variable major polyadhesin subunits SefA or SafA and the conservative minor SefD or SafD subunits (Fig. 1). The SefB chaperone of *S. enteritidis* assists in the assembly of two distinct cell-surface structures, SEF14 and SEF18, which are homopolymers of SefA and SefD subunits, respectively (Clouthier *et al.*, 1994). The SafD subunit is identical for *S. enteritidis*, *S.* Typhi, *S. Paratyphi A*, *S. choleraesuis* and *S. typhimurium*, and the SefD subunit is identical for *S. Paratyphi A* and *S. enteritidis*. Therefore SefD and SafD subunits and monoclonal antibodies to them can be used for medical diagnostics of the main *Salmonella* infections.

Acknowledgements

This work was supported by grants from the European Commission/Research Executive Agency under a Marie Curie International Incoming Fellowship (235538) and a grant from the Academy of Finland (112900) to V.Z., and the FORMAS (221-2007-1057) and Swedish Research Council (K2008-58X-20689-01-3) to A.Z.

References

Aberg V & Almqvist F (2007) Pilicides – small molecules targeting bacterial virulence. *Org Biomol Chem* **5**: 1827–1834.

Adams LM, Simmons CP, Rezmann L, Strugnell RA & Robins-Browne RM (1997) Identification and characterization of a K88- and CS31A-like operon of a rabbit enteropathogenic *Escherichia coli* strain which encodes fimbriae involved in the colonization of rabbit intestine. *Infect Immun* **65**: 5222–5230.

Adinda W, Garofalo C, Nguyen H *et al.* (2008) Intervening with urinary tract infections using anti-adhesives based on the crystal structure of the FimH–oligomannose-3 complex. *PLoS ONE* **3**: e2040.

Ahrens R, Ott M, Ritter A, Hoschuetzky H, Buehler T, Lottspeich F, Boulnois GJ, Jann K & Hacker J (1993) Genetic analysis of the gene cluster encoding nonfimbrial adhesin I from an *Escherichia coli* uropathogen. *Infect Immun* **61**: 2505–2512.

Allen BL, Gerlach GF & Clegg S (1991) Nucleotide sequence and functions of *mrk* determinants necessary for expression of type 3 fimbriae in *Klebsiella pneumoniae*. *J Bacteriol* **173**: 916–920.

Alvarez ML, Pinyerd HL, Crisantes JD, Rigano MM, Pinkhasov J, Walmsley AM, Mason HS & Cardineau GA (2006) Plant-made subunit vaccine against pneumonic and bubonic plague is orally immunogenic in mice. *Vaccine* **24**: 2477–2490.

Anantha RP, McVeigh AL, Lee LH, Agnew MK, Cassels FJ, Scott DA, Whittam TS & Savarino SJ (2004) Evolutionary and functional relationships of colonization factor antigen I and other class 5 adhesive fimbriae of enterotoxigenic *Escherichia coli*. *Infect Immun* **72**: 7190–7201.

Anderson BN, Ding AM, Nilsson LM, Kusuma K, Tchesnokova V, Vogel V, Sokurenko EV & Thomas WE (2007) Weak rolling adhesion enhances bacterial surface colonization. *J Bacteriol* **189**: 1794–1802.

Anderson GW, Worsham PL, Bolt CR, Andrews GP, Welkos SL, Friedlander AM & Burans JP (1997) Protection of mice from fatal bubonic and pneumonic plague by passive immunization with monoclonal antibodies against the F1 protein of *Yersinia pestis*. *Am J Trop Med Hyg* **56**: 471–473.

Anderson KL, Billington J, Pettigrew D, Cota E, Simpson P, Roversi P, Chen H, Urvil P, du Merle L & Barlow P (2004a) An atomic resolution model for assembly, architecture, and function of the Dr adhesins. *Mol Cell* **101**: 647–657.

Anderson KL, Cota E, Simpson P, Chen HA, du Merle L, Le Bougúenec C & Matthews S (2004b) Complete resonance assignments of a 'donor-strand complemented' AfaE: the afimbrial adhesin from diffusely adherent *E. coli*. *J Biomol NMR* **29**: 409–410.

Anisimov AP, Bakhteeva IV, Panfertsev EA *et al.* (2009) The subcutaneous inoculation of pH 6 antigen mutants of *Yersinia pestis* does not affect virulence and immune response in mice. *J Med Microbiol* **58**: 26–36.

Aprikian P, Tchesnokova V, Kidd B, Yakovenko O, Yarov-Yarovoy V, Trinchina E, Vogel V, Thomas W & Sokurenko E (2007) Interdomain interaction in the FimH adhesin of *Escherichia coli* regulates the affinity to mannose. *J Biol Chem* **282**: 23437–23446.

Bahrani FK & Mobley HLT (1994) *Proteus mirabilis* MR/P fimbrial operon: genetic organization, nucleotide sequence, and conditions for expression. *J Bacteriol* **176**: 3412–3419.

Bakker D, Vader CEM, Roosendaal B, Mooj FR, Oudega B & de Graaf FK (1991) Structure and function of periplasmic chaperone-like proteins involved in the biosynthesis of K88

and K99 fimbriae in enterotoxigenic *Escherichia coli*. *Mol Microbiol* **5**: 875–886.

Bann JG, Pinkner JS, Frieden C & Hultgren SJ (2004) Catalysis of protein folding by chaperones in pathogenic bacteria. *P Natl Acad Sci USA* **101**: 17389–17393.

Barnhart MM, Sauer FG, Pinkner JS & Hultgren SJ (2003) Chaperone-subunit-usher interactions required for donor strand exchange during bacterial pilus assembly. *J Bacteriol* **185**: 2723–2730.

Barbe V, Vallenet D, Fonknechten N *et al.* (2004) Unique features revealed by the genome sequence of *Acinetobacter* sp. ADP1, a versatile and naturally transformation competent bacterium. *Nucleic Acids Res* **32**: 5766–5779.

Bäumler AJ & Heffron F (1995) Identification and sequence analysis of *lpfABCDE*, a putative fimbrial operon of *Salmonella typhimurium*. *J Bacteriol* **177**: 2087–2097.

Bäumler AJ, Tsolis RM, Bowe FA, Kusters JG, Hoffmann S & Heffron F (1996) The *pef* fimbrial operon of *Salmonella typhimurium* mediates adhesion to murine small intestine and is necessary for fluid accumulation in the infant mouse. *Infect Immun* **64**: 61–68.

Beaulieu JF (1999) Integrins and human intestinal cell functions. *Front Biosci* **4**: D310–D321.

Benchimol S, Fuks A, Jothy S, Beauchemin N, Shirota K & Stanners CP (1989) Carcinoembryonic antigen, a human tumor marker, functions as an intercellular adhesion molecule. *Cell* **57**: 327–334.

Ben-Efraim S, Aronson M & Bichowsky-Slomnicki L (1961) New antigenic component of *Pasteurella pestis* formed under specific conditions of pH and temperature. *J Bacteriol* **81**: 704–714.

Berger CN, Billker O, Meyer TF, Servin AL & Kansau I (2004) Differential recognition of members of the carcinoembryonic antigen family by Afa/Dr adhesins of diffusely adhering *Escherichia coli* (Afa/Dr DAEC). *Mol Microbiol* **52**: 963–983.

Bergsten G, Wullt B & Svanborg C (2005) *Escherichia coli*, fimbriae, bacterial persistence and host response induction in the human urinary tract. *Int J Med Microbiol* **295**: 487–502.

Bernier C, Gounon P & Le Bouguénec C (2002) Identification of an aggregative adhesion fimbria (AAF) type III-encoding operon in enteroaggregative *Escherichia coli* as a sensitive probe for detecting the AAF-encoding operon family. *Infect Immun* **70**: 4302–4311.

Bertin Y, Girardeau J-P, Der Vartanian M & Martin C (1993) The ClpE protein involved in biogenesis of the CS31A capsule-like antigen is a member of a periplasmic chaperone family in Gram-negative bacteria. *FEMS Microbiol Lett* **108**: 59–68.

Betis F, Brest P, Hofman V, Guignot J, Bernet-Camard MF, Rossi B, Servin A & Hofman P (2003a) The Afa/Dr adhesins of diffusely adhering *Escherichia coli* stimulate interleukin-8 secretion, activate mitogen-activated protein kinases, and promote polymorphonuclear transepithelial migration in T84 polarized epithelial cells. *Infect Immun* **71**: 1068–1074.

Betis F, Brest P, Hofman V, Guignot J, Kansau I, Rossi B, Servin A & Hofman P (2003b) Afa/Dr diffusely adhering *Escherichia coli* infection in T84 cell monolayers induces increased neutrophils transepithelial migration, which in turn promotes cytokine-dependent upregulation of decay-accelerating factor (CD55), the receptor for Afa/Dr adhesins. *Infect Immun* **71**: 1774–1783.

Bilge SS, Clausen CR, Lau W & Moseley SL (1989) Molecular characterization of a fimbrial adhesin, F1845, mediating diffuse adherence of diarrhea-associated *Escherichia coli* to HEp-2 cells. *J Bacteriol* **171**: 4281–4289.

Bonci A, Chiesurin A, Muscas P & Rossolini GM (1997) Relatedness and phylogeny within the family of periplasmic chaperones involved in the assembly of pili or capsule-like structures of gram-negative bacteria. *J Mol Evol* **44**: 299–309.

Bork P, Holm L & Sander C (1994) The immunoglobulin fold: structural classification, sequence patterns and common core. *J Mol Biol* **242**: 309–320.

Bouckaert J, Berglund J, Schembri M *et al.* (2005) Receptor binding studies disclose a novel class of high-affinity inhibitors of the *Escherichia coli* FimH adhesin. *Mol Microbiol* **55**: 441–455.

Bouckaert J, Mackenzie J, de Paz JL *et al.* (2006) The affinity of the FimH fimbrial adhesin is receptor-driven and quasi-independent of *Escherichia coli* pathotypes. *Mol Microbiol* **61**: 1556–1568.

Boulton IC & Gray-Owen SD (2002) Neisserial binding to CEACAM1 arrests the activation and proliferation of CD41T lymphocytes. *Nat Immunol* **3**: 229–236.

Bower JM, Eto DS & Mulvey MA (2005) Covert operations of uropathogenic *Escherichia coli* within the urinary tract. *Traffic* **6**: 18–31.

Bradbury J (2002) *Neisseria gonorrhoeae* evades host immunity by switching off T lymphocytes. *Lancet* **359**: 681.

Brest P, Betis F, Cuburu N, Selva E, Herrant M, Servin A, Auberger P & Hofman P (2004) Increased rate of apoptosis and diminished phagocytic ability of human neutrophils infected with Afa/Dr diffusely adhering *Escherichia coli* strains. *Infect Immun* **72**: 5741–5749.

Brodbeck WG, Liu D, Sperry J, Mold C & Medof ME (1996) Localization of classical and alternative pathway regulatory activity within the decay-accelerating factor. *J Immunol* **156**: 2528–2533.

Brunder W, Khan AS, Hacker J & Karch H (2001) Novel type of fimbriae encoded by the large plasmid of sorbitol-fermenting enterohemorrhagic *Escherichia coli* O157:H2. *Infect Immun* **69**: 4447–4457.

Cane G, Moal VL, Pagès G, Servin AL, Hofman P & Vouret-Craviari V (2007) Up-regulation of intestinal vascular endothelial growth factor by Afa/Dr diffusely adhering *Escherichia coli*. *PLoS ONE* **2**: e1359.

Cantey JR, Blake RK, Williford JR & Moseley SL (1999) Characterization of the *Escherichia coli* AF/R1 pilus operon: novel genes necessary for transcriptional regulation and for pilus-mediated adherence. *Infect Immun* **67**: 2292–2298.

Capitani G, Eidam O & Grütter MG (2006) Evidence for a novel domain of bacterial outer membrane ushers. *Proteins* **65**: 816–823.

Caras IW, Weddell GN, Davitz MA, Nussenzweig V & Martin DW (1987) Signal for attachment of a phospholipid membrane anchor in decay accelerating factor. *Science* **238**: 1280–1283.

Carnoy C & Moseley SL (1997) Mutational analysis of receptor binding mediated by the Dr family of *Escherichia coli* adhesins. *Mol Microbiol* **23**: 365–379.

Carroll MC, Alicot EM, Katzman PJ, Klickstein LB, Smith JA & Fearon DT (1988) Organization of the genes encoding complement receptors type 1 and 2, decay-accelerating factor, and C4-binding protein in the RCA locus on human chromosome 1. *J Exp Med* **167**: 1271–1280.

Cathelyn JS, Crosby SD, Lathem WW, Goldman WE & Miller VL (2006) RovA, a global regulator of *Yersinia pestis*, specifically required for bubonic plague. *P Natl Acad Sci USA* **103**: 13514–13519.

Cegelski L, Marshall GR, Eldridge GR & Hultgren SJ (2008) The biology and future prospects of antivirulence therapies. *Nat Rev Microbiol* **6**: 17–27.

Chapman DAG, Zavialov AV, Chernovskaya TV, Karlyshev AV, Zav'yalova GA, Vasiliev AM, Dudich IV, Abramov VM, Zav'yalov VP & Macintyre S (1999) Structure and functional significance of the FGL sequence of the periplasmic chaperone, Caf1M, of *Yersinia pestis*. *J Bacteriol* **181**: 2422–2429.

Chattopadhyay S, Feldgarden M, Weissman SJ, Dykhuizen DE, van Belle G & Sokurenko EV (2007) Haplotype diversity in 'source-sink' dynamics of *Escherichia coli* urovirulence. *J Mol Evol* **64**: 204–214.

Chen T, Zimmermann W, Parker J, Chen I, Maeda A & Bolland S (2001) Biliary glycoprotein (BGPa, CD66a, CEACAM1) mediates inhibitory signals. *J Leukocyte Biol* **70**: 335–340.

Chen TH & Elberg SS (1977) Scanning electron microscopic study of virulent *Yersinia pestis* and *Yersinia pseudotuberculosis* type 1. *Infect Immun* **15**: 972–977.

Chessa D, Dorsey CW, Winter M & Bäumler AJ (2008) Binding specificity of *Salmonella* plasmid-encoded fimbriae assessed by glycomics. *J Biol Chem* **283**: 8118–8124.

Chichester JA, Musiychuk K, Farrance C, Mett V, Lyons J, Mett V & Yusibov (2009) A single component two-valent LcrV-F1 vaccine protects non-human primates against pneumonic plague. *Vaccine* **27**: 3471–3474.

Chiu CH, Tang P, Chu C, Hu S, Bao Q, Yu J, Chou Y-Y, Wang H-S & Lee Y-S (2005) The genome sequence of *Salmonella enterica* serovar Choleraesuis, a highly invasive and resistant zoonotic pathogen. *Nucleic Acids Res* **33**: 1690–1698.

Choudhury D, Thompson A, Stojanoff V, Langermann S, Pinkner J, Hultgren SJ & Knight SD (1999) X-ray structure of the FimC-FimH chaperone–adhesin complex from uropathogenic *Escherichia coli*. *Science* **285**: 1061–1066.

Cleri DJ, Vernaleo JR, Lombardi LJ, Rabbar MS, Mathew A, Marton R & Reyelt MC (1997) Plague pneumonia disease caused by *Yersinia pestis*. *Semin Respir Infect* **12**: 12–23.

Clouthier SC, Müller KH, Doran JL, Collinson SK & Kay WW (1993) Characterization of three fimbrial genes, *sefABC*, of *Salmonella enteritidis*. *J Bacteriol* **175**: 2523–2533.

Clouthier SC, Collinson SK & Kay WW (1994) Unique fimbriae-like structures encoded by *sefD* of the SEF14 fimbrial gene cluster of *Salmonella enteritidis*. *Mol Microbiol* **12**: 893–901.

Cornelis GR & Wolf-Watz H (1997) The *Yersinia* Yop virulon: a bacterial system for subverting eukaryotic cells. *Mol Microbiol* **23**: 861–867.

Cota E, Chen HA, Anderson KL *et al.* (2004) Letter to the editor: complete resonance assignments of the 'donor-strand complemented' AfaD: the afimbrial invasin from diffusely adherent *E coli*. *J Biomol NMR* **29**: 411–412.

Cota E, Jones C, Simpson P *et al.* (2006) The solution structure of the invasive tip complex from Afa/Dr fibrils. *Mol Microbiol* **62**: 356–366.

Coyne KE, Hall SE, Thompson S, Arce MA, Kinoshita T, Fujita T, Anstee DJ, Rosse W & Lublin DM (1992) Mapping of epitopes, glycosylation sites, and complement regulatory domains in human decay accelerating factor. *J Immunol* **149**: 2906–2913.

Craig L, Pique ME & Tainer JA (2004) Type IV pilus structure and bacterial pathogenicity. *Nat Rev Microbiol* **2**: 363–378.

Crump JA, Luby SP & Mintz ED (2004) The global burden of typhoid fever. *B World Health Organ* **82**: 346–353.

Cusumano CK & Hultgren SJ (2009) Bacterial adhesion – a source of alternate antibiotic targets. *IDrugs* **12**: 699–705.

Davitz MA, Low MG & Nussenzweig V (1986) Release of decay-accelerating factor (DAF) from the cell membrane by phosphatidylinositol-specific phospholipase C (PIPLC). Selective modification of a complement regulatory protein. *J Exp Med* **163**: 1150–1161.

De Bord KL, Anderson DM, Marketon MM, Overheim KA, DePaolo RW, Ciletti NA, Jabri B & Schneewind O (2006) Immunogenicity and protective immunity against bubonic plague and pneumonic plague by immunization of mice with the recombinant V10 antigen, a variant of LcrV. *Infect Immun* **74**: 4910–4914.

De Greve H, Wyns L & Bouckaert J (2007) Combining sites of bacterial fimbriae. *Curr Opin Struc Biol* **17**: 506–512.

Deisenhofer J (1981) Crystallographic refinement and atomic models of a human Fc fragment and its complex with fragment B of protein A from *Staphylococcus aureus* at 2.9- and 2.8-Å resolution. *Biochemistry* **20**: 2361–2370.

De Jong B & Ekdahl B (2006) The comparative burden of salmonellosis in the European Union member states, associated and candidate countries. *BMC Public Health* **6**: 4.

DeLano WL (2002) Unraveling hot spots in binding interfaces: progress and challenges. *Curr Opin Struct Biol* **12**: 14–20.

Delepelaire P (2004) Type I secretion in Gram-negative bacteria. *Biochim Biophys Acta* **1694**: 149–161.

Del Prete G, Santi L, Andrianaivoarimanana V, Amedei A, Domarle O, D' Elios MM, Arntzen CJ, Rahalison L & Mason HS (2009) Plant-derived recombinant F1, V, and F1-V fusion antigens of *Yersinia pestis* activate human cells of the innate and adaptive immune system. *Int J Immunopath Ph* **22**: 133–143.

Deng W, Liou SR, Plunkett G, Mayhew GF, Rose DJ, Burl V, Kodoyianni V, Schwartz DC & Blattner FR (2003)

Comparative genomics of *Salmonella enterica* serovar Typhi strains Ty2 and CT18. *J Bacteriol* **185**: 2330–2337.

Derewenda U, Mateja A, Devedjiev Y, Routzahn KM, Evdokimov AG, Derewenda ZS & Waugh DS (2004) The structure of *Yersinia pestis* V-antigen, an essential virulence factor and mediator of immunity against plague. *Structure (Cambridge)* **12**: 357–358.

Diard S, Toribio AL, Boum Y, Vigier F, Kansau I, Bouvet O & Servin A (2006) Environmental signals implicated in Dr fimbriae release by pathogenic *Escherichia coli*. *Microbes Infect* **8**: 1851–1858.

Dobrindt U, Blum-Oehler G, Hartsch T, Gottschalk G, Ron RZ, Fünfstück R & Hacker J (2001) S-Fimbria-encoding determinant *sfaI* is located on pathogenicity island III536 of uropathogenic *Escherichia coli* strain 536. *Infect Immun* **69**: 4248–4256.

Dodson KW, Jacob-Dubuisson F, Striker RT & Hultgren SJ (1993) Outer-membrane PapC molecular usher discriminately recognizes periplasmic chaperone-pilus subunit complexes. *P Natl Acad Sci USA* **90**: 3670–3674.

Dodson KW, Pinkner JS, Rose RG, Magnusson T, Hultgren S & Waksman G (2001) Structural basis of the interaction of the pyelonephritic *E. coli* adhesin to its human kidney receptor. *Cell* **105**: 733–743.

Donda A, Mori L, Shamshiev A *et al.* (2000) Locally inducible CD66a (CEACAM1) as an amplifier of the human intestinal T cell response. *Eur J Immunol* **30**: 2593–2603.

Du Y, Rosqvist R & Forsberg Å (2002) Role of fraction 1 antigen of *Yersinia pestis* in inhibition of phagocytosis. *Infect Immun* **70**: 1453–1460.

Dutt AK, Akhtar R & McVeigh M (2006) Surat plague of 1994 re-examined. *Southeast Asian J Trop Med Public Health* **37**: 755–760.

Edwards RA, Cao J & Schifferli DM (1996) Identification of major and minor chaperone proteins involved in the export of 987P fimbriae. *J Bacteriol* **178**: 3426–3433.

Edwards RA, Schifferli DM & Maloy SR (2000) A role for *Salmonella* fimbriae in intraperitoneal infections. *P Natl Acad Sci USA* **97**: 1258–1262.

Elias WP, Czeczulin JR, Henderson IR, Trabulsi LR & Nataro JP (1999) Organization of biogenesis genes for aggregative adherence fimbria II defines a virulence gene cluster in enteroaggregative *Escherichia coli*. *J Bacteriol* **181**: 1779–1785.

Elvin SJ, Eyles JE, Howard KA, Ravichandran E, Somavarappu S, Alpar HO & Williamson ED (2006) Protection against bubonic and pneumonic plague with a single dose microencapsulated subunit vaccine. *Vaccine* **24**: 4433–4439.

Emmerth M, Goebel W, Miller SI & Hueck CJ (1999) Genomic subtraction identifies *Salmonella typhimurium* prophages, F-related plasmid sequences, and a novel fimbrial operon, *stf*, which are absent in *Salmonella typhi*. *J Bacteriol* **181**: 5652–5661.

Erilov D, Puorger C & Glockshuber R (2007) Quantitative analysis of nonequilibrium, denaturant-dependent protein folding transitions. *J Am Chem Soc* **129**: 8938–8939.

Eto DS, Jones TA, Sundsbak JL & Mulvey MA (2007) Integrin-mediated host cell invasion by Type 1-piliated uropathogenic *Escherichia coli*. *PLoS Pathog* **3**: e100.

Eyles JE, Williamson ID & Alpar HO (2000) Protection studies following bronchopulmonary and intramuscular immunisation with *Yersinia pestis* F1 and V subunit vaccines co-encapsulated in biodegradable microspheres: a comparison of efficacy. *Vaccine* **18**: 3266–3271.

Fahlgren A, Baranov V, Frangsmyr L, Zoubir F, Hammarstrom ML & Hammarstrom S (2003) Interferon-gamma tempers the expression of carcinoembryonic antigen family molecules in human colon cells: a possible role in innate mucosal defence. *Scand J Immunol* **58**: 628–641.

Fang L, Nowicki BJ, Dong YL & Yallampalli C (1999) Localized increase in nitric oxide production and the expression of nitric oxide synthase isoforms in rat uterus with experimental intrauterine infection. *Am J Obstet Gynecol* **181**: 601–609.

Fang L, Nowicki B & Yallampalli C (2001) Differential expression of uterine NO in pregnant and nonpregnant rats with intrauterine bacterial infection. *Am J Physiol Reg I* **280**: R1356–R1363.

Fischer H, Ellström P, Ekström K, Gustafsson L, Gustafsson M & Svanborg C (2007) Ceramide as a TLR4 agonist; a putative signalling intermediate between sphingolipid receptors for microbial ligands and TLR4. *Cell Microbiol* **9**: 1239–1251.

Folkesson A, Advani A, Sukupolvi S, Pfeifer JD, Normark S & Löfdahl S (1999) Multiple insertions of fimbrial operons correlate with the evolution of *Salmonella* serovars responsible for human disease. *Mol Microbiol* **33**: 612–622.

Forero M, Yakovenko O, Sokurenko EV, Thomas WE & Vogel V (2006) Uncoiling mechanics of *Escherichia coli* Type I fimbriae are optimized for catch bonds. *PLoS Biol* **4**: e298.

Foxman B & Brown P (2003) Epidemiology of urinary tract infections: transmission and risk factors, incidence and costs. *Infect Dis Clin N Am* **17**: 227–241.

Foxman B, Barlow R, D'Arcy H, Gillespie B & Sobel JD (2000) Urinary tract infection: self-reported incidence and associated costs. *Ann Epidemiol* **10**: 509–515.

Fronzes R, Remaut H & Waksman G (2008) Architectures and biogenesis of non-flagellar protein appendages in Gram-negative bacteria. *EMBO J* **27**: 2271–2280.

Fronzes R, Christie PJ & Waksman G (2009a) The structural biology of type IV secretion systems. *Nat Rev Microbiol* **7**: 703–714.

Fronzes R, Schäfer E, Wang L, Saibil HR, Orlova EV & Waksman G (2009b) Structure of a type IV secretion system core complex. *Science* **323**: 266–268.

Fujita T, Inoue T, Ogawa K, Iida K & Tamura N (1987) The mechanism of action of decay-accelerating factor (DAF) DAF inhibits the assembly of C3 convertases by dissociating C2a and Bb. *J Exp Med* **166**: 1221–1228.

Galván EM, Chen H & Schifferli DM (2006) The Psa fimbriae of *Yersinia pestis* interact with phosphatidylcholine on alveolar epithelial cells and pulmonary surfactant. *Infect Immun* **75**: 1272–1279.

Galyov EE, Smirnov OY, Karlyshev AV, Volkovoy KI, Denesyuk AI, Nazimov IV, Rubtsov KS, Abramov VM, Dalvadyanz SM & Zav'yalov VP (1990) Nucleotide sequence of the *Yersinia pestis* gene encoding F1 antigen and the primary structure of the protein. *FEBS Lett* **277**: 230–232.

Galyov EE, Karlyshev AV, Chernovskaya TV, Dolgikh DA, Smirnov OY, Volkovoy KI, Abramov VM & Zav'yalov VP (1991) Expression of the envelope antigen F1 of *Yersinia pestis* is mediated by the product of *caf1M* gene having homology with the chaperone PapD of *Escherichia coli*. *FEBS Lett* **286**: 79–82.

Garcia MI, Labigne A & Le Bouguénec C (1994) Nucleotide sequence of the afimbrial-adhesin-encoding *afa-3* gene cluster and its translocation via flanking IS1 insertion sequences. *J Bacteriol* **176**: 7601–7613.

Garcia MI, Gounon P, Courcoux P, Labigne A & Le Bouguenec C (1996) The afimbrial adhesive sheath encoded by the *afa-3* gene cluster of pathogenic *Escherichia coli* is composed of two adhesins. *Mol Microbiol* **19**: 683–693.

Gerlach RG & Hensel M (2007) Protein secretion systems and adhesins: the molecular armory of Gram-negative pathogens. *Int J Med Microbiol* **297**: 401–415.

Giske CG, Monnet DL, Cars O & Carmeli Y (2008) Clinical and economic impact of common multidrug-resistant Gram-negative bacilli. *Antimicrob Agents Ch* **52**: 813–821.

Glynn A, Roy CJ, Powell BS, Adamovicz JJ, Freytag LC & Clements JD (2005) Protection against aerosolized *Yersinia pestis* challenge following homologous and heterologous prime-boost with recombinant plague antigens. *Infect Immun* **73**: 5256–5261.

Gohl O, Friedrich A, Hoppert M & Averhoff B (2006) The thin pili of *Acinetobacter* sp. strain BD413 mediate adhesion to biotic and abiotic surfaces. *Appl Environ Microb* **72**: 1394–1401.

Goluszko P, Niesel D, Nowicki B, Selvarangan R, Nowicki S, Hart A, Pawelczyk E, Das M, Urvil P & Hasan R (2001) Dr operon-associated invasiveness of *Escherichia coli* from pregnant patients with pyelonephritis. *Infect Immun* **69**: 4678–4680.

Goluszko P, Goluszko E, Nowicki B, Nowicki S, Popov V & Wang H-Q (2005) Vaccination with purified Dr fimbriae reduces mortality associated with chronic urinary tract infection due to *Escherichia coli* bearing Dr adhesin. *Infect Immun* **73**: 627–631.

Gossert AD, Bettendorff P, Puorger C, Vetsch M, Herrmann T, Glockshuber R & Wüthrich K (2008) NMR structure of the *Escherichia coli* Type 1 pilus subunit FimF and its interactions with other pilus subunits. *J Mol Biol* **375**: 752–763.

Grunert F & Kuroki M (1998) CEA family members expressed on hematopoeitic cells and their possible role in cell adhesion and signaling. *Cell Adhesion and Communication Mediated by the CEA Family-Basic and Clinical Perspective* (Stanners CP, ed), pp. 99–120. Harwood Academic Publishers, Amsterdam.

Guignot J, Peiffer I, Bernet-Camard M-F, Lublin DM, Carnoy C, Moseley SL & Servin A (2000) Recruitment of CD55 and CD66e brush border-associated glycosylphosphatidylinositol-anchored proteins by members of the Afa/Dr diffusely adhering family of *Escherichia coli* that infect the human polarized intestinal Caco-2/TC7 cells. *Infect Immun* **68**: 3554–3563.

Guignot J, Hudault S, Kansau I, Chau I & Servin AL (2009) DAF and CEACAMs receptor-mediated internalization and intracellular lifestyle of Afa/Dr diffusely adhering *Escherichia coli* into epithelial cells. *Infect Immun* **77**: 517–531.

Gupta ML & Sharma A (2007) Pneumonic plague, Northern India, 2002. *Emerg Infect Dis* **13**: 664–666.

Hamid N & Jain SK (2007) Immunological, cellular and molecular events in typhoid fever. *Indian J Biochem Bio* **44**: 320–330.

Hammar M, Bian Z & Normark S (1996) Nucleator-dependent intercellular assembly of adhesive curli organelles in *E coli*. *P Natl Acad Sci USA* **93**: 6562–6566.

Hammarstrom S (1999) The carcinoembryonic antigen (CEA) family: structures, suggested functions and expression in normal and malignant tissues. *Semin Cancer Biol* **9**: 67–81.

Hart A, Pham T, Nowicki S, Whorton EB, Martens MG, Anderson GD & Nowicki BJ (1996) Gestational pyelonephritis-associated *Escherichia coli* isolates represent a nonrandom, closely related population. *Am J Obstet Gynecol* **174**: 983–989.

Hart A, Nowicki BJ, Reisner B, Pawelczyk E, Goluszko P, Urvil P, Anderson G & Nowicki S (2001) Ampicillin-resistant *Escherichia coli* in gestational pyelonephritis: increased occurrence and association with the colonization factor Dr adhesin. *J Infect Dis* **183**: 1526–1529.

Hart E, Tauschek M, Bennett-Wood V, Hartland EL & Robins-Browne RM (2009) Rabbit-specific fimbriae, Ral, alter the patterns of *in vitro* adherence and intestinal colonisation of rabbits by human-specific enteropathogenic *E. coli*. *Microbes Infect* **11**: 803–810.

Hasan RJ, Pawelczyk E, Urvil PT, Venkatarajan MS, Goluszko P, Kur J, Selvarangan R, Nowicki S, Braun WA & Nowicki BJ (2002) Structure–function analysis of decay-accelerating factor: identification of residues important for binding of the *Escherichia coli* Dr adhesin and complement regulation. *Infect Immun* **70**: 4485–4493.

Heath DG, Anderson GW, Mauro JM, Welkos SL, Andrews GP, Adamovicz J & Friedlander AM (1998) Protection against experimental bubonic and pneumonic plague by a recombinant capsular F1-V antigen fusion protein vaccine. *Vaccine* **16**: 1131–1137.

Hill J, Copse C, Leary S, Stagg AJ, Williamson ED & Titball RW (2003) Synergistic protection of mice against plague with monoclonal antibodies specific for the F1 and V antigens of *Yersinia pestis*. *Infect Immun* **71**: 2234–2238.

Hill J, Eyles JE, Elvin SJ, Healey GD, Lukaszewski RA & Titball RW (2006) Administration of antibody to the lung protects mice against pneumonic plague. *Infect Immun* **74**: 3068–3070.

Holmgren A & Branden CI (1989) Crystal structure of chaperone protein PapD reveals an immunoglobulin fold. *Nature* **342**: 248–251.

Honarvar S, Choi B-K & Schifferli DM (2003) Phase variation of the 987P-like CS18 fimbriae of human enterotoxigenic *Escherichia coli* is regulated by site-specific recombinases. *Mol Microbiol* **48**: 157–171.

Honko AN, Sriranganathan N, Lees CJ & Mizel SB (2006) Flagellin is an effective adjuvant for immunization against lethal respiratory challenge with *Yersinia pestis*. *Infect Immun* **74**: 1113–1120.

Hu CX, Xu ZR, Li WF, Niu D, Lu P & Fu LL (2009) Secretory expression of K88 (F4) fimbrial adhesin FaeG by recombinant *Lactococcus lactis* for oral vaccination and its protective immune response in mice. *Biotechnol Lett* **31**: 991–997.

Huang XZ & Lindler LE (2004) The pH6 antigen is an antiphagocytic factor produced by *Yersinia pestis* independent of *Yersinia* outer proteins and capsule antigen. *Infect Immun* **72**: 7212–7219.

Hung DL, Knight SD, Woods RM, Pinkner JS & Hultgren SJ (1996) Molecular basis of two subfamilies of immunoglobulin-like chaperones. *EMBO J* **15**: 3792–3805.

Hung DL, Pinkner JS, Knight SD & Hultgren SJ (1999) Structural basis of chaperone self-capping in P pilus biogenesis. *P Natl Acad Sci USA* **96**: 8178–8183.

Iriarte M & Cornelis GR (1995) MyfF, an element of the network regulating the synthesis of fibrillae in *Yersinia enterocolitica*. *J Bacteriol* **177**: 738–744.

Iriarte M, Vanooteghem JC, Delor I, Diaz R, Knutton S & Cornelis GR (1993) The Myf fibrillae of *Yersinia enterocolitica*. *Mol Microbiol* **9**: 507–520.

Jacob-Dubuisson F, Striker R & Hultgren SJ (1994) Chaperone assisted self-assembly of pili independent of cellular energy. *J Biol Chem* **269**: 12447–12455.

Jalajakumar MB, Thomas CJ, Halter R & Manning PA (1989) Genes for biosynthesis and assembly of CS3 pili of CFA/II enterotoxigenic *Escherichia coli*: novel regulation of pilus production by bypassing an amber codon. *Mol Microbiol* **12**: 1685–1695.

Jedrzejczak R, Dauter Z, Dauter M, Piątek R, Zalewska B, Mroz M, Bury K, Nowicki B & Kur J (2006) Structure of DraD invasin from uropathogenic *Escherichia coli*: a dimer with swapped beta-tails. *Acta Crystallogr D* **62**: 157–164.

Joardar V, Lindeberg M, Jackson RW *et al*. (2005) Whole-genome sequence analysis of *Pseudomonas syringae* pv. phaseolicola 1448A reveals divergence among pathovars in genes involved in virulence and transposition. *J Bacteriol* **187**: 6488–6498.

Johnson JR (1991) Virulence factors in *Escherichia coli* urinary tract infection. *Clin Microbiol Rev* **4**: 80–128.

Johnson JR, Skubitz KM, Nowicki BJ, Jacques-Palaz K & Rakita RM (1995) Nonlethal adherence to human neutrophils mediated by Dr antigen-specific adhesins of *Escherichia coli*. *Infect Immun* **63**: 309–316.

Jones CH, Pinkner JS, Nicholes AV, Slonim LN, Abraham SN & Hultgren SJ (1993) FimC is a periplasmic PapD-like chaperone that directs assembly of type 1 pili in bacteria. *P Natl Acad Sci USA* **90**: 8397–8401.

Jones CH, Dodson K & Hultgren SJ (1996) Structure, function and assembly of adhesive P pili. *Urinary Tract Infections: Molecular Pathogenesis and Clinical Management* (Mobley HLT & Warren JW, eds), pp. 175–219. ASM Press, Washington, DC.

Jones T, Adamovicz JJ, Cyr SL, Bolt CR, Bellerose N, Pitt LM, Lowell GH & Burt DS (2006) Intranasal Protollin^{TM}/F1-V vaccine elicits respiratory and serum antibody responses and protects mice against lethal aerosolized plague infection. *Vaccine* **24**: 1625–1632.

Jouve M, Garcia MI, Courcoux P, Labigne A, Gounon P & Le Bouguénec C (1997) Adhesion to and invasion of HeLa cells by pathogenic *Escherichia coli* carrying the *afa-3* gene cluster are mediated by the AfaE and AfaD proteins, respectively. *Infect Immun* **56**: 4082–4089.

Kammerer R, Hahn S, Singer BB, Luo JS & von Kleist S (1998) Biliary glycoprotein (CD66a), a cell adhesion molecule of the immunoglobulin superfamily, on human lymphocytes: structure, expression and involvement in T cell activation. *Eur J Immunol* **28**: 3664–3674.

Kammerer R, Stober D, Singer BB, Obrink B & Reimann J (2001) Carcinoembryonic antigen-related cell adhesion molecule 1 on murine dendritic cells is a potent regulator of T cell stimulation. *J Immunol* **166**: 6537–6544.

Karlyshev AV, Galyov EE, Abramov VM & Zav'yalov VP (1992a) *caf1R* gene and its role in the regulation of capsule formation of *Y. pestis*. *FEBS Lett* **305**: 37–40.

Karlyshev AV, Galyov EE, Smirnov OY, Guzaev AP, Abramov VM & Zav'yalov VP (1992b) A new gene of the *f1* operon of *Y. pestis* involved in the capsule biogenesis. *FEBS Lett* **297**: 77–80.

Karlyshev AV, Galyov EE, Smirnov OY, Abramov VM & Zav'yalov VP (1994) Structure and regulation of a gene cluster involved in capsule formation of *Y pestis*. *Biological Membranes: Structure, Biogenesis and Dynamic, NATO-ASI Serias*, *Vol. H-82* (Op den Kamp JAF, ed), pp. 321–330. Springer-Verlag, New York, NY.

Kaul AK, Khan S, Martens MG, Crosson JT, Lupo VR & Kaul R (1999) Experimental gestational pyelonephritis induces preterm births and low birth weights in C3H/HeJ mice. *Infect Immun* **67**: 5958–5966.

Keller R, Ordoñez JG, de Oliveira RR, Trabulsi LR, Baldwin TJ & Knutton S (2002) Afa, a diffuse adherence fibrillar adhesin associated with enteropathogenic *Escherichia coli*. *Infect Immun* **70**: 2681–2689.

Kida Y, Kobayashi M, Takao S, Akira T, Yoshimasa O, Sigemasa H, Toshikazu Y & Kohji H (2005) Interleukin-1 stimulates cytokines, prostaglandin E2 and matrix metalloproteinase-1 production via activation of MAPK/AP-1 and NF-kB in human gingival fibroblasts. *Cytokine* **29**: 159–168.

Kline KA, Fälker S, Dahlberg S, Normark S & Henriques-Normark B (2009) Bacterial adhesins in host–microbe interactions. *Cell Host Microbe* **5**: 580–592.

Knight SD, Berglund J & Choudhury D (2000) Bacterial adhesins: structural studies reveal chaperone function and pilus biogenesis. *Curr Opin Chem Biol* **4**: 653–660.

Knutton S, McConnel MM, Rowe B & McNeish AS (1989) Adhesion and ultrastructural properties of human enterotoxigenic *Escherichia coli* producing colonization factor antigens III and IV. *Infect Immun* **57**: 3364–3371.

Korotkova N, Cota E, Lebedin Y, Monpouet S, Guignot J, Servin AL, Matthews S & Moseley SL (2006a) A subfamily of Dr adhesions of *Escherichia coli* bind independently to decay-accelerating factor and the N-domain of carcinoembrionic antigen. *J Biol Chem* **281**: 29120–29130.

Korotkova N, Le Trong I, Samudrala R, Korotkov K, Van Loy CP, Bui AL, Moseley SL & Stenkamp RE (2006b) Crystal structure and mutational analysis of the DaaE adhesin of *Escherichia coli*. *J Biol Chem* **281**: 22367–22377.

Korotkova N, Chattopadhyay S, Tabata TA, Beskhlebnaya V, Vigdorovich V, Kaiser BK, Strong RK, Dykhuizen DE, Sokurenko EV & Moseley SL (2007) Selection for functional diversity drives accumulation of point mutations in Dr adhesins of *Escherichia coli*. *Mol Microbiol* **64**: 180–194.

Korotkova N, Yang Y, Le Trong I, Cota E, Demeler B, Marchant J, Thomas WE, Stenkamp RE, Moseley SL & Matthews S (2008a) Binding of Dr adhesins of *Escherichia coli* to carcinoembryonic antigen triggers receptor dissociation. *Mol Microbiol* **67**: 420–434.

Korotkova N, Yarova-Yarovaya Y, Tchesnokova V, Yazvenko N, Carl MA, Stapleton AE & Moseley SL (2008b) *Escherichia coli* DraE adhesin-associated bacterial internalization by epithelial cells is promoted independently by decay-accelerating factor and carcinoembryonic antigen-related cell adhesion molecule binding and does not require the DraD invasin. *Infect Immun* **76**: 3869–3880.

Korpela T, Macintyre-Ayane S, Zavialov A, Battchikova N, Petrovskaya L, Zav'yalov V & Korobko V (1999) Microbial protein expression system. US patent 6919198.

Kuehn MJ, Heuser J, Normark S & Hultgren SJ (1992) P pili in uropathogenic *E. coli* are composite fibres with distinct fibrillar adhesive tips. *Nature* **356**: 252–255.

Kumar S, Balakrishna K, Agarwal GS, Merwyn S, Rai GP, Batra HV, Sardesai AA & Gowrishankar J (2009) Th1-type immune response to infection by pYV-cured phoP-phoQ null mutant of *Yersinia pseudotuberculosis* is defective in mouse model. *Antonie van Leeuwenhoek* **95**: 91–100.

Lalioui L & Le Bouguénec C (2001) *afa-8* Gene cluster is carried by a pathogenicity island inserted into the $tRNA^{Phe}$ of human and bovine pathogenic *Escherichia coli* isolates. *Infect Immun* **69**: 937–948.

Lalioui L, Jouve M, Gounon P & Le Bouguénec C (1999) Molecular cloning and characterization of the *afa-7* and *afa-8* gene clusters encoding Afimbrial adhesins in *Escherichia coli* strains associated with diarrhea or septicemia in calves. *Infect Immun* **10**: 5048–5059.

Lane MC & Mobley HLT (2007) Role of P-fimbrial-mediated adherence in pyelonephritis and persistence of uropathogenic *Escherichia coli* (UPEC) in the mammalian kidney. *Kidney Int* **72**: 19–25.

Langermann S, Palaszynski S, Barnhart M *et al.* (1997) Prevention of mucosal *Escherichia coli* infection by FimH-adhesin-based systemic vaccination. *Science* **276**: 607–611.

Langermann S, Möllby R, Burlein J *et al.* (2000) Vaccination with FimH adhesin protects cynomolgus monkeys from colonization and infection by uropathogenic *Escherichia coli*. *J Infect Dis* **181**: 774–778.

Layton AN & Galyov EE (2007) *Salmonella*-induced enteritis: molecular pathogenesis and therapeutic implications. *Expert Rev Mol Med* **9**: 1–17.

Le Bouguénec C (2005) Adhesins and invasins of pathogenic *Escherichia coli*. *Int J Med Microbiol* **295**: 471–478.

Le Bouguénec C & Bertin Y (1999) AFA and F17 adhesins produced by pathogenic *Escherichia coli* strains in domestic animals. *Vet Res* **30**: 317–342.

Le Bouguénec C & Servin AL (2006) Diffusely adherent *Escherichia coli* strains expressing Afa/Dr adhesins (Afa/Dr DAEC): hitherto unrecognized pathogens. *FEMS Microbiol Lett* **256**: 185–194.

Leffler H & Svanborg-Edén C (1980) Chemical identification of a glycosphingolipid receptor for *E. coli* attaching to human urinary tract epithelial cells and agglutinating human erythrocytes. *FEMS Microbiol Lett* **8**: 127–134.

Leffler H & Svanborg-Edén C (1981) Glycolipid receptors for uropathogenic *Escherichia coli* on human erythrocytes and uroepithelial cells. *Infect Immun* **34**: 920–929.

Lemaitre N, Sebbane F, Long D & Hinnebusch BJ (2006) *Yersinia pestis* YopJ suppresses tumour necrosis factor alpha induction and contributes to apoptosis of immune cells in the lymph node but is not required for virulence in a rat model of bubonic plague. *Infect Immun* **74**: 5126–5131.

Levine MM, Ristaino P, Marley G *et al.* (1984) Coli surface antigens 1 and 3 of colonization factor antigen II-positive enterotoxigenic *Escherichia coli*: morphology, purification, and immune responses in humans. *Infect Immun* **44**: 409–420.

Li B & Yang R (2008) Interaction between *Yersinia pestis* and the host immune system. *Infect Immun* **76**: 1804–1811.

Li B, Jiang L, Song Q *et al.* (2005) Protein microarray for profiling antibody responses to *Yersinia pestis* live vaccine. *Infect Immun* **73**: 3734–3739.

Li H, Qian L, Chen Z, Thibault D, Liu G, Liu T & Thanassi DG (2004) The outer membrane usher forms a twin-pore secretion complex. *J Mol Biol* **344**: 1397–1407.

Li Y, Cui Y, Hauck Y *et al.* (2009a) Genotyping and phylogenetic analysis of *Yersinia pestis* by MLVA: insights into the worldwide expansion of Central Asia plague foci. *PLoS ONE* **4**: e6000.

Li Y, Han W, Lei L, Li Z & Shi L (2009b) MrkD adhesin of *Klebsiella pneumoniae* expression, purification and analysis of adhesive activity. *Wei Sheng Wu Xue Bao* **49**: 638–642.

Li Y-F, Poole S, Rasulova F, McVeigh AL, Savarino SJ & Xia D (2007) A receptor-binding site as revealed by the crystal structure of CfaE, the colonization factor antigen I fimbrial adhesin of enterotoxigenic *Escherichia coli*. *J Biol Chem* **282**: 23970–23980.

Lindberg F, Lund B, Johansson L & Normark S (1987) Localization of the receptor binding protein adhesin at the tip of the bacterial pilus. *Nature* **328**: 84–87.

Lindler LE & Tall BD (1993) *Yersinia pestis* pH6 antigen forms fimbriae and is induced by intracellular association with macrophages. *Mol Microbiol* **8**: 311–324.

Lindler LE, Klempner MS & Straley SC (1990) *Yersinia pestis* pH6 antigen: genetic, biochemical, and virulence characterization of a protein involved in the pathogenesis of bubonic plague. *Infect Immun* **58**: 2569–2577.

Linke D, Riess T, Autenrieth IB, Lupas A & Kempf VA (2006) Trimeric autotransporter adhesins: variable structure, common function. *Trends Microbiol* **14**: 264–270.

Lintermans PF, Pohl P, Deboeck F, Bertels A, Schlicker C, Vandekerckhove J, van Damme J, van Montagu M & de Greve H (1988) Isolation and nucleotide sequence of the F17-A gene encoding the structural protein of the F17 fimbriae in bovine enterotoxigenic *Escherichia coli*. *Infect Immun* **56**: 1475–1484.

Liu F, Chen H, Galván EM, Lasaro MA & Schifferli DM (2006) Effects of Psa and F1 on the adhesive and invasive interactions of *Yersinia pestis* with human respiratory tract epithelial cells. *Infect Immun* **74**: 5636–5644.

Lopes VC, Velayudhan BT, Halvorson DA & Nagaraja KV (2006) Preliminary evaluation of the use of the *sefA* fimbrial gene to elicit immune response against *Salmonella enterica* serotype *Enteritidis* in chickens. *Avian Dis* **50**: 185–190.

Louvard D, Kedinger M & Hauri HP (1992) The differentiating intestinal epithelial cell: establishment and maintenance of functions through interactions between cellular structures. *Annu Rev Cell Biol* **8**: 157–195.

Lublin DM & Atkinson JP (1989) Decay-accelerating factor: biochemistry, molecular biology, and function. *Annu Rev Immunol* **7**: 35–58.

MacIntyre S, Zyrianova IM, Chernovskaya TV, Leonard M, Rudenko EG, Zav'yalov VP & Chapman DAG (2001) An extended hydrophobic interactive surface of *Yersinia pestis* Caf1M chaperone is essential for subunit binding and F1 capsule assembly. *Mol Microbiol* **39**: 12–25.

Makoveichuk E, Cherepanov P, Lundberg S, Forsberg Å & Olivecrona G (2003) pH6 antigen of *Yersinia pestis* interacts with plasma lipoproteins and cell membranes. *Lipid Res* **44**: 320–330.

Marketon MM, Depaolo RW, Debord KL, Jabri B & Schneewind O (2005) Plague bacteria target immune cells during infection. *Science* **309**: 1739–1741.

Marklund B-I, Tennent JM, Garcia E, Hamers A, Bdga M, Lindberg F, Gaastra W & Normark S (1992) Horizontal gene transfer of the *Escherichia coli pap* and *prs* pili operons as a mechanism for the development of tissue-specific adhesive properties. *Mol Microbiol* **6**: 2225–2242.

Massad G & Mobley HLT (1994) Genetic organization and complete sequence of the *Proteus mirabilis pmf* fimbrial operon. *Gene* **150**: 101–104.

Massad G, Fulkerson GF, Watson DC & Mobley HL (1996) *Proteus mirabilis* ambient-temperature fimbriae: cloning and nucleotide sequence of the *atf* gene cluster. *Infect Immun* **64**: 4390–4395.

McClelland M, Sanderson KE, Spieth J *et al.* (2001) Complete genome sequence of *Salmonella enterica* serovar Typhimurium LT2. *Nature* **413**: 852–856.

McClelland M, Sanderson KE, Clifton SW *et al.* (2004) Comparison of genome degradation in Paratyphi A and Typhi, human-restricted serovars of *Salmonella enterica* that cause typhoid. *Nat Genet* **36**: 1268–1274.

Merckel MC, Tanskanen J, Edelman S, Westerlund-Wikström B, Korhonen TK & Goldman A (2003) The structural basis of receptor-binding by *Escherichia coli* associated with diarrhea and septicemia. *J Mol Biol* **331**: 897–905.

Meslet-Cladiere LM, Pimenta A, Duchaud E, Holland IB & Blight MA (2004) *In vivo* expression of the mannose-resistant fimbriae of *Photorhabdus temperata* K122 during insect infection. *J Bacteriol* **186**: 611–622.

Mo L, Zhu XH, Huang HY, Shapiro E, Hasty DL & Wu XR (2004) Ablation of the Tamm-Horsfall protein gene increases susceptibility of mice to bladder colonization by type 1-fimbriated *Escherichia coli*. *Am J Physiol Renal Physiol* **286**: F795–802.

Mueller CA, Broz P, Muller SA, Ringler P, Erne-Brand F, Sorg I, Kuhn M, Engel A & Cornelis GR (2005) The V-antigen of *Yersinia* forms a distinct structure at the tip of injectisome needles. *Science* **310**: 674–676.

Munera D, Hultgren S & Fernandez LA (2007) Recognition of the N-terminal lectin domain of FimH adhesin by the usher FimD is required for type 1 pilus biogenesis. *Mol Microbiol* **64**: 333–346.

Musson JA, Morton M, Walker N, Harper HM, McNeill HV, Williamson ED & Robinson JH (2006) Sequential proteolytic processing of the capsular Caf1 antigen of *Yersinia pestis* for MHC class II restricted presentation to T lymphocytes. *J Biol Chem* **281**: 26129–26135.

Nakajima A, Iijima H, Neurath MF *et al.* (2002) Activation-induced expression of carcinoembryonic antigen-cell adhesion molecule 1 regulates mouse T lymphocyte function. *J Immunol* **168**: 1028–1035.

Nataro JP & Kaper JB (1998) Diarrheagenic *Escherichia coli*. *Clin Microbiol Rev* **11**: 142–201.

Ng TW, Akman L, Osisami M & Thanassi DG (2004) The usher N terminus is the initial targeting site for chaperone–subunit complexes and participates in subsequent pilus biogenesis events. *J Bacteriol* **186**: 5321–5331.

Niemann HH, Schubert WD & Heinz DW (2004) Adhesins and invasins of pathogenic bacteria: a structural view. *Microbes Infect* **6**: 101–112.

Nilsson LM, Thomas WE, Sokurenko EV & Vogel V (2006a) Elevated shear stress protects *Escherichia coli* cells adhering to surfaces via catch bonds from detachment by soluble inhibitors. *Appl Environ Microb* **72**: 3005–3010.

Nilsson LM, Thomas WE, Trintchina E, Vogel V & Sokurenko EV (2006b) Catch bond-mediated adhesion without a shear threshold: trimannose versus monomannose interactions with

the FimH adhesin of *Escherichia coli*. *J Biol Chem* **281**: 16656–16663.

Nilsson LM, Yakovenko O, Tchesnokova V, Thomas WE, Schembri MA, Vogel V, Klemm P & Sokurenko EV (2007) The cysteine bond in the *Escherichia coli* FimH adhesin is critical for adhesion under flow conditions. *Mol Microbiol* **65**: 1158–1169.

Nilsson LM, Thomas WE, Sokurenko EV & Vogel V (2008) Beyond induced-fit receptor-ligand interactions: structural changes that can significantly extend bond lifetimes. *Structure* **16**: 1047–1058.

Nishiyama M, Vetsch M, Puorger C, Jelesarov I & Glockshuber R (2003) Identification and characterization of the chaperone subunit complex-binding domain from the Type 1 pilus assembly platform FimD. *J Mol Biol* **330**: 513–525.

Nishiyama M, Horst R, Eidam OT *et al.* (2005) Structural basis of chaperone–subunit complex recognition by the type 1 pilus assembly plarform FimD. *EMBO J* **24**: 1–12.

Nouvion AL & Beauchemin N (2009) CEACAM1 as a central modulator of metabolism, tumor progression, angiogenesis and immunity. *Med Sci (Paris)* **25**: 247–252.

Nowicki B, Moulds J, Hull R & Hull S (1988) A hemagglutinin of uropathogenic *Escherichia coli* recognizes the Dr blood group antigen. *Infect Immun* **56**: 1057–1060.

Nowicki B, Hart A, Coyne KE, Lublin DM & Nowicki S (1993) Short consensus repeat-3 domain of recombinant decay-accelerating factor is recognized by *Escherichia coli* recombinant Dr adhesin in a model of a cell–cell interaction. *J Exp Med* **178**: 2115–2121.

Nowicki B, Martens M, Hart A & Nowicki S (1994) Gestational age-dependent distribution of *Escherichia coli* fimbriae in pregnant patients with pyelonephritis. *Ann NY Acad Sci* **730**: 290–291.

Nowicki B, Fang L, Singhal J, Nowicki S & Yallampalli C (1997) Lethal outcome of uterine infection in pregnant but not in nonpregnant rats and increased death rate with inhibition of nitric oxide. *Am J Reprod Immunol* **38**: 309–312.

Nuccio S-P & Bäumler AJ (2007) Evolution of the chaperone/usher assembly pathway: fimbrial classification goes greek. *Microbiol Mol Biol R* **71**: 551–575.

Öbrink B (1997) CEA adhesion molecules: multifunctional proteins with signal-regulatory properties. *Curr Opin Cell Biol* **9**: 616–626.

Pak J, Pu Y, Zhang ZT, Hasty DL & Wu XR (2001) Tamm-Horsfall protein binds to type 1 fimbriated *Escherichia coli* and prevents *E. coli* from binding to uroplakin Ia and Ib receptors. *J Biol Chem* **276**: 9924–9930.

Payne D, Tatham D, Williamson ED & Titball RW (1998) pH6 antigen of *Yersinia pestis* binds to β1-linked galactosyl residues in glycosphingolipids. *Infect Immun* **66**: 4545–4548.

Peiffer I, Servin A & Bernet-Camard M-F (1998) Piracy of decay-accelerating factor (CD55) signal transduction by the diffusely adhering strain *Escherichia coli* C1845 promotes cytoskeletal F-actin rearrangements in cultured human intestinal INT407 cells. *Infect Immun* **66**: 4036–4042.

Peiffer I, Blanc-Potard A-B, Bernet-Camard M-F, Guignot J, Barbat A & Servin A (2000a) Afa/Dr diffusely adhering *Escherichia coli* C1845 infection promotes selective injuries in the junctional domain of polarized human intestinal Caco-2/TC7 cells. *Infect Immun* **68**: 3431–3442.

Peiffer I, Guignot J, Barbat A, Carnoy C, Moseley SL, Nowicki BJ, Servin A & Bernet-Camard M-F (2000b) Structural and functional lesions in brush border of human polarized intestinal Caco-2/TC7 cells infected by members of the Afa/Dr diffusely adhering family of *Escherichia coli*. *Infect Immun* **68**: 5979–5990.

Pereverzev YV, Prezhdo OV, Forero M, Sokurenko EV & Thomas WE (2005) The two-pathway model for the catch-slip transition in biological adhesion. *Biophys J* **89**: 1446–1454.

Pereverzev YV, Prezhdo OV & Sokurenko EV (2009) Allosteric role of the large-scale domain opening in biological catch-binding. *Phys Rev E Stat Nonlin Soft Matter Phys* **79**: 051913.

Perry RD & Fetherston JD (1997) *Yersinia pestis* – etiologic agent of plague. *Clin Microbiol Rev* **10**: 35–66.

Pettigrew D, Anderson KL, Billington J *et al.* (2004) High resolution studies of the Afa/Dr adhesin DraE and its interaction with chloramphenicol. *J Biol Chem* **279**: 46851–46857.

Pettigrew DM, Roversi P, Davies SG, Russell AJ & Lea SM (2009) A structural study of the interaction between the Dr haemagglutinin DraE and derivatives of chloramphenicol. *Acta Crystallogr D* **65**: 513–522.

Pham TQ, Goluszko P, Popov V, Nowicki S & Nowicki BJ (1997) Molecular cloning and characterization of Dr-II A nonfimbrial adhesin-I-like adhesin isolated from gestational pyelonephritis-associated *Escherichia coli* that binds to decay-accelerating factor. *Infect Immun* **10**: 4309–4318.

Piątek R, Zalewska B, Kolaj O, Ferens M, Nowicki B & Kur J (2005) Molecular aspects of biogenesis of *Escherichia coli* Dr fimbriae: characterization of DraB–DraE complexes. *Infect Immun* **73**: 135–145.

Pinkner JS, Remaut H, Buelens F *et al.* (2006) Rationally designed small compounds inhibit pilus biogenesis in uropathogenic bacteria. *P Natl Acad Sci USA* **103**: 17897–17902.

Poole ST, McVeigh AL, Anantha RP, Lee LH, Akay YM, Pontzer EA, Scott DA, Bullitt E & Savarino SJ (2007) Donor strand complementation governs intersubunit interaction of fimbriae of the alternate chaperone pathway. *Mol Microbiol* **63**: 1372–1384.

Powell BS, Andrews GP, Enama JT, Jendrek S, Bolt C, Worsham P, Pullen JK, Ribot W, Hines H, Smith L, Heath DG & Adamovicz JJ (2005) Design and testing for a non-tagged F1-V fusion protein as vaccine antigen against bubonic and pneumonic plague. *Biotechnol Prog* **21**: 1490–1510.

Proft T & Baker EN (2009) Pili in Gram-negative and Gram-positive bacteria – structure, assembly and their role in disease. *Cell Mol Life Sci* **66**: 613–635.

Pujol C, Klein KA, Romanov GA, Palmer LE, Cirota C, Zhao Z & Bliska JB (2009) *Yersinia pestis* can reside in autophagosomes

and avoid xenophagy in murine macrophages by preventing vacuole acidification. *Infect Immun* **77**: 2251–2261.

Puorger C, Eidam O, Capitani G, Erilov D, Grütter MG & Glockshuber R (2008) Infinite kinetic stability against dissociation of supramolecular protein complexes through donor strand complementation. *Structure* **16**: 631–642.

Read TD, Dowdell M, Satola SW & Farley MM (1996) Duplication of pilus gene complexes of *Haemophilus influenzae* biogroup aegyptius. *J Bacteriol* **178**: 6564–6570.

Remaut H, Rose RJ, Hannan TJ, Hultgren SJ, Radford SE, Ashcroft AE & Waksman G (2006) Donor-strand exchange in chaperone-assisted pilus assembly proceeds through a concerted β strand displacement mechanism. *Mol Cell* **22**: 831–842.

Remaut H, Tang C, Henderson N, Pinkner J, Wang T, Hultgren S, Thanassi D, Waksman G & Li H (2008) Fiber formation across the bacterial outer membrane by the chaperone/usher pathway. *Cell* **133**: 640–652.

Remer KA, Bartrow M, Roeger B, Moll H, Sonnenborn U & Oelschlaeger TA (2009) Split immune response after oral vaccination of mice with recombinant *Escherichia coli* Nissle 1917 expressing fimbrial adhesin K88. *Int J Med Microbiol* **299**: 467–478.

Rey-Campos J, Rubinstein P & de Cordoba SR (1988) A physical map of the human regulator of complement activation gene cluster linking the complement genes CR1, CR2, DAF, and C4BP. *J Exp Med* **167**: 664–669.

Richardson JS & Richardson DC (2002) Natural beta-sheet proteins use negative design to avoid edge-to-edge aggregation. *P Natl Acad Sci USA* **99**: 2754–2759.

Riegman N, Kusters R, van Veggel H, Bergmans H, van Bergen P, Henegouwen E, Hacker J & van Die I (1990) F1C fimbriae of a uropathogenic *Escherichia coli* strain: genetic and functional organization of the *foc* gene cluster and identification of minor subunits. *J Bacteriol* **172**: 1114–1120.

Rose RJ, Welsh TS, Waksman G, Ashcroft AE, Radford SE & Paci E (2008) Donor-strand exchange in chaperone-assisted pilus assembly revealed in atomic detail by molecular dynamics. *J Mol Biol* **375**: 908–919.

Rougeaux C, Berger CN & Servin AL (2008) CEACAM1-4L down-regulates hDAF-associated signaling after being recognized by the Dr adhesin of diffusely adhering *Escherichia coli*. *Cell Microbiol* **10**: 632–654.

Runco LM, Myrczek S, Bliska JB & Thanassi DG (2008) Biogenesis of the fraction 1 capsule and analysis of the ultrastructure of *Yersinia pestis*. *J Bacteriol* **190**: 3381–3385.

Saarela S (1999) *Functional and Molecular Characterization of the GafD Fimbrial Lectin of Escherichia coli*. Academic Dissertation University of Helsinki, Finland.

Saarela S, Taira S, Nurmiaho-Lassila E-L, Makkonen A & Rhen M (1995) The *Escherichia coli* G-fimbrial lectin protein participates both in fimbrial biogenesis and in recognition of the receptor *N*-acetyl-D-glucosamine. *J Bacteriol* **177**: 1477–1484.

Saarela S, Westerlund-Wikström B, Rhen M & Korhonen TK (1996) The GafD protein of the G (F17) fimbrial complex confers adhesiveness of *Escherichia coli* to laminin. *Infect Immun* **64**: 2857–2860.

Sabhnani L & Rao DN (2000) Identification of immunodominant epitope of F1 antigen of *Yersinia pestis*. *FEMS Immunol Med Mic* **27**: 155–162.

Sabhnani L, Manocha M, Sridevi K, Shashikiran D, Rayanade R & Rao DN (2003) Developing subunit immunogens using B and T cell epitopes and their constructs derived from the F1 antigen of *Yersinia pestis* using novel delivery vehicles. *FEMS Immunol Med Mic* **38**: 215–229.

Salih O, Remaut H, Waksman G & Orlova EV (2008) Structural analysis of the Saf pilus by electron microscopy and image processing. *J Mol Biol* **379**: 174–187.

Sanchez R, Kanarek L, Koninkx J, Hendriks H, Lintermans P, Bertels A, Charlier G & Van Driessche E (1993) Inhibition of adhesion of enterotoxigenic *Escherichia coli* cells expressing F17 fimbriae to small intestinal mucus and brush-border membranes of young calves. *Microb Pathogenesis* **15**: 407–419.

Santi L, Giritch A, Roy CJ, Marillonnet S, Klimyuk V, Gleba Y, Webb R, Arntzen CJ & Mason HS (2006) Protection conferred by recombinant *Yersinia pestis* antigens produced by a rapid and highly scalable plant expression system. *P Natl Acad Sci USA* **103**: 861–866.

Sauer FG, Futterer K, Pinkner JS, Dodson KW, Hultgren SJ & Waksman G (1999) Structural basis of chaperone function and pilus biogenesis. *Science* **285**: 1058–1061.

Sauer FG, Barnhart M, Choudhury D, Knight SD, Waksman G & Hultgren SJ (2000) Chaperone-assisted pilus assembly and bacterial attachment. *Curr Opin Struc Biol* **10**: 548–556.

Sauer FG, Pinkner JS, Waksman G & Hultgren SJ (2002) Chaperone priming of pilus subunits facilitates a topological transition that drives fiber formation. *Cell* **111**: 543–551.

Sauer FG, Remaut H, Hultgren SJ & Waksman G (2004) Fiber assembly by the chaperone–usher pathway. *Biochim Biophys Acta* **1694**: 259–267.

Saulino ET, Thanassi DG, Pinkner JS, Hultgren SJ, Lombardo MJ, Roth R & Heuser J (1998) Ramifications of kinetic partitioning on usher-mediated pilus biogenesis. *EMBO J* **17**: 2177–2185.

Savarino SJ, Fox P, Deng Y & Nataro JP (1994) Identification and characterization of a gene cluster mediating enteroaggregative *Escherichia coli* aggregative adherence fimbria I biogenesis. *J Bacteriol* **176**: 4949–4957.

Scaletsky ICA, Michalski J, Torres AG, Dulguer MV & Kaper JB (2005) Identification and characterization of the locus for diffuse adherence, which encodes a novel afimbrial adhesin found in atypical enteropathogenic *Escherichia coli*. *Infect Immun* **73**: 4753–4765.

Schembri MA, Sokurenko EV & Klemm P (2000) Functional flexibility of the FimH adhesin: insights from a random mutant library. *Infect Immun* **68**: 2638–2646.

Sebbane F, Lemaitre N, Sturdevant DE, Rebeil R, Virtaneva K, Porcella SF & Hinnebusch BJ (2006) Adaptive response of *Yersinia pestis* to extracellular effectors of innate immunity

during bubonic plague. *P Natl Acad Sci USA* **103**: 11766–11771.

Sebbane F, Jarrett C, Gardner D, Long D & Hinnebusch BJ (2009) The *Yersinia pestis caf1M1A1* fimbrial capsule operon promotes transmission by flea bite in a mouse model of bubonic plague. *Infect Immun* **77**: 1222–1229.

Selvarangan R, Goluszko P, Singhal J, Carnoy C, Moseley S, Hudson B, Nowicki S & Nowicki B (2004) Interaction of Dr adhesin with collagen Type IV is a critical step in *Escherichia coli* renal persistence. *Infect Immun* **72**: 4827–4835.

Servin AL (2005) Pathogenesis of Afa/Dr diffusely adhering *Escherichia coli*. *Clin Microbiol Rev* **18**: 264–292.

Sharma RK, Sodhi A & Batra HV (2005a) Involvement of c-Jun N-terminal kinase in rF1 mediated activation of murine peritoneal macrophages *in vitro*. *J Clin Immunol* **3**: 215–223.

Sharma RK, Sodhi A, Batra HV & Tuteja U (2005b) Phosphorylation of p42/44 MAP kinase is required for rF1-induced activation of murine peritoneal macrophages. *Mol Immunol* **42**: 1385–1392.

Smiley ST (2008a) Current challenges in the development of vaccines for pneumonic plague. *Expert Rev Vaccines* **7**: 209–221.

Smiley ST (2008b) Immune defense against pneumonic plague. *Immunol Rev* **225**: 256–271.

So SS & Thanassi DG (2006) Analysis of the requirements for pilus biogenesis at the outer membrane usher and the function of the usher C-terminus. *Mol Microbiol* **60**: 364–375.

Sodhi A, Sharma RK, Batra HV & Tuteja U (2004) Recombinant fraction 1 protein of *Yersinia pestis* activates murine peritoneal macrophages *in vitro*. *Cell Immunol* **229**: 52–61.

Sokurenko EV, Courtney HS, Abraham SN, Klemm P & Hasty DL (1992) Functional heterogeneity of Type 1 fimbriae of *Escherichia coli*. *Infect Immun* **60**: 4709–4719.

Sokurenko EV, Courtney HS, Ohman DE, Klemm P & Hasty DL (1994) Heterogeneity due to minor sequence variations among *fimH* genes. *J Bacteriol* **176**: 748–755.

Sokurenko EV, Courtney HS, Maslow J, Siitonen A & Hasty DL (1995) Quantitative differences in adhesiveness of Type 1 fimbriated *Escherichia coli* due to structural differences in *fimH* genes. *J Bacteriol* **177**: 3680–3686.

Sokurenko EV, Chesnokova V, Doyle RJ & Hasty DL (1997) Diversity of the *Escherichia coli* Type 1 fimbrial lectin: differential binding to mannosides and uroepithelial cells. *J Biol Chem* **272**: 17880–17886.

Sokurenko EV, Chesnokova V, Dykhuizen DE, Ofek I, Wu X-R, Krogfelt KA, Struve C, Schembri MA & Hasty DL (1998) Pathogenic adaptation of *Escherichia coli* by natural variation of the FimH adhesin. *P Natl Acad Sci USA* **95**: 8922–8926.

Soto GE & Hultgren SJ (1999) Bacterial adhesins: common themes and variations in architecture and assembly. *J Bacteriol* **181**: 1059–1071.

Stahlhut SG, Chattopadhyay S, Struve C, Weissman SJ, Aprikian P, Libby SJ, Fang FC, Krogfelt KA & Sokurenko EV (2009) Population variability of the FimH type 1 fimbrial adhesin in *Klebsiella pneumoniae*. *J Bacteriol* **191**: 1941–1950.

Strindelius L, Folkesson A, Normark S & Sjöholm I (2004) Immunogenic properties of the *Salmonella* atypical fimbriae in BALB/c mice. *Vaccine* **22**: 1448–1456.

Sung MA, Fleming K, Chen HA & Matthews S (2001) The solution structure of PapGII from uropathogenic *Escherichia coli* and its recognition of glycolipid receptors. *EMBO Rep* **2**: 621–627.

Tchesnokova V, Aprikian P, Yakovenko O, LaRock C, Kidd B, Vogel V, Thomas W & Sokurenko E (2008) Integrin-like allosteric properties of the catch-bond forming FimH adhesin of *E coli*. *J Biol Chem* **283**: 7823–7833.

Thanassi DG, Saulino ET & Hultgren SJ (1998) The chaperone/usher pathway: a major terminal branch of the general secretory pathway. *Curr Opin Microbiol* **1**: 223–231.

Thanassi DG, Stathopoulos C, Dodson K, Geiger D & Hultgren SJ (2002) Bacterial outer membrane ushers contain distinct targeting and assembly domains for pilus biogenesis. *J Bacteriol* **184**: 6260–6269.

Thomas RJ, Webber D, Collinge A *et al.* (2009) Different pathologies but equal levels of responsiveness to the recombinant F1 and V antigen vaccine and ciprofloxacin in a murine model of plague caused by small- and large-particle aerosols. *Infect Immun* **77**: 1315–1323.

Thomas WE, Trintchina E, Forero M, Vogel V & Sokurenko EV (2002) Bacterial adhesion to target cells enhanced by shear force. *Cell* **109**: 913–923.

Thomas WE, Nilsson LM, Forero M, Sokurenko EV & Vogel V (2004) Shear-dependent 'stick-and-roll' adhesion of type 1 fimbriated *Escherichia coli*. *Mol Microbiol* **53**: 1545–1557.

Thomas WE, Vogel V & Sokurenko E (2008) Biophysics of catch bonds. *Annu Rev Biophys* **37**: 399–416.

Thompson JA, Grunert F & Zimmerman W (1991) Carcinoembryonic antigen family: molecular biology and clinical perspective. *J Clin Lab Anal* **5**: 344–366.

Tieng V, Le Bouguenec C, du Merle L, Bertheau P, Desreumaux P, Janin A, Charron D & Toubert A (2002) Binding of *Escherichia coli* adhesin AfaE to CD55 triggers cell-surface expression of the MHC class I-related molecule MICA. *P Natl Acad Sci USA* **99**: 2977–2982.

Torres AG, Blanco M, Valenzuela P *et al.* (2009) The long polar fimbriae genes of pathogenic *Escherichia coli* strains as reliable markers to identify virulent isolates. *J Clin Microbiol* **47**: 2442–2451.

Tripathi V, Chitralekha KT, Bakshi AR, Tomar D, Deshmukh RA, Baig MA & Rao DN (2006) Inducing systemic and mucosal immune responses to B-T construct of F1 antigen of *Yersinia pestis* in microsphere delivery. *Vaccine* **24**: 3279–3289.

van den Broeck W, Cox E, Oudega C & Goddeeris BM (2000) The F4 fimbrial antigen of *Escherichia coli* and its receptors. *Vet Microbiol* **71**: 223–244.

van Ham SM, van Alphen L, Mooj FR & van Putten JPM (1994) The fimbrial gene cluster of *Haemophilus influenzae* type b. *Mol Microbiol* **13**: 673–684.

Van Loy CP, Sokurenko EV & Moseley SL (2002) The major structural subunits of Dr and F1845 fimbriae are adhesins. *Infect Immun* **70**: 1694–1702.

Van Molle I, Moonens K, Buts L, Garcia-Pino A, Panjikar S, Wyns L, De Greve H & Bouckaert J (2009) The F4 fimbrial chaperone FaeE is stable as a monomer that does not require self-capping of its pilin-interactive surfaces. *Acta Crystallogr D* **65**: 411–420.

Velan B, Bar-Haim E, Zauberman A, Mamroud E, Shafferman A & Cohen S (2006) Discordance in the effects of *Yersinia pestis* on dendritic cell functions: induction of maturation and paralysis of migration. *Infect Immun* **74**: 6365–6376.

Verdonck F, Joensuu JJ, Stuyven E, De Meyer J, Muilu M, Pirhonen M, Goddeeris BM, Mast J, Niklander-Teeri V & Cox E (2009) The polymeric stability of the *Escherichia coli* F4 (K88) fimbriae enhances its mucosal immunogenicity following oral immunization. *Vaccine* **26**: 5728–5735.

Verger D, Bullitt E, Hultgren SJ & Waksman G (2007) Crystal structure of the P pilus rod subunit PapA. *PLoS Pathogens* **3**: e73.

Verger D, Rose RJ, Paci E, Costakes G, Daviter T, Hultgren S, Remaut H, Ashcroft AE, Radford SE & Waksman G (2008) Structural determinants of polymerization reactivity of the P pilus adaptor subunit PapF. *Structure* **16**: 1724–1731.

Vetsch M, Pourger C, Spirig T, Grauschopf U, Weber-Ban EU & Glockshuber R (2004) Pilus chaperones represent a new type of protein folding catalyst. *Nature* **431**: 329–333.

Viboud GI & Bliska JB (2005) *Yersinia* outer proteins: role in modulation of host cell signaling responses and pathogenesis. *Annu Rev Microbiol* **59**: 69–89.

Virdi JS & Sachdeva P (2005) Molecular heterogeneity in *Yersinia enterocolitica* and *Y. enterocolitica*-like species – implications for epidemiology, typing and taxonomy. *FEMS Immunol Med Mic* **45**: 1–10.

Vitagliano L, Ruggiero A, Pedone C & Berisio R (2008) Conformational states and association mechanism of *Yersinia pestis* Caf1 subunits. *Biochem Biophys Res Commun* **372**: 804–810.

Waksman G & Hultgren SJ (2009) Structural biology of the chaperone–usher pathway of pilus biogenesis. *Nat Rev Microbiol* **7**: 765–774.

Wang H, Min G, Glockshuber R, Sun TT & Kong XP (2009) Uropathogenic *E. coli* adhesin-induced host cell receptor conformational changes: implications in transmembrane signaling transduction. *J Mol Biol* **392**: 352–361.

Watts C (2004) The exogenous pathway for antigen presentation on major histocompatibility complex class II and CD1 molecules. *Nat Immun* **5**: 685–692.

Weissman SJ, Chattopadhyay S, Aprikian P, Obata-Yasuoka M, Yarova-Yarovaya Y, Stapleton A, Ba-Thein W, Dykhuizen D, Johnson JR & Sokurenko EV (2006) Clonal analysis reveals high rate of structural mutations in fimbrial adhesins of extraintestinal pathogenic *Escherichia coli*. *Mol Microbiol* **59**: 975–988.

Welkos SL, Andrews GP, Lindler LE, Snellings NJ & Strachan SD (2004) Mu dI1(Ap lac) mutagenesis of *Yersinia pestis* plasmid pFra and identification of temperature-regulated loci associated with virulence. *Plasmid* **51**: 1–11.

Wellens A, Garofalo C, Nguyen H *et al.* (2008) Intervening with urinary tract infections using anti-adhesives based on the crystal structure of the FimH–oligomannose-3 complex. *PLoS ONE* **3**: e2040.

Westerlund B & Korhonen TK (1993) Bacterial proteins binding to the mammalian extracellular matrix. *Mol Microbiol* **9**: 687–694.

Westerlund B, Kuusela P, Risteli J, Risteli L, Vartio T, Rauvala H, Virkola R & Korhonen TK (1989) The O75X adhesin of uropathogenic *Escherichia coli* is a type IV collagen-binding protein. *Mol Microbiol* **3**: 329–337.

Westerlund-Wikström B & Korhonen TK (2005) Molecular structure of adhesin domains in *Escherichia coli* fimbriae. *Int J Med Microbiol* **295**: 479–486.

Willems RJL, van der Heide HGJ & Mooi FR (1992) Characterization of a *Bordetella pertussis* fimbrial gene cluster which is located directly downstream of the filamentous haemagglutinin gene. *Mol Microbiol* **6**: 2661–2671.

Williamson ED, Eley SM, Stagg AJ, Green M, Russell P & Titball RW (1997) A sub-unit vaccine elicits IgG in serum, spleen cell cultures and bronchial washings and protects immunized animals against pneumonic plague. *Vaccine* **15**: 1079–1084.

Williamson ED, Flick-Smith HC, LeButt C, Rowland CA, Jones SM, Waters EL, Gwyther RJ, Miller J, Packer PJ & Irving M (2005) Human immune response to a plague vaccine comprising recombinant F1 and V antigens. *Infect Immun* **73**: 3598–3608.

Wolf MK, De Haan LAM, Cassels FJ, Willshaw GA, Warren R, Boedeker EC & Gaastra W (1997) The CS6 colonization factor of human enterotoxigenic *Escherichia coli* contains two heterologous major subunits. *FEMS Microbiol Lett* **148**: 35–42.

Wroblewska-Seniuk K, Selvarangan R, Hart A *et al.* (2005) Dra/AfaE adhesin of uropathogenic Dr/Afa1 *Escherichia coli* mediates mortality in pregnant rats. *Infect Immun* **73**: 7597–7601.

Yakovenko O, Sharma S, Forero M, Tchesnokova V, Aprikian P, Kidd B, Mach A, Vogel V, Sokurenko E & Thomas WE (2008) FimH forms catch bonds that are enhanced by mechanical force due to allosteric regulation. *J Biol Chem* **283**: 11596–11605.

Yamamoto D, Hernandes RT, Blanco M *et al.* (2009) Invasiveness as a putative additional virulence mechanism of some atypical Enteropathogenic *Escherichia coli* strains with different uncommon intimin types. *BMC Microbiol* **9**: 146.

Yang Y & Isberg RR (1997) Transcriptional regulation of the *Yersinia pseudotuberculosis* pH6 antigen adhesin by two envelope-associated components. *Mol Microbiol* **24**: 499–510.

Yen MR, Peabody CR, Partovi SM, Zhai Y, Tseng YH & Saier MH (2002) Protein-translocating outer membrane porins of gram-negative bacteria. *Biochim Biophys Acta* **1562**: 6–31.

Yu S & Lowe AW (2009) The pancreatic zymogen granule membrane protein, GP2, binds *Escherichia coli* type 1 Fimbriae. *BMC Gastroenterol* **9**: 58.

Yu X, Visweswaran GR, Duck Z, Marupakula S, MacIntyre S, Knight SD & Zavialov AV (2009) Caf1A usher possesses a Caf1 subunit-like domain that is crucial for Caf1 fibre secretion. *Biochem J* **418**: 541–551.

Zalewska B, Piątek R, Konopa G, Nowicki B, Nowicki S & Kur J (2003) Chimeric Dr fimbriae with a herpes simplex virus Type 1 epitope as a model for a recombinant vaccine. *Infect Immun* **71**: 5505–5513.

Zalewska B, Piątek R, Bury K, Samet A, Nowicki B, Nowicki S & Kur J (2005) A surface-exposed DraD protein of uropathogenic *Escherichia coli* bearing Dr fimbriae may be expressed and secreted independently from DraC usher and DraE adhesion. *Microbiology* **151**: 2477–2486.

Zalewska-Piątek B, Bury K, Piątek R, BruŸdziak P & Kur J (2008) Type II secretory pathway for surface secretion of DraD invasin from the uropathogenic *Escherichia coli* Dr^+ strain. *J Bacteriol* **190**: 5044–5056.

Zavialov A, Zav'yalova G, Korpela T & Zav'yalov V (2007) FGL chaperone-assembled fimbrial polyadhesins: anti-immune armament of Gram-negative bacterial pathogens. *FEMS Microbiol Rev* **31**: 478–514.

Zavialov AV & Knight SD (2007) A novel self-capping mechanism controls aggregation of periplasmic chaperone Caf1M. *Mol Microbiol* **64**: 153–164.

Zavialov AV, Batchikova NV, Korpela T, Petrovskaya LE, Korobko VG, Kersley J, MacIntyre S & Zav'yalov VP (2001) Secretion of recombinant proteins via the chaperone/usher pathway in *Escherichia coli*. *Appl Environ Microb* **67**: 1805–1814.

Zavialov AV, Kersley J, Korpela T, Zav'yalov VP, MacIntyre S & Knight SD (2002) Donor strand complementation mechanism in the biogenesis of non-pilus systems. *Mol Microbiol* **45**: 983–995.

Zavialov AV, Berglund J, Pudney AF, Fooks LJ, Ibrahim TM, MacIntyre S & Knight SD (2003) Structure and biogenesis of the capsular F1 antigen from *Yersinia pestis*: preserved folding energy drives fiber formation. *Cell* **113**: 587–596.

Zavialov AV, Tischenko VM, Fooks LJ, Brandsdal BO, Aquist J, Zav'yalov VP, MacIntyre S & Knight SD (2005) Resolving the energy paradox of chaperone-mediated fibre assembly. *Biochem J* **389**: 685–694.

Zav'yalov VP, Chernovskaya TV, Navolotskaya EV, Karlishev AV, MacIntyre S, Vasiliev AM & Abramov VM (1995a) Specific high affinity binding of human interleukin 1β by Caf1A usher protein of *Yersinia pestis*. *FEBS Lett* **371**: 65–68.

Zav'yalov VP, Zav'yalova GA, Denesyuk AI & Korpela T (1995b) Modelling of steric structure of a periplasmic molecular chaperone Caf1M of *Yersinia pestis*, a prototype member of a subfamily with characteristic structural and functional features. *FEMS Immunol Med Mic* **11**: 19–24.

Zav'yalov VP, Abramov VM, Cherepanov PG, Spirina GV, Chernovskaya TV, Vasiliev AM & Zav'yalova GA (1996) pH6 antigen (PsaA protein) of *Yersinia pestis*, a novel bacterial Fc-receptor. *FEMS Immunol Med Mic* **14**: 53–57.

Zav'yalov VP, Chernovskaya TV, Chapman DAG *et al.* (1997) Influence of the conserved disulphide bond, exposed to the putative binding pocket, on the structure and function of the immunoglobulin-like periplasmic molecular chaperone, Caf1M, of *Yersinia pestis*. *Biochem J* **324**: 571–578.

Zhou H, Monack DM, Kayagaki N, Wertz I, Yin J, Wolf B & Dixit VM (2005) *Yersinia* virulence factor YopJ acts as a deubiquitinase to inhibit NF-kB activation. *J Exp Med* **202**: 1327–1332.